Investigation into the start-up and operation of upflow anaerobic sludge bed reactors

In fulfilment of the requirements for the degree of Master of Science

Rory Stott

Supervisor: Prof Sue Harrison
Co-supervisor: Dr David Ikumi

Department of Chemical Engineering
Faculty of Engineering and the Built Environment
University of Cape Town

30 June 2021

Plagiarism Declaration

1. I know that plagiarism is wrong. Plagiarism is to use another's work and to pretend that it is one's own.
2. I have used the Harvard system for citation and referencing. Each significant contribution to, and quotation in, this report from the work, or works, of other people has been attributed, and has been cited and referenced.
3. This report is my own unaided work, except for assistance received from the teaching staff.
4. I have not allowed, and will not allow, anyone to copy my work with the intention of passing it off as his or her own work.

Signed by candidate

_____

Signature

APPLICATION FORM

Please Note:
Any person planning to undertake research in the Faculty of Engineering and the Built Environment (EBE) at the University of Cape Town is required to complete this form **before** collecting or analysing data.The objective of submitting this application *prior* to embarking on research is to ensure that the highest ethical standards in research, conducted under the auspices of the EBE Faculty, are met. Please ensure that you have read, and understood the **EBE Ethics in Research Handbook**(available from the UCT EBE, Research Ethics website) prior to completing this application form: http://www.ebe.uct.ac.za/usr/ebe/research/ethics.pdf

APPLICANT'S DETAILS		
Name of principal researcher, student or external applicant		Rory Stott
Department		Chemical Engineering
Preferred email address of applicant:		sttror001@myuct.ac.za
If a Student	Your Degree: e.g., MSc, PhD, etc.,	MSc
	Name of Supervisor (if supervised):	Sue Harrison, David Ikumi, Madelyn Johnstone-Robertson
If this is a researchcontract, indicate the source of funding/sponsorship		~~Click here to enter text.~~ NRF , CWRC
Project Title		Investigation of the trade-offs between methane productivity and yield in wastewater anaerobic digestion

I hereby undertake to carry out my research in such a way that:

- there is no apparent legal objection to the nature or the method of research; and
- the research will not compromise staff or students or the other responsibilities of the University;
- the stated objective will be achieved, and the findings will have a high degree of validity;
- limitations and alternative interpretations will be considered;
- the findings could be subject to peer review and publicly available; and
- I will comply with the conventions of copyright and avoid any practice that would constitute plagiarism.

SIGNED BY	Full name	Signature	Date
Principal Researcher/ Student/External applicant	Rory Stott	Signed by candidate	~~Click here to enter a date.~~ 05/05/2017

APPLICATION APPROVED BY	Full name	Signature	Date
Supervisor (where applicable)	STL HARRISON ~~Click here to enter text.~~		~~Click here to enter a date.~~ 5/5/2017
HOD (or delegated nominee) Final authority for all applicants who have answered NO to all questions in Section1; and for all Undergraduateresearch (Including Honours).	Adeniyi Isafiade ~~Click here to enter text.~~	Digitally signed by Adeniyi J Isafiade Date: 2018.10.11 13:24:23 +02'00'	Oct 2018 ~~Click here to enter a date.~~
Chair : Faculty EIR Committee For applicants other than undergraduate students who have answered YES to any of the above questions.	~~Click here to enter text.~~		~~Click here to enter a date.~~

pp

Acknowledgements

I would like to thank the following people/organisations for their support with this investigation:

Newlands and Prospecton SAB for the sludges used as inocula used in the experimental investigations, more specifically to Joanne Crimes and Wrenay Arjoon for their correspondence and help with procurement of the sludges.

Joachim Macke for building my reactors, as well as aiding in their conceptualisation, providing knowledge of where to source the materials, and help with building the feed drums and other ancillary components.

Njabulo Thela and Hector Mafungwa for keeping an eye on my reactors and notifying me of any leaking pipes etc, as well as to Tich Samkange and Emmanuel Ngoma for their support for the laboratory experiments.

Prof George Ekama for help with modelling pH.

The financial assistance of the Water Research Commission and National Research Foundation (NRF) towards this research is hereby acknowledged. Opinions expressed and conclusions arrived at, are those of the author and are not necessarily to be attributed to the NRF.

Finally, I would like to thank Dr David Ikumi for his care in helping and guiding me.

Abstract

High-rate anaerobic biological wastewater treatment using the upflow anaerobic sludge bed (UASB) reactor technology offers the potential to reform wastewater treatment. However, the lack of clarity regarding the mechanisms responsible for self-immobilisation of the microbial consortia involved, known as granulation, presents an obstacle to the wide-spread use of this technology. In this study, two laboratory-scale UASB reactors were commissioned for the purpose of generating datasets for model development. A sucrose-based feed was used for the experiments, which were conducted at 37°C. Deterioration of the sludge granules used as inoculum into undesirable bulking-type sludge resulted in refocusing the study to investigate the granulation process. After consulting the literature on granulation, an experimental investigation into the effect of providing additional hydraulic mixing by recycling reactor effluent on granulation was conducted. It was hypothesised that the additional hydraulic mixing would result in the formation of more settleable granules. However, it was found that inclusion of the additional hydraulic mixing resulted in a less dense sludge bed which contained more visual signs (presence of both more loosely-bound exogenous polymeric substance and long filaments presumed to be *Methanosaeta Spp.*) of bulking-type sludge. In hindsight it was found that application of too low a sludge loading rate in the experimental investigations was the cause of the granulation issues, but that this was exacerbated by the additional hydraulic mixing. Apart from granulation issues, a low effluent pH of 6.5 was obtained from the reactors during the experimental investigations in spite of a high feed pH of 8.0. It was hypothesised that the production of VFA and consumption of NH_3 were the primary causes of the acidity generation. A fixed-conversion model of the digester pH was developed to investigate the conversions of the relevant weak acid and base species present and the effects of these conversions on the digester pH. It was found that the dissolution of CO_2 to satisfy the vapour-liquid equilibrium between the headspace CO_2 partial pressure and dissolved carbonic acid concentration was predominantly responsible for the decrease in pH across the reactors. It is on the basis of these findings that both hypotheses were refuted.

Table of Contents

List of Figures

List of Tables

Glossary of Terms

Aerobic	Requiring oxygen
Alkalinity	The quantity of protons required to return a solution to its reference pH
Activated sludge process	An aerobic wastewater treatment process used for removal of organics (COD) which can incorporate nutrient removal processes
Anaerobic	The absence of oxygen
Anaerobic digester	A vessel in which the anaerobic digestion process takes place
Anaerobic digestion	The biodegradation of organic matter in the absence of oxygen
Chemical oxygen demand	The quantity of electrons available expressed as the equivalent mass of oxygen (2 mol-e/mol-O_2) required to oxidise a compound to its most oxygen-saturated form.
Feedstock	The material, often a waste(water) stream, fed to an anaerobic digester
Fit-for-purpose	In the context of water, this refers to water of different qualities (i.e. having different levels of pollutants) being suitable for different purposes, the effect of which is that not all water needs be treated to potable standards to be re-used
Fluidise	To render solid particles fluid-like properties by passing a fluid upwards through them
H_2CO_3*	The combination of the H_2CO_3 and dissolved CO_2 concentrations
Inoculum	The microorganisms used as a seed to start up a bioreactor
Minimum doubling time	The time taken for a microbial species to grow to double its population at a certain temperature when growing at their maximum rate
Monod kinetics	A kinetic model for the growth of microorganisms based on the consumption of one limiting substrate
Organic loading rate	The rate at which COD is fed to a digester per unit reactor volume, usually with the units kg-COD/m^3.day
Physico-chemical	Relating specifically to both physical and chemical properties
Plug-flow	An idealised fluid flow pattern in which there is no deviation in velocity in the plane perpendicular to the fluid flow
Primary sludge	The settleable fraction of raw sewage that is separated in the primary settling tank (this settling stage is known as primary treatment)
Specific methanogenic activity	The CH_4-producing capacity of an anaerobic sludge sample reported as g-COD_{CH4}/g-VSS.day, where 1 g-COD_{CH4}=350 mL_{CH4} at STP
Shear rate	The rate of change of velocity between two adjacent fluid layers, with units of s^{-1}
Sludge loading rate	The rate at which COD is fed to the microorganisms within the digester on the basis of volatile suspended solids i.e. kg-COD/kg-VSS.day
Steady state	A state in which a process or system has stabilized to the extent that the variables defining the process are constant with respect to time
Substrate	The material fed to an anaerobic digester
Waste activated sludge	The sludge produced from the aerobic digestion of sewage following primary treatment

Acronyms and Abbreviations

CH_4	Methane
AD	Anaerobic digestion
ADM1	Anaerobic Digestion Model No 1
COD	Chemical oxygen demand
DWW	Domestic wastewater
EPS	Exogenous polymeric substance
g-COD_{CH4}	An equivalent mass of CH_4 in terms of COD, i.e.
g-COD_{feed}	The COD concentration of the feed to an AD
HAc	Acetic acid
K_s	A constant used in Monod kinetics representing the substrate concentration at which microorganisms attain half their maximum specific growth
LB-EPS	Loosely-bound exogenous polymeric substances
OLR	Organic loading rate
PN	Proteins
PN-EPS	Proteinaceous exogenous polymeric substances
PS	Polysaccharides
PS-EPS	Polysaccharine exogenous polymeric substances
SLR	Sludge loading rate
TB-EPS	Tightly-bound exogenous polymeric substances
TSS	Total suspended solids
UASB	Upflow anaerobic sludge bed
VFA	Volatile fatty acids
VSS	Volatile suspended solids
WW	Wastewater
WWTP	Wastewater treatment plant

1. Introduction

1.1 The untapped potential of wastewaters

Two common characteristics of domestic wastewaters (DWW), and indeed many industrial wastewaters, are the presence of inorganic nutrients and organic compounds (Seghezzo *et al.*, 1998). In addition to this, components that are recalcitrant or inhibitory to biodegradation may also be present (Chen *et al.*, 2008). The generalised aim of wastewater treatment is to ensure that no environmental harm is caused by the release of the treated wastewater into a receiving water body (Chernicharo *et al.*, 2015). Typically, this means removing the nutrients and organic compounds, as well as ensuring adequate pathogen destruction where relevant (Seghezzo *et al.*, 1998). More recently, awareness has also grown around the need to remove micro-pollutants known as endocrine disruptor chemicals (EDC) from wastewaters (Bolong *et al.*, 2009). Removing the aforementioned pollutants through wastewater treatment processes is necessary since failure to do so adequately can result in eutrophication, which can cause large-scale imbalances in natural ecosystems and water bodies (Heisler *et al.*, 2008), as well as allowing the proliferation of pathogenic microorganisms. Water scarcity is a significant issue in largely populated arid-climatic regions. Even where water supply is not lacking, its abstraction has environmental consequences (Rijsberman, 2006). In either case, it is prudent to treat water resources frugally.

At present, organic compounds and nutrients in DWW are generally treated as burdensome substances requiring elimination (Wang *et al.*, 2015). The most ubiquitous domestic wastewater treatment plant (WWTP) strategy is to eliminate the nutrients Nitrogen (N) and Phosphorus (P) through nutrient removal processes, and to remove the organic compounds, measured as chemical oxygen demand (COD), through the aerobic activated sludge process (Sperling and Chernicharo, 2005; Grady Jr *et al.*, 2011; Chernicharo *et al.*, 2015). In this process the N and chemical energy present in the organic matter is lost completely through their conversion to N_2 and CO_2 gases. This approach also generates large quantities of primary and waste-activated sludges, which are usually stabilised using anaerobic digestion (Angelidaki *et al.*, 2003). Due to the prevalence of this substance elimination approach, WWTPs treating organic-rich wastewaters account for 4% of the electricity consumption in the US and other developed countries (Wang *et al.*, 2015). Typically half of this electricity consumption is required for the compression of air for the aerobic treatment process (McCarty *et al.*, 2011). In addition to the environmental burdens associated with electricity production, the nutrient removal processes in WWTP are estimated to produce 3% of N_2O (a powerful greenhouse gas and ozone depletor) emissions globally (Law *et al.*, 2012). At the same time, much energy and resources are used to fix atmospheric N_2 and mine limited P-reserves to supply the agricultural industry (Cordell and White, 2011; McCarty *et al.*, 2011). Furthermore, the limited availability of P is resulting in the rise of farm input costs, which affects food prices (Cordell and White, 2011).

The treatment and reuse of wastewater not only presents an effective means to minimising our demand for fresh water, but also to recover nutrients and energy from the contaminating compounds. The idea of reusing wastewater brings up the concept of ‘fit-for-purpose’ water, meaning that different criteria exist for the quality of the water depending on its intended use. In the case of reusing DWW, repurposing it for agricultural use represents the opportunity for the agricultural sector to demand less freshwater as well as nutrients which are already present in DWW (McCarty *et al.*, 2011).

Energy can be recovered from the organic compounds in DWW and suitable industrial wastewaters (typically from the food, pharmaceutical and pulp and paper industries (van Lier *et al.*, 2015)) through the anaerobic digestion (AD) process. In AD, the biodegradable organic compounds undergo a series of biological transformations until they are eventually converted into biogas, a combination of CH_4 and CO_2 (Angelidaki *et al.*, 2003). This biogas can either be upgraded to a fuel similar to compressed natural gas, or combusted in a generator for electricity production (Zacharof and Lovitt, 2013). The energy potential for AD of raw DWW is so great that converting WWTP from the conventional scheme (with the activated sludge process) to one using AD as the primary treatment process can result in the WWTP producing energy above its own needs (McCarty *et al.*, 2011). Energy consumption can also be reduced

outside of the WWTP if nutrients are recovered, due to decreased dependence on the Haber-Bosch process for combined nitrogen species for fertiliser production (McCarty *et al.*, 2011). Since AD does not eliminate the potential to recover nutrients, and provides energy from the breakdown of organic compounds, focusing the design of WWTP around the AD unit operation allows for the three goals of water reuse, nutrient recovery and energy recovery to be realised. Ultimately, this scheme represents the potential to increase resource efficiency within an important and large-scale sector, thus significantly reducing waste generation and the need for raw materials.

1.2 Anaerobic wastewater treatment

In terms of reactor design, applications of AD are divided between the digestion of slurries (high solids & COD concentrations), including sewage sludges, and wastewaters (relatively low presence of solids & potentially dilute). As mentioned, AD is a biological process in which biodegradable organic compounds (substrate) are converted by a diverse range of microorganisms. Effective treatment of the substrate refers to the removal of this substrate through its conversion into gaseous CH_4, which then spontaneously separates from the slurry or wastewater treated due to its low solubility (Kleerebezem *et al.*, 2015). As a rule of thumb, particulate organic matter is biodegraded much more slowly than soluble organic compounds (Eastman and Ferguson, 1981). Since microorganisms catalyse this treatment process by consuming the substrate, the rate at which substrate is degraded is therefore governed largely by the concentration of microorganisms in the reactor (van Lier *et al.*, 2015). A convenient characteristic of the microorganisms prevalent in AD processes is their ability to secrete exogenous polymeric substances (EPS) that allow them to bind together as a macroscopic sludge (Schmidt and Ahring, 1996). In the case where the substrate is a slurry containing solids that are mostly recalcitrant to degradation, it is usually not feasible to separate the slurry from the microorganisms and thus retain these 'biocatalysts' for substrate degradation. However, in the case of wastewater (WW) AD, the solid sludge (biomass) exists as a discrete phase to the wastewater, thus it is possible to selectively retain a high concentration of highly active biomass (biocatalyst) in the reactor.

Novel reactor systems that selectively retain biomass were developed from the 1970s onwards to take advantage of this fact, and are typically termed 'high-rate' anaerobic reactors due to the higher volumetric rates of treatment attainable when biomass is retained to achieve high biomass concentrations (van Lier *et al.*, 2015). The development of such systems was necessary to make AD a feasible option for treatment of most WW due to the impractically large reactor volumes required should a standard reactor design without biomass retention be implemented (van Lier *et al.*, 2015). These systems provide an alternative to activated sludge systems for treatment of organic-rich industrial WW with many advantages. Activated sludge processes consume roughly 1 kWh-electricity/kg-$COD_{removed}$, while AD can produce 1.5 kWh-electricity/kg-$COD_{removed}$ through combustion of the CH_4 generated in a generator, assuming a 40% efficiency for the conversion of thermal energy to electrical energy (van Lier *et al.*, 2015). Furthermore, sludge production is reduced tenfold, representing a significant reduction in WWTP operating costs for sludge disposal. In addition, the reactor footprint is typically 90% smaller than for the activated sludge process (van Lier *et al.*, 2015).

Of the high-rate anaerobic reactor systems installed for industrial WW treatment, over 90% are a design known as the upflow anaerobic sludge bed (UASB) reactor (van Lier *et al.*, 2015). The UASB reactor technology was developed in the 1980s for treatment of industrial WW, but was soon incorporated into the sewage treatment strategy for India and Latin American countries (Chernicharo *et al.*, 2015). By 2012, UASB reactor technology was found to be the third most employed technology for municipal WW treatment by number, and fourth by design flow after only 25 years of use for sewage treatment in Latin America (Chernicharo *et al.*, 2015). In sewage WWTP, use of the UASB reactor as the dominant unit operation for removal of organic compounds (followed by aerobic post-treatment) typically reduces capital and operational expenditure by 20-50% and >50% compared with activated sludge-based WWTP (Chernicharo *et al.*, 2015).

The mechanism by which the UASB reactor is able to retain highly active sludge is through the formation of settleable sludge granules. These granules form as a result of the behaviour of AD microorganisms in response to favourable conditions. If granulation proceeds well upon reactor start-up, the sludge granules are dense and settleable, allowing WW to be pumped upwards through the sludge bed without

eluting the granules. The success of the UASB reactor system is therefore reliant on the formation of these settleable sludge granules (Chui *et al.*, 1993; Fukuzaki *et al.*, 1995; Schmidt and Ahring, 1996; Hulshoff Pol *et al.*, 2004; van Lier *et al.*, 2015). However, sludge granulation does not always occur as desired and, if conditions are unfavourable, loose flocs may form that are prone to flotation, thus resulting in a deterioration of reactor performance due to loss of the active biomass as well as the presence of this biomass in the effluent (Hulshoff Pol. *et al.*, 1982; De Beer *et al.*, 1996; Halalsheh *et al.*, 2005; Wang *et al.*, 2017). The improper application of UASB reactors soon after its advent damaged its credibility amongst water authorities (Chernicharo *et al.*, 2015). It is therefore imperative to understand which conditions lead to the formation of granules to fully realise the potential of this technology.

It must be noted that the low nutrient removal aspect of AD can be considered a drawback where the effluent cannot be used for irrigation, which results in the need for further treatment of the wastewater following AD. However, such further treatment provides the added advantage of nutrient repurposing rather than simply nutrient removal. Furthermore, post-treatment is also often required to remove residual COD and pathogens. 'Complete' AD of the wastewater (consumption of the biodegradable COD) can actually be detrimental if nutrient removal processes, which also require readily biodegradable COD, are to follow (Chernicharo *et al.*, 2015). In this situation, the scheme chosen for treating the wastewater requires careful evaluation. Specifically, it is important to understand the compromise between energy recovery from AD and the ability to treat, and potentially recover, fit-for-purpose water.

1.3 Scope of investigation

To design AD reactor systems, knowledge of the kinetics of the process are required for determination of the reactor volume required to treat a wastewater of a certain flow rate and strength (COD concentration). Furthermore, in a system as described above, where incomplete degradation of the substrate COD may be desired, it is useful to have a model that describes the conversion of the substrate upon specification of the wastewater and reactor system characteristics. The development of such a model provides the opportunity to perform virtual experiments without wasting resources and using minimal time and labour. This allows for the analysis of the performance of various scenarios or process configurations for overall process optimisation.

The organic loading rate (OLR) is the operational parameter with the greatest effect on the AD process, and is defined as the mass of COD fed to the reactor per unit volume per unit time (units of kg-COD/$m^3_{reactor}$.day). This parameter takes into account the reactor volume, wastewater flow rate and strength. It represents the amount of substrate fed to the reactor, and therefore influences the productivity and yield of CH_4. If a similar conversion of all compounds in the wastewater is expected at two OLR, then the productivity of CH_4 will be higher at the higher OLR. In reality, increasing the OLR may result in a decrease in CH_4 yield because higher substrate conversion rates would be required from the microorganisms to maintain the same CH_4 yield on substrate fed, which is not feasible if the microorganisms are already 'saturated' with substrate. Furthermore, in most cases the OLR can only be increased by decreasing the hydraulic retention time (HRT) of the reactor because the COD concentration of the wastewater is not something that is controlled. This results in a lower contact time between the substrate and the microorganisms in the reactor, which may also decrease the CH_4 yield attained if the contact time is insufficient.

The initial aim of this study was to investigate the influence of the OLR on reactor performance – specifically the CH_4 yield, CH_4 productivity and effluent characteristics. Because wastewater AD in full-scale installations is performed using continuous flow-through systems with biomass retention, a UASB reactor system was designed, built and commissioned to make this investigation relevant. A large concentration of well-granulated sludge was used as the inoculum for this experiment. However, deterioration of these granules occurred, followed by sludge washout which persisted until the experiment was eventually terminated.

This emphasised the need to provide the correct conditions for granulation for successful UASB reactor operation. The aim of this study was therefore modified to investigate the causes for granule

deterioration in the OLR experiment. A review of the relevant literature indicated the importance of the reactor hydrodynamic conditions for granule formation. In light of this, a new experimental plan was devised, focusing on the effect of supplementary hydraulic mixing on the start-up and granulation of the UASB reactors. Furthermore, a simple stoichiometric model capable of predicting the effluent pH, gas production and gas composition of the UASB reactors was developed to further investigate the relationship between UASB reactor physiology and pH. This model was developed to elucidate the factors responsible for the low effluent pH produced during the laboratory experiments.

1.4 Plan of development

In Chapter 2, a review of the relevant AD literature is presented. This review introduces the fundamentals and background of the AD process in Section 2.1 and covers the microbiology and factors influencing the process in more detail in Sections 2.2 and 2.3. An extensive review of the phenomenon of sludge granulation in UASB reactors is then presented in Section 2.4, followed by modelling considerations in Section 2.5, and eventually the proposed experimental plans and hypotheses in Section 2.6.

The design of the laboratory-scale experimental UASB reactors is presented in Chapter 3, followed by the design of the experiments, and finally specific analytical techniques and protocols used to perform the experiments. The development of the steady state model for pH prediction is documented in Chapter 4.

The results and discussion of the experiments performed are presented in Chapter 5. The results of the first experiment are discussed in Section 5.1, followed by the results of the Granulation experiment in Section 5.2, and finally the results of the modelling experiments in Section 5.3.

The conclusions of the investigation are made and presented in Chapter 6, followed by recommendations on how to improve the methodology used.

2. Literature Review

2.1 Introduction to AD

AD is a bioprocess whereby organic carbon is sequentially utilised by an anaerobic mixed microbial community until it is converted to its most oxidised and reduced forms, namely CO_2 and CH_4 respectively (Angelidaki *et al.*, 2003). This combination of CO_2 and CH_4 is called biogas, of which CH_4 usually comprises around 60% (Chynoweth *et al.*, 2000), although the CH_4 concentration obtained varies based on environmental conditions and feedstocks (Buswell and Mueller, 1952). Biogas is a readily combustible fuel that can be used to produce heat or electricity or both, or upgraded to natural gas or further processed to a liquid fuel for automotive use (Angelidaki *et al.*, 2003). AD is a particularly efficient biofuel production process, with a recovery of Gibbs Free Energy typically 2-3 times higher than in other biofuel production processes such as bioethanol or biodiesel (Kleerebezem *et al.*, 2015). In Western Europe and the United States, anaerobically produced biogas is used to generate nearly 13000 GWh of electricity annually. This accounts for 1.2% and nearly 10% of the total and renewable electricity productions respectively in these countries (Zacharof and Lovitt, 2013). Some 3405 GWh of electricity was produced using biogas in Italy alone in 2011, and China's annual production of biogas reached 248 billion m^3 (from 26.5 million biodigesters) in 2010 (Mao *et al.*, 2015).

Most organic carbon-containing waste streams are appropriate as feedstocks for AD, making it an attractive option for treatment of these streams. Although energy crops are also considered as feedstocks (Weiland, 2003), the most popular applications of AD are for waste treatment and are as follows (Angelidaki *et al.*, 2003):

- Treatment of primary and waste activated sludge resulting from primary (settling) and secondary (aerobic) sewage treatment processes, thus stabilising and lowering the quantity of sludge
- Treatment of industrial wastewaters containing organic carbon, usually from biomass, fermentation, pharmaceutical, food processing and pulp and paper industries (van Lier *et al.*, 2015)
- Processing of livestock waste to generate methane and improve the quality of manure as a fertiliser
- Processing of the organic fraction of municipal solid waste to both decrease the need for landfilling or incineration, to reduce methane production in landfill and to recycle nutrients to the agricultural sector
- Raw sewage treatment – at present, only significant in countries with the warm ambient temperatures associated with tropical climate such as Brazil, Colombia, Mexico and India (Chernicharo *et al.*, 2015)

The use of high-rate AD reactors to treat wastewaters contaminated by organics can also be significantly advantageous over traditional aerobic treatment for a number of reasons. Aerobic treatment consumes energy due to the power needed for aeration, and produces 3-20 times more sludge (Seghezzo *et al.*, 1998) which is often costly to dispose of (Speece, 1983; Angelidaki *et al.*, 2003). In addition to this, higher organic loading rates (OLR) may be processed in UASB reactors than in aerobic reactors (Seghezzo *et al.*, 1998). This is because the rate of AD is only dependent on the quantity and activity of biomass within the reactor, and not on oxygen mass transfer rates as is often the case in aerobic treatment (Fang and Chui, 1993). The use of AD processes also has numerous environmental advantages, most notably because the CH_4 produced can replace conventional fuels, and the agricultural use of the nutrient-rich digestate can reduce inorganic nutrient requirements (McCarty *et al.*, 2011; Mao *et al.*, 2015). Because biogas is derived from geologically recently-fixed carbon in waste streams, its combustion does not result in the release of additional carbon dioxide (Angelidaki *et al.*, 2003; Haberl *et al.*, 2012). An assessment by McCarty et al. (2011) found that the treatment of sewage using AD can convert sewage treatment systems into net energy producers. This is especially significant considering that wastewater treatment accounts for 4% of the U.S. electricity demand (Wang *et al.*, 2015). However, it must be noted that the lack of nutrient removal in AD is often

a disadvantage where it is not possible to use the treated wastewater for irrigation purposes (McCarty *et al.*, 2011). In addition to this, the effluent COD from most high-rate wastewater (WW) AD reactor systems is often too high to meet environmental regulations, and pathogen removal in WW AD is low (Seghezzo *et al.*, 1998). A polishing step is therefore often required to remove residual COD, nutrients and pathogens (Seghezzo *et al.*, 1998; Chernicharo *et al.*, 2015). It must be noted, however, that the use of AD for removing biodegradable COD prior to nutrient removal may be detrimental to the nutrient removal processes which require a carbon-source if insufficient residual COD is left to power these processes, thus this scheme requires careful evaluation (Seghezzo *et al.*, 1998; Chernicharo *et al.*, 2015). Where nutrient removal is not desired, the development of anaerobic membrane bioreactors presents a method to satisfactorily remove COD to meet effluent standards without the need for post-treatment, and has been made more feasible by a relatively recent development to counteract the effect of membrane fouling (Kim *et al.*, 2011). In the study performed by Kim et al. (2011), a two-stage setup comprising an anaerobic fluidized bed reactor (AFBR) followed by an anaerobic fluidized bed membrane reactor (AFBMR) was used. Both reactors contained granular activated carbon as the carrier particles, while only the AFBMR contained a submerged polyvinylidenefluoride membrane with a pore size of 0.1 µm through which the effluent was pumped. This setup allowed for the reduction of influent COD, in the form of propionate and acetate, from ~500 mg-COD/L to ~7 mg-COD/L.

2.2 The Microbiology of AD

The overall AD process comprises four main sub-processes: hydrolysis, acidogenesis, acetogenesis and methanogenesis. A conceptual model of these stages and the dominant (bio)chemical species that characterise them are illustrated in Figure 2-1.

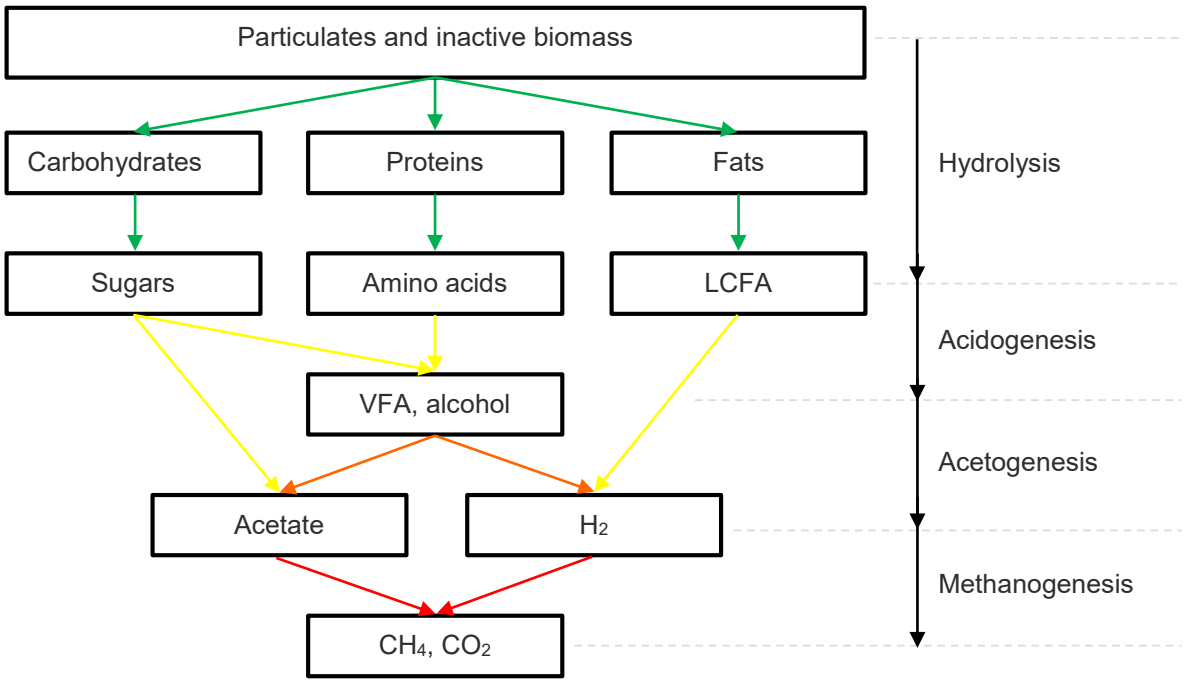

Figure 2-1: Diagram of the AD process, adapted from Mao et al (2015) and Batstone et al (2002). The green, yellow, orange and red arrows represent hydrolysis, acidogenesis, acetogenesis and methanogenesis respectively

Hydrolysis of solid particulates, inactive (dead) biomass and soluble complex organic compounds such as carbohydrate polymers, proteins and fats occurs as a result of extracellular enzymes secreted by hydrolytic acidogenic microbes (Adney *et al.*, 1991; Batstone *et al.*, 2002; Lee *et al.*, 2014). The products of hydrolysis, namely simple sugars, amino acids and long chain fatty acids (LCFAs) are then converted through intracellular processes by acidogenic bacteria to form volatile fatty acids (VFAs), alcohols and H_2 (Lee *et al.*, 2014; Mao *et al.*, 2015). The VFAs and alcohols are converted to acetate and H_2 by

acetogenic bacteria (Mao *et al.*, 2015). The acetate and H_2 are then converted by aceticlastic and hydrogenotrophic methanogens respectively to form methane and CO_2 (Speece, 1983; Pind *et al.*, 2003).

Typically, around 70% of the CH_4 generated is formed from acetic acid through the activity of the aceticlastic methanogens, with the balance being produced by hydrogenotrophic methanogens using H_2 and CO_2 (Gujer and Zehnder, 1983; Speece, 1983). Only two genera (belonging to two different families) of aceticlastic methanogens exist, namely *Methanosarcina* and *Methanosaeta* (Chui, 1994; Garcia *et al.*, 2000). The latter was formerly known (and widely referred to) as *Methanothrix* (Schmidt and Ahring, 1996; Garcia *et al.*, 2000). *Methanosaeta spp.* are slow-growing scavengers (doubling time of 4-7 days at 37°C, K_s = 30 mg/L) that utilise acetate as their sole carbon-source (McCarty and Mosey, 1991; Garcia *et al.*, 2000). Their cells are rod-shaped (0.8 x 2.0 µm), and form long sheathed filaments that tend to aggregate in flocs (McCarty and Mosey, 1991; Garcia *et al.*, 2000). *Methanosarcina spp.* on the other hand are poorer scavengers, but faster-growing (doubling time of 1.5 days, K_s = 400 mg/L), and some can utilise methanol, methylamines, acetate and H_2/CO_2 (McCarty and Mosey, 1991; Garcia *et al.*, 2000). *Methanosarcina spp.* cells are coccoid-shaped and grow together in clumps (McCarty and Mosey, 1991; Garcia *et al.*, 2000). *Methanosarcina spp.* also have a wider pH range of growth, and thrive at a pH range between 6 and 8, while *Methanosaeta spp.* prefer the range 6.8 to 7.8 (Ten Brummeler *et al.*, 1985).

As indicated by their large doubling times, the aceticlastic methanogens are notoriously slow growing (Speece, 1983; McCarty and Mosey, 1991), and are generally some of the most sensitive species to inhibitory compounds (Chen *et al.*, 2008). This is in contrast with the acidogenic bacteria which, in general, are much faster growing (minimum doubling time of 30 min) and less sensitive to inhibition (Mosey, 1983; Chen *et al.*, 2008). Aceticlastic methanogenesis is therefore usually the process to be affected both first and worst by the presence of inhibitors or sub-optimal process conditions, leading to an accumulation of the VFAs produced by acidogenic bacteria (Dogan *et al.*, 2005; Chen *et al.*, 2008).

A close relationship exists between the hydrogenotrophic methanogens and the acetogens due to the conversion of higher VFAs to acetate and H_2 (acetogenesis) being thermodynamically favourable only at H_2 partial pressures of less than 10^{-4} atm (Speece, 1983). According to McCarty & Mosey (1991), the higher VFAs propionate and butyrate are not characteristically produced unless the H_2 partial pressure exceeds 10^{-6} atm and the pH is acidic respectively. This is because fermentation of sugars to acetate provides a higher energy yield, thus acetate is the preferred product of acidogenesis (Mosey, 1983). Propionate producing bacteria grow quickly at neutral pH and high substrate concentrations (McCarty and Mosey, 1991). Production of propionate by these bacteria is only observed at high H_2 partial pressures due to the need for the bacteria to dehydrogenate the cofactor NADH (formed in the conversion of glucose to pyruvate) (Sam-Soon *et al.*, 1987). This process usually happens spontaneously through the release of H_2 gas, but since this is not thermodynamically feasible at high H_2 partial pressures they regenerate NAD^+ through the production of propionic acid (Sam-Soon *et al.*, 1987). Hydrogenotrophic methanogens are typically 10 times more active than aceticlastic methanogens (Chui, 1994), with minimum doubling times of 6 hours (Mosey, 1983). They are effective scavengers adept at maintaining the H_2 partial pressure favourable for acetogenesis (Mosey, 1983; Speece, 1983). However, it can be seen that a sensitive dynamic exists between the AD consortia and, in the case of a shock loading of substrate, both VFA concentrations and H_2 partial pressure can rise above that required for stable operation of acetogenesis and methanogenesis, resulting in the inhibition of these processes (Dogan *et al.*, 2005).

VFA accumulation affects methanogenesis by lowering the pH below the optimal range for methanogens (Şentürk *et al.*, 2010). It has also been proposed that the undissociated form of VFA can also be directly inhibitory by permeating the cell wall and lowering cytoplasmic pH (Pullammanappallil *et al.*, 2001). This effect is exacerbated at a low pH where a greater proportion of the VFA are in their undissociated state (Pullammanappallil *et al.*, 2001). Propionate is considered to be the most inhibitory and recalcitrant VFA in the AD process, while the toxicity of the acetate and butyrate are only realised at relatively high concentrations at normal pH values (Lee *et al.*, 2014). Dogan et al. (2005) found that acetate, propionate and butyrate caused a 50% reduction in methanogenic activity at concentrations of 13000 mg/L, 3500 mg/L and 15000 mg/L respectively (unfortunately no pH data available).

Furthermore, propionate is particularly persistent in AD, and propionate degradation has been found to be performed by the slow-growing bacterium *Syntrophobacter wolinii* that is unlikely to be found in significant quantities under normal digester operation since propionate is their sole carbon source in AD (McCarty and Mosey, 1991).

McCarty & Mosey (1991) proposed that the AD process behaviour is greatly influenced by the population dynamics of the various consortia involved. They propose that under shock loading conditions, acetate and propionate will accumulate, decreasing the pH and inhibiting further propionate production but triggering butyrate production instead (McCarty and Mosey, 1991). Butyrate and acetate levels are expected to drop relatively quickly, but propionate may persist due to the need for the population of propionate degraders to establish itself (McCarty and Mosey, 1991).

2.3 Factors influencing the AD process

2.3.1 Temperature

Increasing temperature increases microbial activity and affects physical properties such as viscosity, surface tension and mass transfer within the AD system (Angelidaki *et al.*, 2003). AD processes are usually operated at mesophilic (25-40°C) or thermophilic (≥45°C) temperatures (Angelidaki *et al.*, 2003). However, methane production still occurs at psychrophilic (0-20°C) temperatures (Rajeshwari *et al.*, 2000; Angelidaki *et al.*, 2003). Angelidaki et al. (2003) warn that fluctuations in temperature hinder process performance because the microbes take time to adapt. The rate of microbial activity is reported to decrease by roughly 50% for every 10°C decrease in temperature within the mesophilic range (Rajeshwari *et al.*, 2000).

The increased microbial activity experienced at higher temperatures means that higher OLRs can be handled (Angelidaki *et al.*, 2003; Mao *et al.*, 2015). Thermophilic processes have been reported to be less stable (Mao *et al.*, 2015), with higher VFA accumulation during process upsets (Nges and Liu, 2010). However, Angelidaki et al. (2003) state that industrial experience has proven otherwise, and that increased rates of hydrolysis are observed as well as destruction of pathogens at higher temperatures. It has been observed that the microbial community's composition does not change noticeably when lowering the process temperature from the mesophilic to psychrophilic range, indicating that the mesophilic organisms are tolerant to low temperatures (Angelidaki *et al.*, 2003).

Temperature affects the solubility of gases. Hence, at low temperatures an appreciable quantity of CH_4 generated can be retained in the effluent stream, especially if the feed stream is dilute, as in the case of treatment of sewage using AD (Singh and Viraraghavan, 1998; Kim *et al.*, 2011; Ferrer *et al.*, 2012; Chernicharo *et al.*, 2015; Kleerebezem *et al.*, 2015). At temperatures of around 20°C, and influent sewage COD < 1000 mg/L, 30-41 % of the CH_4 produced during digestion of sewage is typically dissolved in the liquid phase (Chernicharo *et al.*, 2015). The equilibrium solubility of CH_4 in water as a function of temperature can be described by Henry's law as presented in Equation 1 and Equation 2 (Ferrer *et al.*, 2012).

$$x_{CH_4,aq} = \frac{P \cdot y_{CH_4}}{H^{CH_4}(T)} \qquad \text{Equation 1}$$

where

$$H^{CH_4}(T) = 10^{\left(\frac{-675.74}{T(K)} + 6.88\right)} \qquad \text{Equation 2}$$

and

$x_{CH_4,aq}$ is the mole fraction of CH_4 in the aqueous phase

P is the total pressure in atm

y_{CH_4} is the mole fraction of CH_4 in the vapour phase

It can be seen that the solubility of CH_4 increases with decreasing temperature. Because CH_4 is produced in the aqueous phase, inadequate mixing within the reactor may limit the transfer of CH_4 from the aqueous phase to the gaseous phase, resulting in an oversaturated concentration of CH_4 within the reactor effluent (Singh and Viraraghavan, 1998; Kim *et al.*, 2011; Ferrer *et al.*, 2012). Kim et al. (2011) found the oversaturation of CH_4 to be on average 1.94 times the equilibrium value. An air-stripping unit can be incorporated following the AD reactor to remove and utilise the dissolved methane present in the effluent stream (McCarty *et al.*, 2011).

2.3.2 pH

As alluded to in Section 2.2, the pH of the reactor is one of the most important parameters in the AD process and is required to be kept in the favourable range for methanogenesis to maintain process operation (Rajeshwari *et al.*, 2000; Angelidaki *et al.*, 2003). The optimal pH range for methanogens is 6.8-7.2 (Rajeshwari *et al.*, 2000). For high-rate digestion of wastewaters using immobilised cells, a larger pH range of 6.5-7.8 still provides satisfactory conditions for methanogens (Hulshoff Pol *et al.*, 1983). It has been observed that the rate of hydrolysis is pH dependent and that the optimal pH is different for different substrates. The optimal pH range for hydrolysis of sludge was found to be 8 – 11, 7 for kitchen waste, and 5.25 – 6 for wastewaters (Lee *et al.*, 2014). The optimal pH range for acidogenic bacteria is 5.5 - 6.5, and it was found that a pH of 6 was optimal in the production of VFA (Wang *et al.*, 2014).

The pH of the AD reactor is determined by the interactions between the dominant weak acid/base subsystems present (McCarty and Mosey, 1991; Musvoto *et al.*, 1997). In AD of domestic WW (DWW), the weak acid/base subsystems commonly of importance (apart from the $H^+/H_2O/OH^-$ subsystem) are the $H_2CO_3/HCO_3^-/CO_3^{2-}$, NH_3/NH_4^+, $H_3PO_4/H_2PO_4^-/HPO_4^{2-}/PO_4^{3-}$, $H_2S/HS^-/S^{2-}$ and VFA/VFA^- subsystems (Moosbrugger *et al.*, 1993; Musvoto *et al.*, 1997). The conversion of VFA, COD, N, P and S found in the substrate to HCO_3^-, VFA^-, NH_3, H_3PO_4 and H_2S – the respective forms in which these elements are predominantly found in anaerobic environments (Loewenthal *et al.*, 1989) – re-establishes the pH (Loewenthal *et al.*, 1989; Musvoto *et al.*, 1997). Alkalinity is a property of aqueous solutions that can be defined as the proton absorbing capacity of a solution relative to some reference state (Loewenthal *et al.*, 1989). If the WW fed to an AD reactor is defined as the reference state (with its own characteristic pH), then the respective production/consumption of acids/bases that dissociated to release a proton lowers the proton absorbing potential of the WW relative to this reference state, thus consuming alkalinity (Loewenthal *et al.*, 1989). If acids/bases are consumed/produced respectively instead, this represents the production of alkalinity relative to the reference state of the WW (Loewenthal *et al.*, 1989).

If alkalinity is not generated during digestion, sodium bicarbonate is often used as a source of alkalinity to maintain a stable pH, especially when process upsets occur and VFA accumulate (Rajeshwari *et al.*, 2000). The VFA:alkalinity ratio has been identified as an indicator of digester stability. According to Behling et al. (1997) the reactor is stable at a ratio below 0.4 mg-VFA/mg-$CaCO_3$, slightly unstable between 0.4 and 0.8 mg-VFA/mg-$CaCO_3$, and significantly unstable above 0.8 mg-VFA/mg-$CaCO_3$. Note that presentation of alkalinity as a mass of $CaCO_3$ corresponds to the proton absorbing capacity of that mass of $CaCO_3$ (e.g. one mole of $CaCO_3$ is equivalent to two mole OH^- alkalinity, or one mole CO_3^{2-} alkalinity).

2.3.3 Substrate composition & the rate-limiting step

Hydrolysis is usually considered the slowest process step in AD (Fang and Chui, 1993; Chernicharo *et al.*, 2015). However, since the organics-containing waste streams used for AD vary in their composition, the rate-controlling step is predominantly dependent on the composition of the substrate (Speece, 1983). Grease, lipids, cellulose and proteins present in the substrate are required to be hydrolysed before being utilised within the cell, thus AD processes fed with these substrates are likely to be limited by hydrolysis (Eastman and Ferguson, 1981; Speece, 1983). However, for substrates that do not contain these recalcitrant and complex organics, methanogenesis is usually rate-limiting (Speece, 1983).

For example, the high COD present in primary and waste activated sludges is 90-99% insoluble, leading to hydrolysis limiting the overall process rate (Lee *et al.*, 2014). This is similarly the case for food waste and the organic fraction of municipal solid waste. However, many food processing wastewaters contain high levels or simple organic compounds which are readily converted to VFA, leading to methanogenesis being rate-limiting (Speece, 1983).

The substrate composition can also influence the pH of the reactor, as well as the methane yield. The liberation of N from N-containing biodegradable organic compounds (mostly proteins and urea (Chen *et al.*, 2008)) results in the production of alkalinity, thus raising the pH of the digester (Ekama *et al.*, 2015). This can lower or negate the need for alkalinity supplementation. If the feed contains significant quantities of NH_3 and/or high concentrations of NH_3 are generated through the degradation of N-containing substrates, inhibition can occur (Nielsen and Angelidaki, 2008). Inhibition from NH_3-toxicity is thought to result from the un-ionised form of NH_3 (Angelidaki *et al.*, 2003). The relative concentrations of NH_3 and NH_4^+ are governed by the pH of the system, where the concentration of the toxic NH_3 form increases with increasing pH (Chen *et al.*, 2008). Lowering the digester pH through the addition of acidity has helped to recover digesters suffering from NH_3 inhibition, supporting the view that the un-ionised NH_3 form is indeed responsible for inhibition (Angelidaki *et al.*, 2003).

Sulphate is a component of many industrial and DWW (Barrera *et al.*, 2014; Wang *et al.*, 2017), and the presence of sulphate in the digestion substrate tends to result in a lower CH_4 yield being attained (Singh and Viraraghavan, 1998). In AD, sulphate-reducing bacteria (SRB) compete with methanogens for substrate, as well as produce sulphide which can lead to inhibition of methanogens (O'Flaherty *et al.*, 1998). The COD/SO_4^{2-} ratio is important, because sulphate reduction by SRB is energetically favoured over methanogenesis. SRB typically have a higher affinity for acetate than methanogens (lower Ks than methanogens), thus SRB outcompete methanogens for acetate consumption at low COD concentrations (Speece, 1983). The reduction reaction of sulphate (SO_4^{2-}) to form sulphide (S^{2-}) requires the oxidation of two mole of COD per mole of sulphide formed, corresponding to 0.67 g-COD/g-SO_4^{2-} converted. This means that 0.67 g-COD will be used for every g-SO_4^{2-} present in the feed, thus having the effect of diverting COD reduction from methane formation to sulphide formation (Singh and Viraraghavan, 1998). The pH optima of methanogens (6.8-7.8) is lower than that of SRB (7.5-8.5), thus operation at a lower pH can help to favour methanogenesis (O'Flaherty *et al.*, 1998).

2.3.4 Retention times & organic loading rates

The hydraulic retention time (HRT) is defined as the average time that the substrate spends in the reactor, and is defined by Equation 3.

$$HRT = \frac{V}{\nu}\ (days)$$ Equation 3

Where V is the working volume of the reactor (m^3), and ν is the volumetric flow rate of the feed (m^3/day). The HRT is closely linked to the initial capital investment of the reactor since a longer HRT results in a larger reactor per volume of feed processed (Speece, 1983; Lee *et al.*, 2014).

The solids retention time (SRT) is defined as the average time that solids spend in the reactor, and is defined by Equation 4.

$$SRT = \frac{M_T}{TSS_e}$$ Equation 4

where

M_T is the total mass of solids present in the reactor and

TSS_e is the total suspended solids concentration of the effluent

In a completely mixed reactor with no means of biomass (solids) retention, the SRT is equal to the HRT (Lee *et al.*, 2014). However, in WW AD, the solid and liquid phases are discrete. In the case where high-rate AD reactors with biomass (solids) retention are used, the SRT can be much longer than the

HRT (Speece, 1983). In WW AD processes, it is important to ensure that the SRT is sufficiently long to prevent washout of the slow-growing methanogens and process instability (Speece, 1983). The SRT also influences the prevalence of microbial species within the reactor (Lee *et al.*, 2014).

The organic loading rate (OLR) is defined as the mass of organic matter fed to the reactor per volume of reactor per day. The mass of organic matter is usually represented by the mass of volatile solids (VS) for solid waste treatment systems, or by chemical oxygen demand (COD) for wastewater treatment systems. This parameter is a function of the COD (or VS) in the feed, and the HRT. The relationship between COD, HRT and OLR is shown in Equation 5.

$$OLR = \frac{COD\ (kg/m^3)}{HRT\ (days)} \qquad \text{Equation 5}$$

The OLR is an important parameter because it represents the amount of organic substrate available to be degraded. Due to the fact that methanogenesis is rate-limiting when simple substrates are used, increasing the OLR tends to result in a transient accumulation of VFAs due to methanogens not being able to keep up with the rate of acidogenesis (Rajeshwari *et al.*, 2000; Chen *et al.*, 2008).

Lastly, the sludge loading rate (SLR) is defined as the mass of COD fed per mass of volatile suspended solids (VSS) per day, and is a parameter particularly important for high-rate AD reactors (as explained in section 2.4.3). The relationship between the SLR, OLR and average VSS concentration in the reactor is shown in Equation 6.

$$SLR = \frac{OLR\left(\frac{kgCOD}{m^3 \cdot day}\right)}{VSS\left(\frac{kgVSS}{m^3}\right)} \qquad \text{Equation 6}$$

2.3.5 Nutrient requirements

To perform adequately, it is essential that the microbial groups receive an adequate amount of nutrients, which are often lacking in industrial wastewaters (Speece, 1983). These nutrients include N, P, undissociated H_2S (at levels lower than are toxic), Ca, Mg, Fe, Co, Ni, Mo, and Se (Speece, 1983).

Supplementation of the nutrient content of wastewaters is essential in the cases where these nutrients are lacking (Speece, 1983; Sperling and Chernicharo, 2005). To determine the quantities with which to supplement a deficient wastewater, Sperling & Chernicharo (2005) advise that the minimum nutrient content be adjusted to that required for the formation of the actual microbial cells. If the composition of the cells, the growth yield and substrate concentration are known, then the concentration of nutrients can be calculated according to Equation 7 (Sperling and Chernicharo, 2005).

$$Nutrient\ conc.(mg/L) = COD_{feed} \cdot Y \cdot \frac{TSS}{VSS} \cdot N_{bac} \qquad \text{Equation 7}$$

where

$Nutrient\ conc.$ is the minimum concentration of the specific nutrient to be calculated (mg/L)

COD_{feed} is the COD concentration of the influent (g-COD/L)

Y is the yield of biomass from the influent COD, and is taken to be 0.15 g-VSS/g-$COD_{removed}$ for carbohydrate-rich wastewaters

$\frac{TSS}{VSS}$ is the ratio of TSS/VSS typical of anaerobic sludge, and is taken to be 1.4 g-TSS/g-VSS

N_{bac} is the typical concentration of the nutrient in the methanogens

Values of N_{bac} are listed in in Table 2-1 which can be used for this calculation.

Table 2-1: Elemental composition of methanogens (Sperling and Chernicharo, 2005)

Macronutrients	Concentration (mg/g-TSS cells)	Trace nutrients	Concentration (mg/g-TSS cells)
N	65	Fe	1.8
P	15	Ni	0.1
K	10	Co	0.075
S	10	Mo	0.06
Ca	4	Zn	0.06
Mg	3	Mn	0.02
		Cu	0.01

However, in the case of high-rate systems where exogenous polymeric substances (EPS) can be produced in significant quantities, this can greatly increase the amount of N required (Sam-Soon *et al.*, 1990). The EPS produced in high-rate AD systems roughly contains an equal concentration of proteins and polysaccharides (Vanderhaegen *et al.*, 1992). Sam-Soon et al. (1990) found in the digestion of a synthetic glucose wastewater that 20 mg-N/g-COD was required to prevent granulation and methanogenesis from being adversely affected.

2.4 UASB reactors for wastewater AD

2.4.1 Wastewater AD

As stated in Section 2.3.4, when dealing with anaerobic digestion (AD) of wastewater (WW) it is important to use an appropriate reactor type that selectively retains biomass within the reactor (Speece, 1983; van Lier *et al.*, 2015). Various reactor types such as the anaerobic contact reactor, anaerobic filter, anaerobic baffled reactor, upflow anaerobic sludge bed (UASB) reactor and fluidised bed reactor have been developed from the 1960s onwards to achieve this goal of enhanced biomass retention (van Lier *et al.*, 2015). Of these reactor types, the UASB reactor technology has dominated in full-scale installations for both domestic (Chernicharo *et al.*, 2015) and industrial (van Lier *et al.*, 2015) WW treatment. UASB reactors were found to be the third most prevalent technology by number, and fourth by design flow, for municipal WW treatment in Latin American countries (Noyola *et al.*, 2012), and they constitute over 90% of the WW AD systems used for industrial WW treatment (van Lier *et al.*, 2015).

As mentioned in Section 1.1, the objectives of WW treatment are to remove organic compounds (measured as COD), nutrients, micro-contaminants and pathogens depending on whether these contaminants are present in the WW. AD as a WW treatment process is used for the removal of the organic compounds through the conversion of the influent COD into CH_4 which separates from the WW spontaneously due to its low solubility (Kleerebezem *et al.*, 2015). A schematic depicting the fate of COD fed to a UASB reactor is shown in Figure 2-2.

As shown in Figure 2-2, COD associated with the organic compounds in the WW is converted to biomass and CH_4. Because the biomass in a UASB is retained in the form of granular sludge, the COD associated with the growth of the granular sludge accumulates in the sludge bed. The balance of the COD either leaves with the effluent stream as unconverted substrate, or as CH_4 in the biogas. The sludge production in AD systems is low – usually around 0.15 g-VSS/g-$COD_{removed}$ and 0.05 g-VSS/g-$COD_{removed}$ for digestion of carbohydrates and VFA respectively (Sperling and Chernicharo, 2005). The ratio of COD/VSS for anaerobic sludge is usually around 1.4-1.5 (Sam-Soon *et al.*, 1987), thus yields of CH_4 of around 0.8 g-COD_{CH4}/g-$COD_{removed}$ and >0.9 g-COD_{CH4}/g-$COD_{removed}$ is expected for carbohydrate and VFA digestion respectively. However, Sam-Soon et al. (1987) measured a sludge yield of 0.09 g-VSS/g-$COD_{removed}$ for treatment of a carbohydrate-based WW, with a COD/VSS ratio of 1.23 g-COD/g-VSS. In this case, a sludge yield of 0.11 g-$COD_{biomass}$/g-$COD_{removed}$ was attained, with a corresponding CH_4 yield of 0.89 g-COD_{CH4}/g-$COD_{removed}$.

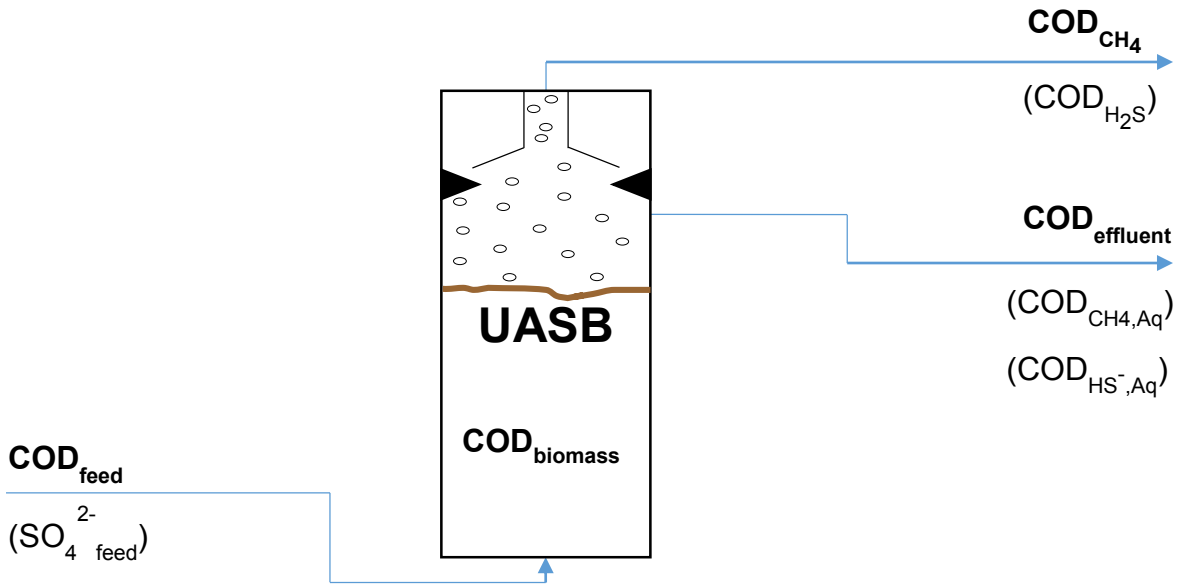

Figure 2-2: Schematic of the fate of the COD sources and sinks in a UASB reactor

Variations on this basic CH_4 yield estimate arise when SO_4^{2-} is present in the WW in significant quantities or the WW is dilute. As mentioned in Section 2.3.3, sulphate-reducing bacteria reduce sulphate, consuming 0.67 g-COD/g-SO_4^{2-} removed. This can result in a significantly lower yield of CH_4 from AD of SO_4^{2-}-containing WW (Singh and Viraraghavan, 1998). Some of this sulphide produced may remain dissolved in the effluent stream depending on the amount of biogas produced due to the effect of the biogas stripping out the sulphide (Barrera *et al.*, 2014). Furthermore, as documented in Section 2.3.1, in the treatment of dilute WW the presence of dissolved CH_4 in the effluent can constitute a significant portion of the total CH_4 produced (Singh and Viraraghavan, 1998; Kim *et al.*, 2011; Ferrer *et al.*, 2012; Chernicharo *et al.*, 2015; Kleerebezem *et al.*, 2015). Domestic WW are often dilute (Seghezzo *et al.*, 1998), and it is common for 30-40% of the CH_4 produced to remain dissolved in the effluent (Chernicharo *et al.*, 2015).

2.4.2 Properties of sludge granules

The UASB reactor was developed in the 1970s (Lettinga *et al.*, 1980), and its success relies predominantly on the formation of well-granulated sludge (Chui *et al.*, 1993; Fukuzaki *et al.*, 1995; Schmidt and Ahring, 1996; Hulshoff Pol *et al.*, 2004; van Lier *et al.*, 2015). Granular sludge refers to aggregates of microorganisms that form spontaneously under certain conditions. These aggregates are usually somewhat spherical, with a diameter of 0.14 to 5 mm, and an inorganic mineral content of 10 to 90% depending on the wastewater (feed) composition (Schmidt and Ahring, 1996). The aggregates are comprised of AD microorganisms immobilised in a matrix of exogenous polymeric substances (EPS), which is usually made up of polysaccharide and protein (in roughly equal proportions) (Vanderhaegen *et al.*, 1992), as well as humic substances (Wang *et al.*, 2017). The main inorganic components of granules are usually Ca, K and Fe (Schmidt and Ahring, 1996). Reported buoyant densities of granules are usually in the range of 1.04-1.08 g/mL, but as high as 1.4 g/mL has been reported (Schmidt and Ahring, 1996). Granular sludge typically exhibits settling velocities of 18-60 m/h, but values as high as 100 m/h have been reported (Schmidt and Ahring, 1996; Hulshoff Pol *et al.*, 2004). With superficial upflow velocities of less than 2 m/h generally used in full-scale installations this high settling velocity allows for an almost complete decoupling of the solids retention time (SRT) from the hydraulic retention time (HRT) (Hulshoff Pol *et al.*, 2004).

Furthermore, well-granulated sludge is particularly active, with typical specific methanogenic activities (SMA) of 0.5-2 g-COD_{CH4}/g-VSS.day (Hulshoff Pol. *et al.*, 1982; Schmidt and Ahring, 1996). The highest SMA demonstrated in a UASB reactor found was 2.2 kg-COD_{CH4}/kg-VSS.day in the digestion of an artificial WW consisting of sucrose and milk powder (Fang and Chui, 1993). This contrasts with flocculent digested sewage sludge from continuous stirred tank type digesters, which usually has a

SMA of 0.04-0.1 kg-COD_{CH4}/kg-VSS.day (Hulshoff Pol. *et al.*, 1982; Hulshoff Pol *et al.*, 1983). This ability for a well-operated UASB reactor to produce and retain high concentrations of highly active biomass allows for high OLR (above 50 kg-COD/L.day) to be accommodated (Hulshoff Pol *et al.*, 1983).

2.4.3 Conditions favouring granulation

The conditions required for granule formation have been the subject of much research over the past 35 years. Microbial growth in UASB reactors tends to result either in the successful formation of granules, or the production of a more flocculent-type sludge that is prone to flotation (Hulshoff Pol. *et al.*, 1982; Fukuzaki *et al.*, 1995; Ghangrekar *et al.*, 2005; Wang *et al.*, 2017). It is therefore important to ensure the correct conditions are applied for the attainment of granular sludge which demonstrates the beneficial characteristics described in Section 2.4.2. Although theories on the exact mechanism(s) behind granule formation are still in development, many factors have been identified as benefitting or interfering with the process of granule formation (Hulshoff Pol *et al.*, 2004). These factors are elaborated on below.

Optimal growth conditions

It has been reported by many researchers that granules form under the conditions beneficial for the growth of the aceticlastic methanogens (Hulshoff Pol *et al.*, 1983; Wiegant and de Man, 1986), in particular the species *Methanosaeta concilii* (Hulshoff Pol *et al.*, 2004). These conditions include provision of an adequate amount of substrate (carbon-source), nutrients and the correct pH. The pH range in which granulation occurs is the same as the acceptable pH for the growth of *Methanosaeta concilii* which is between 6.5-7.8 (Hulshoff Pol *et al.*, 1983). Essential nutrients also need to be present in sufficient quantities to ensure that growth is not limited (Hulshoff Pol *et al.*, 1983). It must be noted that the N-requirement of UASB reactors (and potentially other high-rate AD reactors) can be significantly higher than that required for incorporation into cell protoplasm (cell synthesis) (Sam-Soon *et al.*, 1990). This is due to the consumption of N for the production of the proteinaceous component of the EPS, and it has been estimated that 0.02 mg-N/mg-COD_{feed} is required to satisfy this consumption for a carbohydrate-based feed (Sam-Soon *et al.*, 1990). Sam-Soon et al. (1990) found that if the N supplied is below 0.02 mg-N/mg-COD_{feed} significant quantities of H_2 accumulated in the biogas, and if dropped below the concentration required for cell synthesis – around 0.0086 mg-N/mg-$COD_{influent}$, acidogenesis was also affected. In addition to this, consumption of this N can affect the digester pH due to the consumption of alkalinity in an equimolar ratio with N (Sam-Soon *et al.*, 1990), thus additional alkalinity may be required if the WW is not well-buffered (or does not contain intrinsic alkalinity in the organically-bound N (Ekama *et al.*, 2015). Sam-Soon & Wentzel (1991) found by trial and error that an alkalinity addition of 1.6 g-$CaCO_3$/mg-COD (added as 2.688 g-$NaHCO_3$/g-COD) buffered their carbohydrate-based wastewater (with negligible alkalinity) sufficiently to prevent the minimum pH in the sludge bed from dropping below 6.6. However, it has been found that a high NH_4^+ concentration of 1000 mg-NH_4^+-N/L inhibited granule formation and propionic degradation, thus it is important to not over-supply N (Hulshoff Pol *et al.*, 1983).

Lastly, it is necessary to ensure that the methanogens are fed sufficiently to prevent starvation (Hulshoff Pol *et al.*, 1983; Ten Brummeler *et al.*, 1985; Schmidt and Ahring, 1996; Ghangrekar *et al.*, 2005). Hulshoff Pol et al. (1983) found that granulation would only occur in reactors fed with a SLR above 0.6 kg-COD/kg-VSS.day when a mixture of VFA was used as the substrate.

Appropriate start-up regime

The type and SMA of the sludge developed depends on the loading rates applied during start up (Ghangrekar *et al.*, 2005), therefore emphasis has been placed on providing the correct conditions during reactor start up (Hulshoff Pol. *et al.*, 1982). Hulshoff Pol et al. (1983) identified three phases of sludge growth when using 12-15 g-VSS/L digested sewage sludge as an inoculum. In the first phase, low OLR were applied (0.5-2 g-COD/L.day), causing the sludge bed to expand due to gas production and growth of filamentous organisms. In the second phase, the decreased HRT results in an increased OLR (2-5 kg-COD/m^3.day) and washout of around 70-85% of the VSS content of the bed due to its flocculent nature (Hulshoff Pol *et al.*, 1983). Phase three is marked by the recovery of the sludge bed VSS, where biomass growth is greater than washout, and occurred when the OLR was further increased

above 3-5 g-COD/L.day. It is necessary to start the reactor up at relatively low OLR and SLR to prevent both overloading of the sludge (which could result in VFA accumulation) as well as to ensure that enough VSS from the inoculum is retained during the washout phase (Hulshoff Pol *et al.*, 1983). The latter issue regarding retention of enough inoculum to prevent complete washout is especially an issue when using digested sewage sludge as an inoculum (Hulshoff Pol *et al.*, 1983). This issue can be addressed somewhat by the inclusion of some granular sludge in the inoculum, but it was found that the addition of granular sludge to the inoculum did not result in the formation of new granules taking place sooner (Hulshoff Pol *et al.*, 1983).

Another issue that can arise is the formation of bulking type sludge that is prone to flotation during periods of underloading or substrate limitation (Hulshoff Pol. *et al.*, 1982; Ten Brummeler *et al.*, 1985; Schmidt and Ahring, 1996). It is therefore important to ensure that the low loading conditions provided during phase 1 described above (where filamentous organisms grow to form a bulking type sludge) are not applied for too long. Ghangrekar et al. (2005) found that the OLR and SLR should be in the ranges of 2.0-4.5 kg-COD/m^3.day and 0.1-0.25 kg-COD/kg-VSS.day respectively to prevent overloading or underloading the UASB during start up when using sucrose as the carbon source. Hulshoff Pol et al. (1983) reported that superficial upflow velocities of around 1 m^3/m^2.day and sludge loading rates of above 0.6 kg-COD/kg-VSS.day are necessary for granulation using a mixture of VFA as the carbon source.

Granulation has been successfully attained using inoculum concentrations of roughly 8-15 kg-VSS/m^3 with digested sewage sludge as the inoculum (Hulshoff Pol *et al.*, 1983; Fang and Chui, 1993). Granulation is usually observed between 25-50 days after start-up if the correct procedure is followed (Hulshoff Pol. *et al.*, 1982; Ghangrekar *et al.*, 2005).

Hydrodynamic conditions

The hydrodynamic conditions within the reactor have been found to play an important role in the granulation process (Vanderhaegen *et al.*, 1992; Ghangrekar *et al.*, 2005; Wang *et al.*, 2017). It is important to keep the upflow velocity in a desirable range to maintain favourable hydrodynamic conditions, such that short-circuiting and dead zones are minimised (Peña *et al.*, 2006). The hydrodynamic conditions result in the 'selection pressure' exerted on the system, where higher upflow velocities result not only in more turbulent conditions, but also in the elution of smaller sludge particles (Hulshoff Pol *et al.*, 2004). Control of the superficial upflow velocity therefore provides the ability to select for the heavier sludge particles to remain within the reactor, thus preventing growth of finely dispersed sludge by limiting growth to a smaller number of nuclei (Hulshoff Pol *et al.*, 2004). However, Vanderhaegen et al. (1992) found that although the presence of mixing and a shear force was essential for granule growth, this mixing need not arise from an upflow of liquid and need not remove smaller particles from the reactor. Wang et al. (2017) recently investigated the effect of various mixing regimes on the sludge flotation potential (SFP) of the sludge from a predominantly sulphidogenic (where COD is used for the purpose of sulphate reduction instead of CH_4 production) UASB treating saline sewage. The SFP is quantified using a test involving flotation of sludge granules using rising gas, and provides a measurement of the likelihood of sludge granules becoming buoyant and causing the sludge bed to float (Wang *et al.*, 2017). An SFP of below 20% indicates a very low likelihood of sludge flotation (Wang *et al.*, 2017). Wang et al. (2017) investigated the effects of mixing intensity and methods of mixing (hydraulic, mechanic and pneumatic), and found that the SFP was reduced from roughly 75% for the original sludge to 11%, 19% and 31% after 30 days of operation at shear rates of 4 to 6 s^{-1} for pneumatically-, mechanically- and hydraulically-mixed reactors respectively. Hulshoff Pol et al. (1989) found that in methanogenic systems, biogas productivities above 1 $m^3/m^3_{reactor}$.day (corresponding to an OLR of 2-3 kg-COD/m^3.day if the COD is mostly degraded) provided enough turbulence to keep the reactor well-mixed.

Polyvalent cations

As already noted, the inorganic content of granules can constitute a significant portion of their mass. Of these inorganic compounds, polyvalent cations are thought to provide linkages between the microorganisms and the EPS they form (Fukuzaki *et al.*, 1995). The most important polyvalent cation is thought to be Ca^{2+}, which is often found in significant quantities in granules and has been found to

improve their settling qualities (Lettinga *et al.*, 1980; Fukuzaki *et al.*, 1995; Yu *et al.*, 2001). Mahoney et al. (1987) found that granules grown under high Ca^{2+} conditions (100 mg-Ca^{2+}/L) were larger and over three times more settleable than those grown without Ca^{2+} supplementation. Hulshoff Pol et al. (1983) found that more *Methanosarcina spp.* were found in granules grown under high Ca^{2+} concentrations. Vanderhaegen et al. (1992) reported that Ca^{2+} concentrations of above 30 mg-Ca^{2+}/L were beneficial to granule formation. The presence of Mg^{2+} has also been reported as beneficial to granulation (Ahring *et al.*, 1993). Ahring et al. (1993) found experimentally that granulation only occurred after the concentrations of Mg^{2+}, NH_4^+, K^+ and PO_4^{3-} were increased. Of these nutrients, the effect of varying Mg^{2+} concentrations were investigated further. It was found that neglecting to add Mg^{2+} at 0.5 mmol/L (12 mg-Mg^{2+}/L) caused the granules to become less dense and contain more rod-shaped bacteria (Ahring *et al.*, 1993). However, high Mg^{2+} concentrations (30 and 100 mmol/L) caused disintegration of the granules (Ahring *et al.*, 1993). Also, Fe and K are usually the second most abundant inorganic component of granules after Ca (Schmidt and Ahring, 1996), thus it is possible that these compounds are also required in excess of the requirements for only cell synthesis.

Wastewater composition

The WW composition is also documented to play an important role in sludge granulation (Hulshoff Pol *et al.*, 1983; Wiegant and de Man, 1986; Sam-Soon *et al.*, 1987). 'Acidogenic' substrates such as sugars result in a greater production of EPS than do purely acetogenic/methanogenic feedstocks (VFA mixtures) (Schmidt and Ahring, 1996). Similarly, degradation of 'high-energy' COD (sugars) results in a greater granule yield as well as better quality granules (Vanderhaegen *et al.*, 1992). Vanderhaegan et al. (1992) also report that the presence of a high protein content in the feed adversely affects granulation, as does NH_4^+ at concentrations above 1500 mg-NH_4^+/L and at pHs above 7.4. Suspended solids present in the feed may adversely affect granulation through displacement of sludge (Lettinga and Hulshoff Pol, 1991) or through provision of too many support particles for microbial growth, leading to dispersed growth that is washed out of the reactor (Hulshoff Pol *et al.*, 2004). Also of note is that compounds inhibitory to methanogenesis affect granulation (Hulshoff Pol *et al.*, 1983), although granular sludge is less susceptible to inhibition than flocculent sludge (Morvai *et al.*, 1992). Finally, the WW composition affects the need for alkalinity supplementation to maintain the pH in the correct range. This is due to the generation and consumption of alkalinity both from solubilisation (hydrolysis) of the feedstock organic compounds and from their conversion in growth-related processes (Ekama *et al.*, 2015), and is discussed in greater detail in Section 2.5.4. If alkalinity is generated during digestion, the recycling of effluent can be beneficial to lower the influent alkalinity requirements (Sam-Soon *et al.*, 1991; Chui *et al.*, 1994). However, at loading rates near the maximum that a specific UASB system can handle, a high recycle ratio (ratio of recycle flow rate to influent flow rate) can magnify upsets caused by an accumulation of VFA in the effluent (Sam-Soon *et al.*, 1991) because the sludge bed is fed both the influent COD as well as the VFA in the recycle.

2.4.4 Granulation theories

Many theories exist on the mechanisms responsible for granule formation (Hulshoff Pol *et al.*, 2004). Although granule formation has been observed in acidification (purely acidogenic) and denitrification reactors, the greater stability of methanogenic granules indicates that a different mechanism is responsible for the formation of methanogenic granules than that for acidogenic or denitrification granules (Hulshoff Pol *et al.*, 1983). Many of these theories propose that *Methanosaeta concilii* is responsible for initiating granulation through the formation of filaments that entwine other microorganisms (Hulshoff Pol *et al.*, 2004). The production of EPS is also recognised as playing a role in immobilising other microbes. Further, the filaments of *Methanosaeta concilii* are thought to stabilise the resulting granules (Hulshoff Pol *et al.*, 2004).

In contrast with this, a very specific theory on the mechanisms of granulation was proposed by Sam-Soon et al. (1987) in which the hydrogenotrophic methanogen *Methanobacterium* Strain *AZ* is hypothesised to be responsible for granule formation. According to Sam-Soon et al. (1987), polypeptide chains secreted by the H_2-utilising *Methanobacterium* Strain *AZ* are responsible for binding other cells into granules. Furthermore, *Methanobacterium* Strain *AZ* only excretes polypeptides at near-neutral pH and high H_2 partial pressure (high substrate concentration/growth conditions) with a limited amount of

cysteine (this organism's only essential amino acid) and an abundance of ammonia (to stimulate over-production of polypeptides) (Sam-Soon *et al.*, 1987). In this theory, these conditions are likely to produce a high sludge yield and lower CH_4 yield, since a significant proportion of the COD utilised contributes to polypeptide production and the organism does not require as much energy for polypeptide production as it does for cell growth (Sam-Soon *et al.*, 1987). Their hypothesis was supported by noting a 50% decrease in sludge yield when 12.2 mg-cysteine was included in the feed (Sam-Soon *et al.*, 1987). In this study a particularly high sludge yield of 0.36 g-VSS/g-$COD_{removed}$ was found, with a low COD/VSS ratio of 1.23 (versus 1.4-1.5 g-COD/g-VSS usually found in anaerobic sludge), indicating that much of the sludge is EPS (Sam-Soon *et al.*, 1987). This theory precludes the possibility for granules to form from the degradation of substrates that do not form H_2, such as acetate. However, evidence against this theory has been found in numerous studies (Morvai *et al.*, 1990, 1992; Ahring *et al.*, 1993; Chen and Lun, 1993) where granulation occurred with acetate as the sole carbon source. Furthermore, the requirement of high H_2 partial pressure implies the need for plug-flow conditions due to the low H_2 partial pressure requirements of the acetogenic bacteria. However, it is unlikely that such a steep profile in the H_2 partial pressure is generated in most UASB systems due to the mixing caused by biogas evolution (Hulshoff Pol *et al.*, 2004). Lastly, Moosbrugger et al. (1990) found granulation to occur using casein as the substrate. Casein has been reported to contain cysteine at 4.6 g-cysteine/kg-protein, thus this further contradicts the hypothesis proposed by Sam-Soon (1987) as the complete theory on granulation.

Another mechanism proposed for granulation considers the thermodynamics of the adhesion of cells to one another or their substrate (Hulshoff Pol *et al.*, 2004). Schmidt & Ahring (1996) describe a four-stage model, originally proposed for biofilm formation by van Loosdrecht & Zehnder (1990), in which cells are transported to the surface of a support material (inert particle, or particulate substrate), to which they adhere reversibly through physicochemical forces. Irreversible attachment then occurs as a result of appendages or EPS formed by the cell, after which they begin to multiply and form granules (Hulshoff Pol *et al.*, 2004). This thermodynamic model was taken further by Thaveesri et al. (1995), who consider the adherence of cells to a support based on the Gibbs Free Energy of adsorption. They found that the maximum free energy of adhesion is obtained when the liquid surface tension is sufficiently high or low (Thaveesri *et al.*, 1995). The hydrophobicity or hydrophilicity of AD microorganisms has been measured using the contact angle technique, the results of which are that most acidogenic bacteria are found to be hydrophilic while methanogens are hydrophobic (Hulshoff Pol *et al.*, 2004). The surface tension model of Thaveesri et al. (1995) predicts that at higher surface tensions (above 55 mN/m) the adhesion of hydrophobic cells is favoured, while at lower surface tensions (below 50 mN/m) the adhesion of hydrophilic cells is favoured. Granules are often observed to be multi-layered where substrates more complex than VFA are used (Vanderhaegen *et al.*, 1992; Fang *et al.*, 1994; Thaveesri *et al.*, 1995). Under such conditions, the exterior of the granules are often richer in hydrophilic acidogens (Vanderhaegen *et al.*, 1992; Fang *et al.*, 1994), which act as 'solid-phase emulsifiers' (Hulshoff Pol *et al.*, 2004). This enhances process stability since tiny gas bubbles are less adhesive to hydrophilic surfaces, thus preventing the likelihood of sludge flotation (Thaveesri *et al.*, 1995).

The results and analysis thereof from the recent study by Wang et al. (2017) into the effects of mixing method (pneumatic, hydraulic and mechanical) and mixing intensity on the granule properties of a sulphidogenic reactor treating synthetic saline sewage show promising insights into controlling the granulation process. Wang et al. (2017) state that sludge flotation is an issue that is often experienced during normal operating conditions and has been linked to sludge properties such as high hydrophobicity, low surface charge, a high ratio of proteins to polysaccharides in the EPS generated and the presence of gas pockets inside granules formed after cells lyse. They classify EPS as either tightly bound to the cell surface (TB-EPS), or loosely-bound EPS (LB-EPS) that forms an indiscrete layer on the granule surface (Wang *et al.*, 2017). In their experiments, four mixing intensities (shear rates between ~0.8-5 s^{-1}) were investigated for each mixing method where each mixing intensity was investigated for a 45 day period (Wang *et al.*, 2017). Wang et al. (2017) found that the ratio of LB-EPS/TB-EPS decreased from 0.5-0.8 to 0.12-0.25 by increasing the shear rate. Furthermore, they found that that the quantity of proteins (PN) and polysaccharides (PS) found in the LB-EPS decreased significantly with increasing mixing intensity (on a basis of total sludge VSS), while the protein and polysaccharide content of the TB-EPS increased slightly with increasing mixing intensity. Moreover, they found that the overall ratio of protein:polysaccharide of the granules decreased from 4-8 mg-

PN/mg-PS to 2-4 mg-PN/mg-PS (Wang *et al.*, 2017). They note that in studies on denitrifying systems it has been observed that a PN/PS ratio above 5 increases the potential of sludge flotation incidents (Wang *et al.*, 2017). Wang et al. (2017) also found that granule size increased with increasing mixing intensity in the range of shear rates investigated, and that hydraulic, mechanical and pneumatic methods of mixing formed the smallest (116 ± 30 um), intermediate (164 ± 18 um) and largest (191 ± 10 um) sized granules respectively (Wang *et al.*, 2017). Increasing mixing intensity also resulted in the granule hydrophobicity dropping from 60-67% to 33-40% (Wang *et al.*, 2017). Wang et al. (2017) also found that the surface charge of the granules decreased with increasing mixing – most notably the reactor with pneumatic mixing – resulting in a lower affinity for gas bubbles to attach to the granule surface. The sludge viscosity decreased in the pneumatically mixed and mechanically mixed reactors with increasing mixing intensity, but did not follow a trend for the hydraulically mixed reactor (Wang *et al.*, 2017). They found the SFP of the granules decreased from ~75% characteristic of the inoculum to 11%, 19% and 31% for the pneumatically-mixed, mechanically-mixed and hydraulically-mixed reactors respectively (Wang *et al.*, 2017). These results reported were found to be relatively stable from 30 days into the experiment, indicating that sludge characteristics could be enhanced in a short time period.

Wang et al. (2017) theorise that inadequate mixing can lead to dead zones and short-circuiting, resulting in a loss of even substrate distribution and mass transfer, as well as overgrowth of EPS (Wang *et al.*, 2017). This can cause starvation conditions for the granules in dead zones, resulting in the consumption of PS-EPS, as well as allowing the LB-EPS to remain intact (Wang *et al.*, 2017). The increased ratio of PN-EPS to PS-EPS can cause sludge flotation, and the increased amount of LB-EPS causes bulking-type sludge which can trap gas bubbles (Wang *et al.*, 2017). LB-EPS is more water retentive than TB-EPS, causing a bulkier sludge of higher viscosity, while TB-EPS does not retain much water and creates a less-viscous sludge bed environment (Wang *et al.*, 2017). Furthermore, the carboxyl and phosphate groups in PS-EPS carry a negative charge, while the amino groups in PN-EPS carry a positive charge (Wang *et al.*, 2017). This suggests that the surface charge and hydrophobicity are dependent on the type of EPS present (Wang *et al.*, 2017). In their statistical analysis of the relationships between sludge properties and SFP, they found a negative correlation between particle size and the SFP (Wang *et al.*, 2017). This could be explained by the lower likelihood of a larger and thus heavier particles from being buoyed by fine gas bubbles (Wang *et al.*, 2017). Sludge hydrophobicity and surface charge were also found to be strongly related to the SFP, which can be explained by the fact that gas bubbles in bioreactors have a negative surface charge (Wang *et al.*, 2017). However, sludge viscosity was not as strongly related to SFP. The LB-EPS that causes the high viscosity has a gel-like sticky texture, and can trap gas bubbles and aggravate sludge flotation (Wang *et al.*, 2017). These results are interesting in that they suggest mixing intensity and method affect EPS structure (change in ratio of TB-EPS:LB-EPS) and composition (change in PN:PS ratio), which affected the granule properties in ways that decreased the SFP (Wang *et al.*, 2017).

2.5 Modelling of AD

2.5.1 General modelling protocol

Four characteristics of a good model are simplicity, description of the most relevant cause-effect relationships, the ability for parameters to be easily identified from experimental data, and the ability to accurately predict the performance under reasonably similar conditions (Donoso-Bravo *et al.*, 2011). According to Donoso-Bravo et al. (2011) the following procedure is generally followed when building a model:

1. Selection of parameters should start with bearing in mind the objectives for the model (i.e. the level of detail that will be required by the model)
2. Derivation of the mathematical expressions to be used
3. Implementation in a maths software program through coding such as using Fortran, C or Matlab
4. Sensitivity analyses can then be performed to determine the most and least influential parameters
5. Checking the experimental data for errors and outliers
6. Formulating and minimising an objective cost function which serves as a measure of the disagreement between the experimental data and calculated values

7. Validation using the experimental data used to determine the parameters
8. Cross validation using other experimental data to test the prediction power of the model

In this text, the term 'conceptual model' refers to the choice of biological and physicochemical processes and species that are included, as well as the interactions (relevant mass/energy flows) between these processes. In light of the above procedure, building the conceptual model is synonymous with 'selection of parameters', in which the processes and species relevant to the model aims are chosen for inclusion. Derivation of the mathematical expressions (step 2) describing the flows of compounds can be developed using mass balances and process stoichiometry, as well as kinetic equations and the kinetic parameters (McCarty and Mosey, 1991).

2.5.2 Development of AD models

Development of AD models began in the early 1970s to satisfy the need to improve the efficiency of the AD process (Donoso-Bravo *et al.*, 2011), as well as to aid in the development of process control strategies (Lyberatos and Skiadas, 1999). As noted in Section 2.2, the AD process can be broken down into four steps. AD models have evolved from describing only the rate-limiting step, to identifying VFAs as a key intermediate and describing their production, and finally towards more sophisticated model frameworks which incorporate more processes and detailed kinetics (Donoso-Bravo *et al.*, 2011).

Gujer & Zehnder (1983) published a description of their conceptual model in which particulate COD in the form of proteins, carbohydrates and lipids is hydrolysed to form amino acids, sugars and fatty acids respectively. The sugars and amino acids are then fermented and the fatty acids anaerobically oxidised to form intermediate VFA, acetate and hydrogen. The intermediate-length VFA are oxidised anaerobically to form more acetate and hydrogen, which are then utilised by aceticlastic and hydrogenotrophic methanogens to form CH_4 and CO_2 (Gujer and Zehnder, 1983). Gujer & Zehnder's conceptual model of 1983 includes the six conversion processes described above, which are mediated by five independent groups of microorganisms, and still forms the basic structure on which the International Water Association AD Model No 1 (ADM1) (Batstone *et al.*, 2002) – the most widely-recognised model at present – is based. However, ADM1 has grown in complexity to include 24 (bio)chemical species and 19 conversion processes, as well as physico-chemical processes which describe the non-biologically-mediated transformations (Batstone *et al.*, 2002; Donoso-Bravo *et al.*, 2011). A schematic of ADM1 is shown in Figure 2-3.

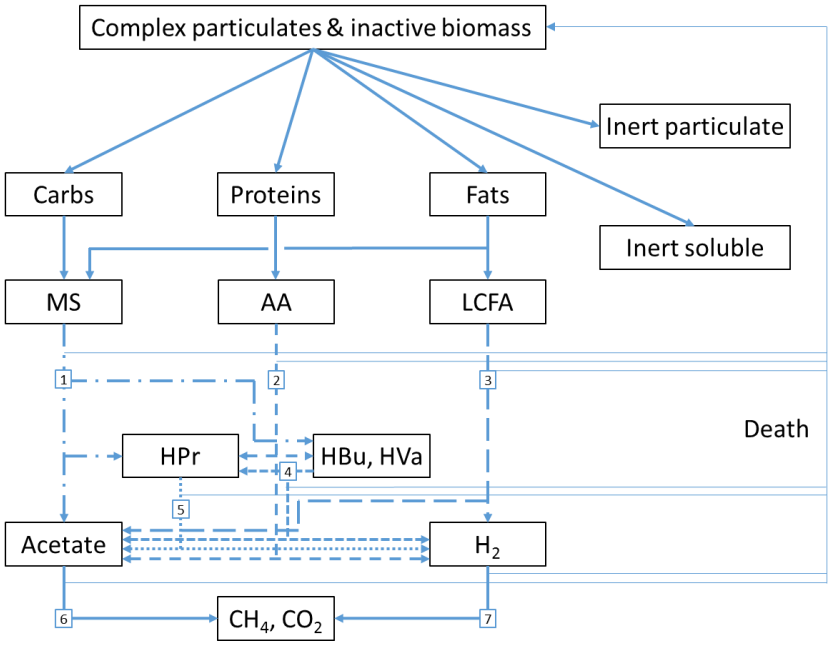

Figure 2-3: The conceptual model of the biochemical processes as implemented in ADM1 (Batstone *et al.*, 2002): (1) acidogenesis of monosaccharides, (2) acidogenesis of amino acids, (3) acetogenesis of LCFA (4) acetogenesis of butyrate and valerate, (5) acetogenesis of propionate, (6) aceticlastic methanogenesis, (7) hydrogenotrophic methanogenesis

This level of complexity in the ADM1 framework has been criticised – especially due to the difficulty in measuring the key chemical species in experiments (Donoso-Bravo *et al.*, 2011), but it also provides scope to customise or simplify the existing framework to suit the needs of the modeller (Hassam *et al.*, 2015).

2.5.3 SDM-3P model

The University of Cape Town (UCT) Water Research Group (WRG) developed and, in 2005, published an AD model that was originally named UCTADM1 (Sötemann et al. 2005) aimed at modelling the digestion of sewage sludge. This model is also based upon the flowsheet developed by Gujer & Zehnder (1983) but includes some modifications (Sötemann et al. 2005):

1. The hydrolysis of complex materials acts upon one group of compounds defined by the empirical formula $C_xH_yO_zN_a$ (e.g. for glucose x = 6, y = 12, z = 6 and z = 0). This is in contrast with the original flowsheet which describes three complex groups of compounds requiring hydrolysis, namely proteins, carbohydrates and lipids.
2. Because the hydrolysis process acts upon one generic compound $C_xH_yO_zN_a$, only one hydrolysis product is included in UCTADM1, namely glucose (as opposed to amino acids, monosaccharides and fatty acids). This choice of substrate characterisation and single hydrolysis product is convenient because it is generally easier to determine the values of x, y, z, and a in the molecular formula than the concentration of proteins, carbohydrates and lipids experimentally. Furthermore, glucose is a convenient intermediate due to the knowledge existing around the acidogenesis of glucose to form VFA, and is of little consequence due to the fact that acidogenesis is unlikely to ever be rate-limiting. Glucose therefore never accumulates, and acts as an intermediate between the complex generic molecule requiring hydrolysis and VFA.
3. Anaerobic oxidation of LCFA is not relevant due to UCTADM1 not including fats as a discrete feedstock.
4. The only VFAs included in UCTADM1 are acetate and propionate, with the distribution of acetate and propionate formed being regulated by the hydrogen partial pressure. Butyrate and valerate are not included due to these VFAs not being found in AD of sewage sludge, even during digester failure.

By characterising the feedstock differently, and including only two VFAs, the UCTADM1 model describes only 10 biological processes and 14 species, representing a significantly simpler model than ADM1. However, because feedstocks are characterised only by the phase in which they are present (particulate or dissolved) and their empirical molecular formula, a model developed under this conceptual framework is less generically applicable than one developed using ADM1 (in which the feedstocks are described in greater detail). Indeed UCTADM1 was developed specifically for the AD of sewage sludge.

This model was then extended to better cater for the context of the conventional domestic wastewater treatment plant, where the feedstocks to the AD include primary sludge (PS) and waste activated sludge (WAS) (Brouckaert *et al.*, 2010). The model, now called SDM-3P, is documented online (Brouckaert *et al.*, 2010; Ikumi *et al.*, 2012; Haile *et al.*, 2015) and has been implemented in the WEST wastewater treatment simulation software package. The major extensions are the inclusion of the element phosphorus, mineral precipitation, further classification of soluble and particulate components into biodegradable and non-biodegradable fractions, and inclusion of microbial species found in biological phosphorus removal systems (Brouckaert *et al.*, 2010). The rationale for doing so revolves around the fact that the phosphate subsystem affects the digester pH, and that precipitation of the phosphate containing minerals $MgNH_4PO_4.6H_2O$ (struvite), $MgKPO_4.6H_2O$ (K-struvite) and $Ca_3(PO_4)_2$ affects the dissolved phosphate concentration (Brouckaert *et al.*, 2010). The empirical formula used to define complex organics in this model was therefore extended to have the generic composition $C_xH_yO_zN_aP_b$.

The SDM-3P model predicts the digester pH by formulating the weak acids and bases in terms of their ion concentrations (ion speciation) (Brouckaert *et al.*, 2010). Although total species concentrations (e.g. for CO_3 = CO_3^{2-} + HCO_3^- + H_2CO_3 + other CO_3 species in solution) are necessary for mass balance calculations, many reaction processes are dependent on the speciation of the ions in the solution

(Brouckaert *et al.*, 2010). Because the equilibrium reactions that determine the speciation of ions in solution proceed fast in comparison to the biological processes, they are assumed to be at equilibrium (Brouckaert *et al.*, 2010). This results in increased numerical stability and faster simulation run times (Batstone *et al.*, 2002; Haile *et al.*, 2015). In addition to this, non-idealities in the aqueous phase are taken into account by correcting for the influence of the solution ionic strength (Haile *et al.*, 2015). In the case of the SDM-3P, an external software program (MINTEQA2) is used to (re)speciate the ions after each time step in the process simulation based on the total species concentrations, temperature and pressure (Brouckaert *et al.*, 2010; Ikumi *et al.*, 2012).

2.5.4 Modelling pH in AD

For simple models where the kinetics are based purely on the rate-limiting step, all other parameters such as pH, species concentrations, gas production etc. are calculated from the conversion occurring in the rate-limiting step (McCarty & Mosey 1991; Sötemann et al. 2005). To further simplify this approach, kinetics can be omitted altogether. The relationships between the abovementioned parameters and the substrate conversion can then be calculated by specifying the conversion of substrate and intermediate compounds if the stoichiometry is known (Sötemann et al. 2005).

Alkalinity is a property of aqueous systems defined as the mass of protons required to return a solution to its 'reference state' (Loewenthal *et al.*, 1989). The reference state of a solution is the state of the solution before any pH altering substances (acids and bases) are added to or removed from the solution (Loewenthal *et al.*, 1989). This approach can be used to model the pH of a solution in which the concentrations of all the dominant acidic and basic species – as well as the form in which they were added to the solution – are known through a proton balance (Loewenthal *et al.*, 1989). Alkalinity is a mass-based parameter (Loewenthal *et al.*, 1989), and can be linked to the conversion of COD-, N-, P- and S-containing compounds in the feedstock to determine the effluent alkalinity.

As mentioned in Section 2.5.4, the interactions between the weak acids/bases present in solution determine the digester pH, where the weak acid/base subsystems that are commonly of importance are the $H_2CO_3/HCO_3^-/CO_3^{2-}$, NH_3/NH_4^+, $H_3PO_4/H_2PO_4^-/HPO_4^{2-}/PO_4^{3-}$ and VFA subsystems (Musvoto *et al.*, 1997). If the total concentrations of the dominant weak acids/bases present are known, as well as the form they are added in, it is possible to calculate the pH using a proton balance as described by Loewenthal et al. (1989). At high ionic strengths, the reactivity of the ions that affect pH changes due to the presence of ionic drag (Kennedy, 1990). Solon et al. (2015) found that pH predictions are affected if corrections are not made for ionic strengths above 0.2 mol/L. To account for high ionic strengths, "mixed" pK_a values that are defined using ionic activity (instead of molar concentration) should be used for pH-related calculations instead of the commonly-used thermodynamic dissociation constants (Kennedy, 1990).

2.5.5 Experimental considerations for data collection

The mode of operation has bearing on the quality of kinetic parameters, and it has been shown that steady state continuous reactor studies return better kinetic parameters, provided various dilution rates are investigated. This is because batch kinetic experiments cannot be used to uniquely determine the parameters for simple Monod-type kinetics (Donoso-Bravo *et al.*, 2011). A less time-consuming technique is to apply substrate pulses and measure the dynamic responses that follow (Donoso-Bravo *et al.*, 2011). However, steady-state data allows the differential equations that describe the system to be simplified to simple algebraic equations, allowing parameters to be found through simple linear regression (Donoso-Bravo *et al.*, 2011). The elemental composition of the feed (C, N, H, O, P) should also be documented, and tracing the courses of these elements can reveal problems with the model or expose unknown processes (Donoso-Bravo *et al.*, 2011). In the context of SDM-3P, the relevant analyses required to inform steps 6-8 in the modelling procedure outlined in Section 2.5.1 are listed in Table 2-2.

Table 2-2: Analyses required for providing data for calibration and/or validation of SDM-3P

Analysis	Influent	Effluent
H_2CO_3* Alkalinity	Filtered	Filtered
pH	Raw	Raw
COD	Centrifuged	Raw & centrifuged
VFAs	NA	Filtered
Dissolved CH_4	NA	Raw
Gaseous CH_4 & CO_2	NA	Gas sampling bag
TKN	Filtered	Raw & filtered
Free & saline ammonia	Filtered	Filtered
Ortho-P	Filtered	Filtered
TSS	NA	Raw
VSS	NA	Raw
Conductivity	Raw	Raw

2.6 Research approach

2.6.1 Initial objectives

The initial objective of this study was to investigate the effect of the OLR on CH_4 yield and productivity, as well as to provide data to inform further development of the SDM-3P model. Although the effect of the OLR on reactor performance has been well-documented in the literature, differences in experimental conditions, and especially substrate composition affect the results obtained. Furthermore, if data is required for model development it is necessary for the analyses performed when generating the data to match the chemical species or quantities used by the model. In this case, it was desired to generate two complete datasets experimentally from the digestion of two defined substrates to inform further development of the SDM-3P model. Doing so specifically requires the measurements listed in Table 2-2 to be performed when steady state operation is achieved at various OLR.

2.6.2 Initial research approach

It was initially desired to perform the experiments using two synthetic wastewaters (WW) with a relatively low COD concentration (1.5 g/L). This required the design and construction of two identical high-rate anaerobic reactors. The UASB reactor type was chosen, and a scaled-down version of the UASB reactors used by Fang & Chui (1993) was used as the basis for the design. The design of the reactors is documented in greater detail in Section 3.1.1. For the substrates, the synthetic WW fed to Reactor 1 (R1) was comprised with sucrose as the sole carbon source, while the synthetic WW fed to Reactor 2 (R2) comprised sucrose and carbyoxymethyl cellulose (CMC) in a ratio of 1:1 in terms of COD. The CMC in the latter synthetic substrate requires hydrolysis, making it more recalcitrant to degradation.

A very well-granulated and active starting inoculum was used. However, issues with flotation of the sludge bed started within weeks after inoculation, after which growth took place mostly as dispersed filamentous bulking-type sludge. In spite of the sludge maintaining its ability to convert sucrose to CH_4, washout of flocculent sludge as well as periodic flotation of the entire sludge bed persisted throughout the experiment, making treatment of the synthetic WW ineffective. Further review of the literature specifically on the conditions governing anaerobic sludge granulation (documented in Section 2.4.2) was performed in response to the deterioration of the sludge granules during the experiment described in the previous section. This led to a number of experimental changes being made in numerous attempts to return the sludge to its granular state. However, the experiment was eventually terminated after a number of interventions failed to return the sludge back to a granular state. More details on this experiment are documented in Section 5.1.

2.6.3 Revised objectives

In the initial experiment, the importance of establishing the correct conditions for cultivating well-granulated sludge was identified as a key requirement for successful UASB operation. The study objectives were therefore re-defined to focus on start-up and granulation of the UASB reactors.

The literature on anaerobic sludge granulation emphasises the role of the mixing conditions within the reactor in granule formation. The specific objective of this study is therefore to investigate the effect of providing a mixing force in addition to the mixing caused by the evolution of biogas bubbles from the sludge bed.

Furthermore, provision of the correct growth conditions for the methanogen *Methanosaeta concilii* is also highlighted as a prerequisite for granulation in the literature. In the initial experiment, the pH dropped to the lower boundary of the desirable range of 6.5-7.8 (Hulshoff Pol *et al.*, 1983), even at steady state and low OLRs, in spite of a high influent pH (~8.0). This is undesirable since any shock to the system, such as increasing the OLR, would likely result in a transient accumulation of VFAs which would lower the pH below the abovementioned range. This highlights the need to understand the dominant mechanisms affecting pH in WW AD. Therefore, a secondary objective of this study is to develop a model to investigate the mechanisms by which alkalinity was consumed, as well as provide a tool to predict the influent alkalinity required to maintain a neutral pH.

2.6.4 Hypotheses

In view of the revised objectives of this study, two new Hypotheses were developed. Hypothesis 1 was formulated to address the effects of mixing on granulation. Hypothesis 2 was developed to address the mechanism responsible for the low effluent pH experienced experimentally.

Hypothesis 1

A reactor recycle loop was included in the original design and build of the UASB reactors for the purposes of aiding reactor mixing and maintaining a consistent upflow velocity. This enabled the effect of hydraulic mixing on reactor start-up to be investigated. From Section 2.4.3 it is expected that increasing the superficial upflow velocity (through increasing the recycle ratio) should increase the shear rate, thus resulting in the growth of more settleable granules due to LB EPS being sheared off (Wang *et al.*, 2017), as well as by minimising the length of the filaments of hydrophobic *Methanosaeta Spp.* which are prone to the attachment of gas bubbles, thereby causing flotation (Thaveesri *et al.*, 1995). Furthermore, the increased upflow velocity in the reactor through the use of a high recycle ratio should increase the suspension of less-settleable particles (Vanderhaegen *et al.*, 1992; Hulshoff Pol *et al.*, 2004) and thereby their washout, therefore applying a greater selection pressure for more settleable sludge granules. This led to the proposal of Hypothesis 1:

> The recycling of effluent in a UASB system increases the superficial upflow velocity and therefore the turbulence and shear forces within the reactor. This increase in shear force aids in preventing the formation of bulking type sludge. Furthermore, the increased upflow velocity results in a greater 'selection pressure' for more settleable sludge particles. The recycling of effluent therefore results in the formation of more settleable sludge ganules.

Key questions:

- How does the settleability differ between granules grown in UASB reactors operated with a high effluent recycle ratio and with no effluent recycle?
- How does the effluent recycle ratio effect cell morphology?
- How does the use of a high effluent recycle ratio affect the LB EPS content of the sludge?
- How does the physical appearance of the sludge granules differ between those grown with a high effluent recycle ratio and those grown with no effluent recycle?
- Does the use of a high effluent recycle ratio reduce the frequency of or prevent sludge bed flotation incidents over a reactor operated with no effluent recycle?

Hypothesis 2

The development of Hypothesis 2 followed the observation that the pH of the effluents of both R1 and R2 (~6.5) was significantly lower than that of the feed (~8.0), even at steady state and low OLR. A drop in pH in an AD reactor usually results from the accumulation of VFA in the effluent due to inhibition or overloading of the methanogen population (Moosbrugger *et al.*, 1993). However, it is unlikely that VFA would accumulate under steady state conditions at low OLRs and feed concentration, which indicates that a mechanism other than VFA production was responsible for the drop in pH between the reactor influent and effluent. A similar observation made by Sam-Soon et al. (1990) was attributed to the uptake of NH_3 for PN EPS generation, which led to the proposal of Hypothesis 2 below:

> The large drop in pH between the influent and effluent fed to/from the UASB reactors (~8.0-~6.5) in the experimental investigations is due to both the uptake of the weak base NH_3 for PN EPS production in addition to the production of the weak acid VFA. Furthermore, the effect of the uptake of NH_3 on pH in the experimental systems investigated is of a similar magnitude to the effect of the VFA produced.

Key questions:

- What are the chemical and biochemical systems and processes that affect pH in the experimental UASB systems investigated?
- What is the mechanism by which uptake of NH_3 affects pH?
- What would the effluent pH be in the absence of VFA?
- What would the effluent pH be if NH_3 uptake is ignored?

2.6.5 Revised research approach

A new experimental plan was devised to test Hypothesis 1. For this granulation experiment, R1 and R2 were operated as duplicate reactors except for the inclusion of the effluent recycle stream for R1. A purely sucrose-based synthetic WW was used due to the benefits of using a readily biodegradable carbohydrate feed on sludge granulation. The experiment was run for 50 days since it was focused on only the start-up of the UASB reactors. Analytical tests relevant to the key questions posed for Hypothesis 1 were performed to provide the results required to assess the validity of the hypothesis. A list of the tests performed is presented in Table 2-3. More information on the experimental design is presented in Section 3.2.

Table 2-3: A list of the analyses performed during the granulation experiment

Analysis	Frequency/no. of measurements over experimental period
Influent and effluent soluble COD	Daily
Effluent pH	Daily
Biogas productivity	Daily
Biogas composition	5 times
Sludge bed TSS & VSS	4 times
Photography	4 times
Micrography	Once

To test Hypothesis 2, a modelling approach was adopted. A steady state, fixed-conversion model was developed which includes only the weak acid/base subsystems dominant in the experimental UASB system. Development of the model involved definition of a conceptual model of the process, followed by derivation of the stoichiometry implied by the conceptual model. Finally, the pH of the reactor was related to the concentrations of the weak acid/base species present in the feed and the conversions thereof. The model could then be used to perform virtual experiments to determine the alkalinities produced or consumed within each weak acid/base subsystem. These virtual experiments were conducted for various scenarios, the results of which provided the data required to accept or reject Hypothesis 2. The development of the model is presented in detail in Chapter 4 and the virtual experiments performed are described in Section 5.3.1.

3. Materials and Methods

3.1 Materials

3.1.1 UASB reactor system design

Introduction

Because this research is focussed on AD of dilute wastewaters, an efficient reactor type that decouples the SRT and HRT was required. The most popular type of AD wastewater treatment reactor is the upflow anaerobic sludge blanket (UASB) reactor (Chernicharo *et al.*, 2015; van Lier *et al.*, 2015). This reactor's popularity stems from its ability to treat wastewater at high OLR and short HRT (van Lier *et al.*, 2015), suited to the treatment of dilute wastewaters. The study by Fang & Chui (1993) has been the most successful in determining the highest OLR achievable in a UASB reactor, achieving ~75% and ~95% total and soluble COD removal respectively at an OLR of 160 g-COD/L.day, and was hence used as a basis for the design of this experimental investigation. The reactors were designed to investigate the trade-off between CH_4 productivity and yield. As a result, the reactor detailed below is designed to meet the need to operate at a large range of OLR.

Effluent recycle

Two issues were presented as a result of using a UASB reactor for the abovementioned aims. The first issue is that although UASB reactors are relatively well-mixed through the production of biogas at higher OLR (Fang and Chui, 1993), they are not completely mixed. This poses problems when trying to model the system, or use data generated using a UASB system for model development, since accounting for spatial variations in concentration add to the complexity of the kinetic equations.

The second problem is that to change the OLR, either the influent COD concentration or the HRT or both need to be changed. However, the wide range of OLR over which the reactors were designed to operate (1-200 g-COD/L.day) require these variables to be changed by at least an order of magnitude each. It was therefore necessary to increase the OLR through changing both the feed concentration and HRT. However, on changing the HRT the upflow velocity, a parameter of great importance in UASB systems (Peña *et al.*, 2006), would change proportionally.

To overcome these potential drawbacks, a recycle stream was included to pump 'clarified' liquor from the gas-liquid-solid-separator (GLSS) zone of the UASB (shown in Figure 3-2) to the reactor influent. The recycle ratio (defined by Equation 8) could then be decreased each time the HRT was decreased, allowing a constant upflow velocity to be maintained at any given feed flow rate (by recycling less effluent to compensate for the greater feed flow rate).

$$\text{Recycle ratio} = \frac{\dot{v}_{\text{recycle}} + \dot{v}_{\text{feed}}}{\dot{v}_{\text{feed}}} \qquad \text{Equation 8}$$

where

$\dot{v}_{recycle}$ is the volumetric flow rate of the recycle stream

$\dot{v}_{feed}$ is the volumetric flow rate of the feed stream

The OLR could then be increased initially by increasing the feed flow rate. A maximum desired feed flow rate of ~30 L/day was decided upon. This decision was made to prevent the HRT from dropping below 1.5 hours, thus ensuring that sufficient contact time between the microorganisms and the substrate is maintained. The feed flow rate was also limited to avoid preparing and storing impractically large volumes of synthetic feed. On attaining the maximum desired feed rate further increases in the OLR could be controlled by increasing the influent COD concentration. By operating at a high recycle ratio initially, the reactor would also be well-mixed. As the recycle ratio is decreased to accommodate the lower HRT, the superficial upflow velocity remains constant. Furthermore, the higher productivity of biogas expected at the higher OLR serves to maintain the homogeneity of the reactor contents. A schematic of the reactor system is shown in Figure 3-1.

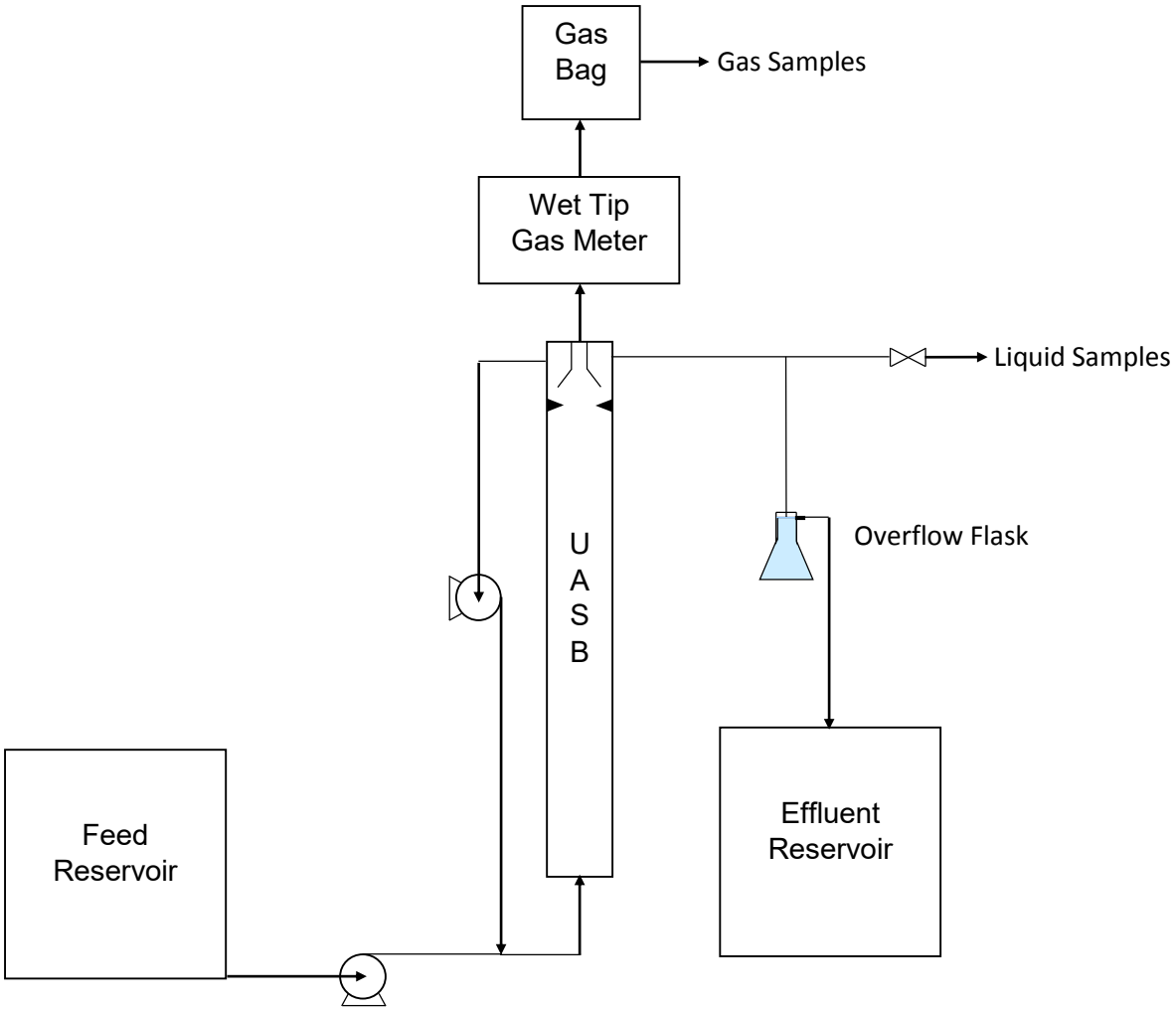

Figure 3-1: Schematic of the experimental setup

Specification of reactor dimensions

To specify the reactor dimensions, it was decided that a cylindrical reactor geometry would be used, and the working volume (total reactor volume minus the GLSS volume) was set at 2 L. This volume was decided upon as being large enough for samples to be taken from the sludge bed for total suspended solids analysis and minimising errors associated with measurement and operational equipment (gas meters, pumps etc.), whilst not requiring unreasonable volumes of feed to be prepared and stored.

To make the data comparable to digestion of a high-strength raw sewage – a research objective outside of this investigation – the initial feed COD was set at 1.5 g/L until an OLR of 22 g-COD/L.day (a safe estimate for the maximum OLR at which a raw sewage AD study would likely run). These two constraints allowed calculation of the minimum HRT to be 1.64 hours.

Using these specifications as starting points, the remaining reactor dimensions were calculated using the following relationships:

$$A = \frac{\dot{v}_{Feed} + \dot{v}_{Recycle}}{u_{Upflow}}$$ Equation 9

Substituting the numerator with Equation 8 after multiplying both sides by $\dot{v}_{Feed}$:

$$A = \frac{\dot{v}_{Feed} \cdot Recycle\ ratio}{u_{Upflow}}$$ Equation 10

Further substituting Equation 3 for $\dot{v}_{Feed}$ yields Equation 11:

$$A = \frac{V_{Reactor} \cdot Recycle\ ratio}{u_{Upflow} \cdot HRT}$$ Equation 11

Where

A is the reactor cross-sectional area in dm^2

u_{Upflow} is the specified upflow velocity in dm/h

$V_{Reactor}$ is the reactor volume in L

As can be seen from Equation 11, to determine the cross-sectional area it is necessary to specify the recycle ratio and upflow velocity in addition to the reactor volume and HRT. The upflow velocity was specified an arbitrary value between 0.5-1.0 m/h – a desirable range for UASB reactors (Saravanan and Sreekrishnan, 2006; Chernicharo *et al.*, 2015). The dimensions were then set to be designed for the conditions occurring at the minimum HRT according to Equation 12. This is because, for a given cross-sectional area, there is a maximum feed flow rate (corresponding to the minimum HRT) above which the recycle flow rate cannot be further decreased to maintain a constant upflow velocity. It was arbitrarily decided that the recycle ratio should be equal to two at this this minimum HRT to ensure that benefits of recycling effluent mentioned previously still occur under these conditions.

$$A = \frac{V_{Reactor} \cdot Recycle\ ratio_{min}}{u_{Upflow} \cdot HRT_{min}}$$ Equation 12

Where

HRT_{min} is the minimum value of the HRT (=1.64 hours)

$Recycle\ ratio_{min}$ is the minimum value of the recycle ratio, corresponding to the minimum HRT

However, the value calculated for the cross-sectional area did not correspond to an available standard diameter of PVC piping. The diameter was adjusted to an available standard size of PVC piping using the MS Excel Solver plugin, which was specified to vary the design upflow velocity. This scaled the upflow velocity to a value of 0.677 m/h to obtain the correct size diameter. A summary of the most relevant reactor dimensions is included in Table 3-1, and a side view illustration of the final reactor design is presented as Figure 3-2 (a diagram including dimensions is included in Appendix B:).

Table 3-1: Reactor dimensions

Reactor body	Inner diameter	67.8 mm
	Height	554 mm
	Diameter of constriction	57.8 mm
GLSS	Inner diameter	106 mm
	Height	226 mm
	Gas collection hood diameter	65 mm

Finally, temperature control systems were installed on both reactors. These systems maintained the reactor temperatures at 37°C using a heating coil which responded to the output of a custom-built feedback controller. The temperature was measured for each reactor using a thermocouple inserted into a purpose-built port 80% up the height of the reactor body (between the top two sludge sampling ports) on the opposite side to the sludge sampling ports.

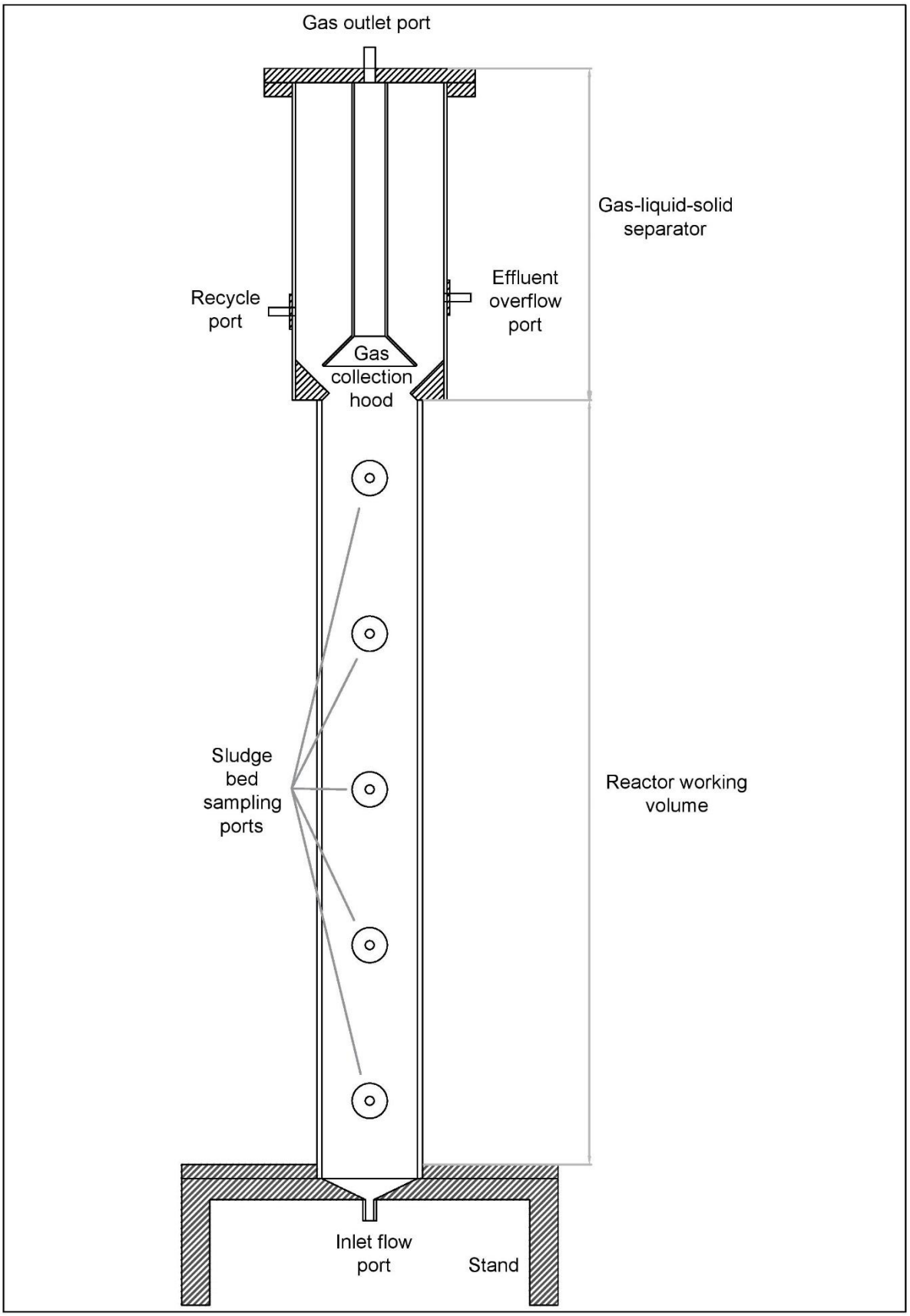

Figure 3-2: Side view of the UASB reactors

Ancillary equipment

For the first experiment, substrate was initially prepared and then autoclaved in 5 L and then 10 L Schott bottles with modified lids that allowed for the connection of feed tubing and an air filter. Eventually, it was arranged for the feed to be stored in a refrigerated room (5°C) due to contamination issues. Stainless steel tubing was installed to transport the feed around the seal of the door. With this approach, feed could be prepared and stored for up to 5 days before contamination (indicated by the presence of turbidity) was observed. Feed drums that could be stationed in the walk-in fridge were then built during the fourth month of the experiment, enabling larger flow rates to be prepared and thus fed to the reactors. These drums are 50 L, and are pictured in Figure 3-3 below.

Figure 3-3: Feed drums used for after start-up of the first experiment

For the second (granulation) experiment, feed was initially prepared in 10 L plastic jerry can-type containers sealed with rubber bungs with a hole each for the connection of feed tubing and an air filter. These containers were also stored in the refrigerated room to prevent contamination. Once the feed flow rate exceeded 3 L/day, four days' worth of feed was prepared at a time and stored in/fed from the drums pictured in Figure 3-3.

Substrate was pumped into both reactors using a Masterflex L/S variable speed drive peristaltic pump (Cole Parmer, Item # EW-77521-47) fitted with two Masterflex pump heads (Cole Parmer, Model 7013-52). Substrate was recycled for both reactors with a pump of the same type fitted with two larger model Masterflex pump heads (Cole Parmer, Model 7014-52).

Volumetric biogas production was measured using Wet Tip Gas Meters, which work using a simple mechanism to measure the biogas produced. More information on these gas meters can be found at http://wettipgasmeter.com/.

Both reactors' effluent ports were connected to a 500 mL filter flask (depicted as "Overflow Flask" in Figure 3-1) raised on a retort stand. These flasks served as a buffer between air and the reactor effluent, allowed for the retention of washed-out sludge, and maintained the head of pressure required in the reactors for the biogas produced to overcome flowing into the bottom of the gas meters. Pipes were attached to the effluent nozzle of each filter flask, allowing the overflow from the flasks to flow into an effluent drum.

A photograph depicting most of the experimental equipment is presented in Figure 3-4.

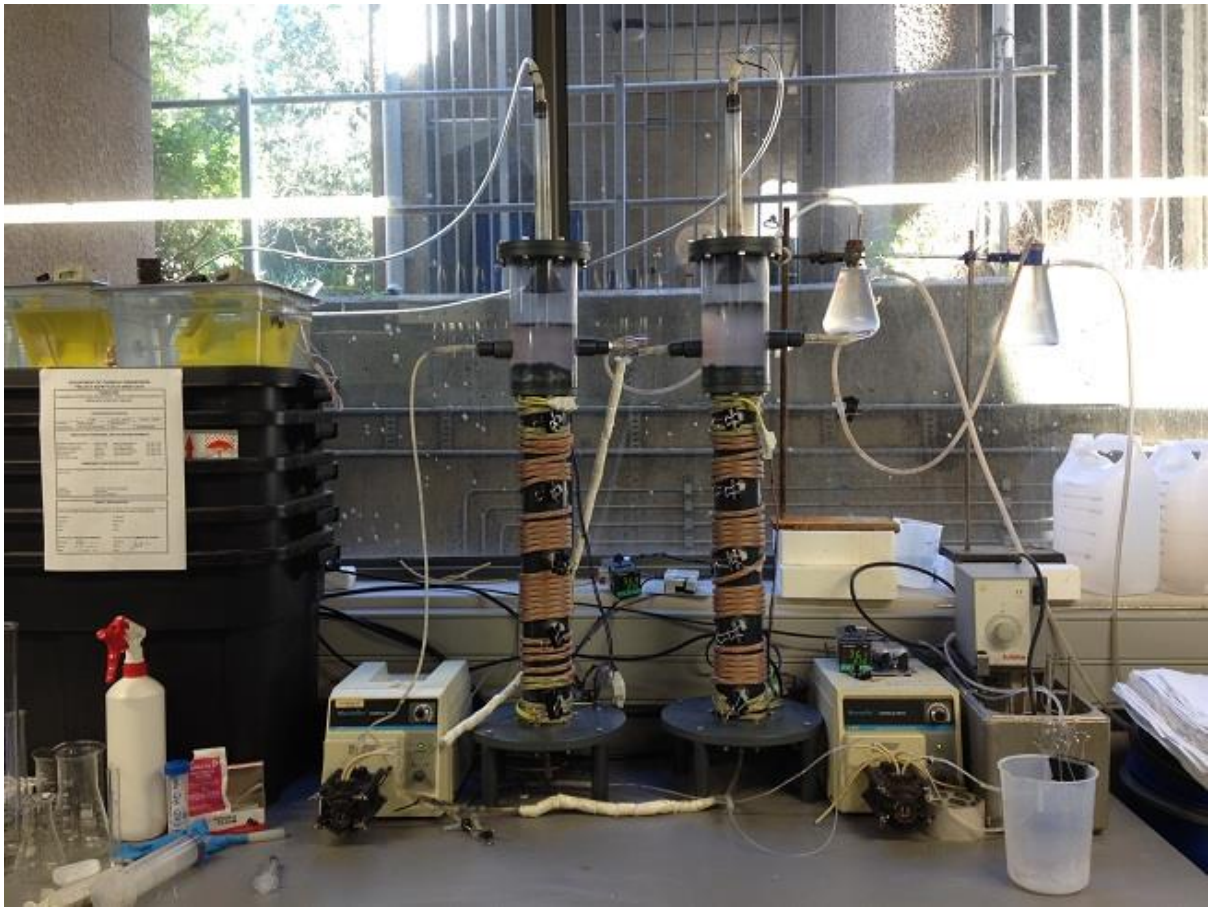

Figure 3-4: The experimental setup

Inocula utilised

For the first experiment, 1 L of well-granulated sludge originating from the South African Breweries' (SAB) Prospecton plant's UASB reactor was used as an inoculum for each reactor, some of which is pictured in Figure 3-5. The sludge granules appear to be very well-defined and are dark brown in colour. The total solids content of this sludge was 182 g/L when settled. Unfortunately the volatile fraction of the total solids was not measured.

For the granulation-focused experiment, 500 mL of granular sludge originating from the SAB Newlands plant's UASB reactor was used for each reactor, some of which is pictured in Figure 3-6. The sludge is agglomerated into granules, but these granules are much less compact than the sludge from the Prospecton plant, and relatively colourless/transparent. There appears to be a large amount of solid substrate/debris present in the Newlands sludge, and it looks like many of the granular agglomerates present have formed on these solid particles. The boundary between the granules and the liquid in-between them was less clear for the Newlands sludge than for the Prospecton sludge, rendering the Newlands sludge suspension more viscous in appearance. When settled, the Newlands sludge contained 84.3 ± 0.6 g-TSS/L and 58.6 ± 0.8 g-VSS/L (VSS/TSS = 69.5%).

The above inocula were taken from reactors operated under the conditions in Table 3-2.

Table 3-2: Operating conditions of UASB reactors treating brewery wastewater

OLR (g-COD/L.day)	8.5-11.7
HRT (h)	12
SLR (g-COD/g-VSS.day)	0.61
pH	7
Influent COD (g/L)	5.9

actor

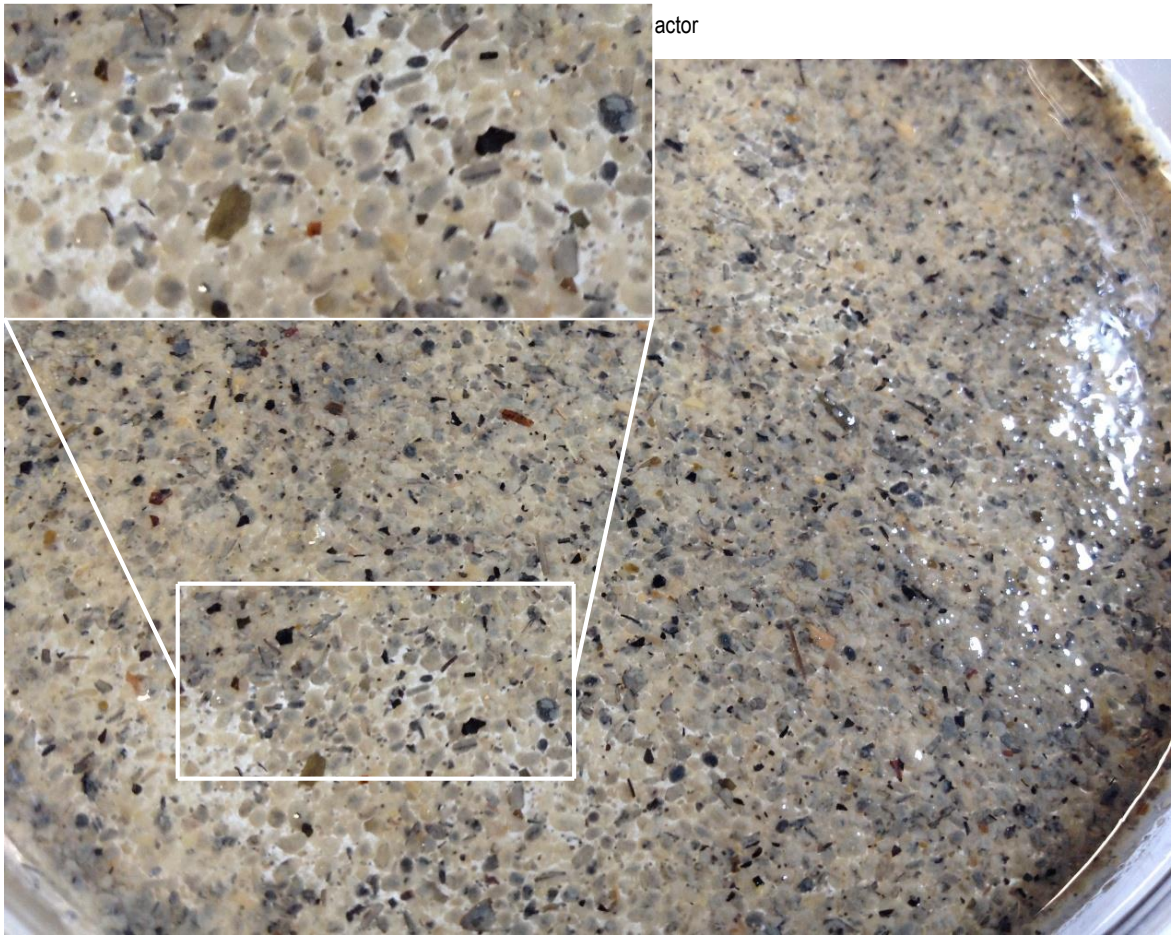

Figure 3-6: Sludge from SAB's Newlands plant's UASB reactor

3.1.2 Substrate composition

Choice of carbon source

For the original experiment, it was desired to test the effects of OLR on reactor performance using both a readily biodegradable and a more recalcitrant carbon source. Sucrose was chosen as the readily biodegradable carbon source due to its wide availability, low price, high solubility, and ease-of use by microorganisms. Carboxymethyl cellulose (CMC) was initially used as a more recalcitrant feedstock for R2, which was fed 50% CMC and 50% sucrose by COD (viscosity of 1% CMC solution = 0.755 Pa.s). At a feed COD of 1.5 g/L, and noting the measured COD of sucrose (brown sugar) (1.08 g-COD/g-sucrose) and CMC (0.90 g-COD/g-CMC), a 50% sucrose/CMC medium by COD equates to 690 mg-sucrose/L and 840 mg-CMC/L. However, CMC was phased out of the feed for R2 and was eventually replaced by sucrose due to reasons discussed in Section 5.1.1. For the granulation experiment, the medium used was identical between both reactors and contained 1.5 g-COD/L equivalent as sucrose (brown sugar).

Nutrient medium

Due to the success of the experiment by Fang & Chui (1993), the nutrient solution was originally based almost solely upon theirs with the exception of the addition of the essential trace element selenium in the form of sodium selenite. However, this mixture exhibited issues with precipitation, which would limit the bioavailability of the nutrients as well as change the pH of the feed solution. It was eventually decided to reformulate the medium using the approach suggested by Sperling and Chernicharo (2005), wherein the nutrient requirements are calculated using a theoretical approach (refer to section 2.3.5). In addition to the nutrient requirements, K_2HPO_4 was added at a concentration higher than necessary for nutrient requirements along with $NaHCO_3$ to buffer the solution against the pH drop resulting from VFA formation. The resulting nutrient medium is shown in Table 3-2.

Table 3-3: Original substrate composition used for most of the first experiment, with the partition of the components into the stock solutions and concentration factor in which they were stored in parenthesis

Medium components	mg/g-COD	mg/L_{feed}	Stock Solution
COD	1000	1500	
Brown sugar	930	1389	Sucrose (100X)
Sodium bicarbonate ($NaHCO_3$)	667	1000	Macronutrients & Buffers (50X)
Ammonium chloride (NH_4Cl)	52	78	
Potassium monohydrogen phosphate (K_2HPO_4)	113	170	
Sodium citrate ($Na_3C_6H_5O_7$))	77	116	
Ferric chloride ($FeCl_3.6H_2O$)	1.83	2.74	Fe (1000X)
EDTA ($C_{10}H_{16}N_2O_8$)	1.83	2.74	
Magnesium sulphate ($MgSO_4.7H_2O$)	6.39	9.58	Mg (1000X)
Nickel sulphate ($NiSO_4.7H_2O$)	0.010	0.151	Micronutrients (500X)
Manganese(II) chloride ($MnCl_2.4H_2O$)	0.014	0.022	
Zinc chloride ($ZnCl_2$)	0.026	0.039	
Cobalt chloride ($CoCl_2.2H_2O$)	0.064	0.095	
Ammonium molybdate ($(NH_4)_6Mo_7O_{24}.4H_2O$)	0.023	0.035	
Copper(II) chloride ($CuCl_2.2H_2O$)	0.006	0.0085	
Sodium borate ($Na_2B_4O_7.10H_2O$)	0.033	0.050	
Sodium selenite ($Na_2SeO_3.5H_2O$)	0.020	0.030	
Ca^{2+}	8	12	From tap water

However, this medium composition exhibited a number of issues. Firstly, the $NaHCO_3$ concentration was increased to 1500 g/L (1000 mg/g-COD) to increase the alkalinity of the feed. The NH_4Cl

concentration was also found to be too low to supply the N required for both cell synthesis and proteinaceous EPS production. The N requirement has been estimated at 20 mg-N/g-COD (Sam-Soon *et al.*, 1990), corresponding to a NH_4Cl concentration of 76 mg-NH_4Cl/g-COD. It was decided to adopt the NH_4Cl concentration used by Fang & Chui (1993) of 260 mg-NH_4Cl/L. Secondly, the concentrations of the divalent cations Ca^{2+} and Mg^{2+} were lower than optimal for granulation. A Ca^{2+} concentration of 150 mg-Ca^{2+}/L was found optimal in a study by Yu et al. (2001). However, the highest Ca^{2+} concentration attainable without causing precipitation was 64 mg-Ca^{2+}/L (including the ~12 mg-Ca^{2+}/L contribution from the tapwater Ca^{2+}), corresponding to a $CaCl_2.2H_2O$ addition of 191 mg-$CaCl_2.2H_2O$/L. It was also not initially noted that the S-requirement of methanogens is higher than the Mg requirement (Table 2-1), and insufficient S was included in the original medium composition as a result. The $MgSO_4$ concentration was therefore increased to account for the S requirement of 2.1 mg-S/g-COD, as well as provide a higher Mg^{2+} concentration. Also, because Fe has often been found to accumulate in granules (Schmidt and Ahring, 1996) the Fe concentration was increased to account for Fe removed from the medium. Lastly, it was decided to increase the concentrations of the micronutrients to those typically used in UASB studies (Ten Brummeler *et al.*, 1985; Fang and Chui, 1993; Thaveesri *et al.*, 1995; Mu and Yu, 2006) to provide a greater margin for error. The resulting substrate composition is shown in Table 3-3. The pH of this medium was ~8.0 when prepared using tap water.

Table 3-4: Revised substrate composition used toward the end of the first experiment and in the second experiment, with the partition of the components into the stock solutions and concentration factors in which they were stored in parenthesis

Medium components	mg/g-COD	mg/L_{feed}	Stock Solution
COD	1000	1500	
Sucrose	930	1389	Sucrose (100X)
Sodium bicarbonate ($NaHCO_3$)	1000	1500	Macronutrients & Buffers (500X)
Ammonium chloride (NH_4Cl)	260	390	
Potassium monohydrogen phosphate (K_2HPO_4)	113	170	
Sodium citrate ($Na_3C_6H_5O_7$))	77	116	
Ferric chloride ($FeCl_3.6H_2O$)	6.67	10	Fe (1000X)
EDTA ($C_{10}H_{16}N_2O_8$)	6.67	10	
Magnesium sulphate ($MgSO_4.7H_2O$)	16.7	25.0	Mg (1000X)
Calcium chloride ($CaCl_2.2H_2O$)	127	191	Ca (1000X)
Nickel sulphate ($NiSO_4.7H_2O$)	0.33	0.50	Micronutrients (500X)
Manganese(II) chloride ($MnCl_2.4H_2O$)	0.33	2.0	
Zinc chloride ($ZnCl_2$)	0.33	0.50	
Cobalt chloride ($CoCl_2.2H_2O$)	0.33	0.50	
Ammonium molybdate ($(NH_4)_6Mo_7O_{24}.4H_2O$)	0.33	0.50	
Copper(II) chloride ($CuCl_2.2H_2O$)	0.33	0.50	
Sodium borate ($Na_2B_4O_7.10H_2O$)	0.33	0.50	
Sodium selenite ($Na_2SeO_3.5H_2O$)	0.33	0.50	
EDTA	3.3	5.0	

3.2 Experimental Design

The first experiment was designed to generate data from the UASB reactor systems for the purpose of model development. It was desired to generate datasets at increasing organic loading rates (OLR) once steady state was reached at each OLR. The experimental plan for the original experiment is documented in Table 6-1 in Appendix C:. This plan was to increase the OLR by 50% once steady state had been reached – indicated by COD removal of above 80% and stable gas production for three consecutive days. Also, the recycle ratios employed were designed to allow a gradual increase in the superficial upflow velocity during the initial start-up period. The objective of the experiment was to measure the quantities listed in Table 2-2 once steady state was achieved at each of the OLR from 6 g-COD/L.day and above. However, only 'Phase 2' (Table 6-1) was reached before deciding to terminate this experiment.

The granulation experiment was designed to investigate the effect of including additional hydraulic mixing on granulation. For the granulation experiment the experimental plan laid out in Table 3-4 was followed. The OLR actually used (presented in Section 5.2.1) differed slightly due to minor errors in substrate preparation. The recycle ratios employed were designed for a gradual increase in the upflow velocity during the initial start-up period. Note that the recycle flow rates and ratios apply only to R1, and that R1 and R2 experienced different superficial upflow velocities as a result of the recycle only being included for R1.

Table 3-5: Experimental plan for the granulation experiment

Phase	1	2	3	4	5	6	7
OLR (g-COD/L.day)	1	1.5	2.25	3.8	5.63	8.4	11.2
HRT (h)	36	24	16	9.5	6.4	4.265	3
COD (g/L)	1.5	1.5	1.5	1.5	1.5	1.5	1.5
Feed flow rate (L/day)	1.33	2.0	3.0	5.0	7.5	11.2	15
R1 Recycle flow rate (L/day)	7.3	19.7	31.7	55.6	79.1	75.4	70.6
R1 Recycle ratio*	6.5	10.8	11.6	12.0	11.6	7.7	5.4
R1 Upflow velocity (m/h)	0.10	0.25	0.4	0.7	1.0	1.0	1.0
R2 Upflow velocity (m/h)	0.015	0.023	0.035	0.058	0.087	0.12	0.19

*Note that R2 was operated without effluent recycling

The analyses performed during the granulation experiment, as well as the frequency with which they were performed, during the granulation experiment are presented in Table 3-5.

Table 3-6: Analyses performed to monitor and document the performance of R1 and R2

Test	Frequency/number of measurement(s)	
	Influent	Effluent
pH	Twice	Daily
COD	Daily	Daily
VFA	-	Five sequential days
Biogas productivity	Daily	
Biogas composition (%CH_4)	Six times	
Sludge bed TSS, VSS and height	Four times	

3.3 Methods

3.3.1 Experimental Protocols

Inoculation

For the first experiment, inoculation was performed on the 08/11/2016 for R2 and 15/11/2016 for R1 (delayed due to a weak plastic joint breaking and needing to be fixed). For each inoculation, 1 L of the granular sludge (described in section 3.1.1) was transferred to a measuring cylinder and then poured through the open lid of the empty reactor. The sludge sampling, liquid effluent and recycle ports were all clamped. The lids were then fitted before the reactors were sparged with N_2 gas for roughly 5 minutes to ensure all oxygen in the sludge and (initially very large) headspace was displaced. Feeding was then initiated at the lowest flow rate of 1.33 L/day. Around 24 hours later the liquid level was higher than the liquid effluent port, which was then unclamped to allow this liquid to overflow out into the effluent flasks, which themselves eventually filled and overflowed into the effluent bottles. The initial average TSS in the working volume of the reactors after inoculation was 91 g/L.

The same procedure was followed for the granulation experiment with the exception that only 500 mL of sludge was added, resulting in initial total and volatile solids concentrations of 21.1 g-TSS/L and 14.6 g-VSS/L respectively. Inoculation of both reactors took place on 26/10/2017 for the granulation experiment.

Substrate preparation

For the first experiment, substrate was initially prepared in 5 L & 10 L Schott bottles. These feed bottles were then connected to the reactors via a peristaltic pump (see specifications in Section 3.1.1) using silicone tubing. The Fe and Macronutrients & buffer stock solutions (see Table 3-2) were added after autoclaving in a laminar flow hood to prevent precipitation from occurring during autoclaving. However, this approach exposed the bottles to an unsterile environment, even if briefly, which often resulted in contamination of the substrate if stored and used for more than two days. In the fourth month of the first experiment it was decided to move the reactors closer to a walk-in refrigerated room, allowing the substrate to be refrigerated for the sake of preventing contamination. New feed drums were constructed using 50 L plastic barrels (Figure 3-3). These drums were connected to the reactors after installing a section of stainless steel tubing that ran through a gap of insulating rubber on the fridge door.

For the granulation experiment, substrate was initially prepared in 10 L plastic jerry can-type containers sealed with rubber bungs with a hole each for the connection of feed tubing and an air filter. Once the feed flow rate exceeded 3 L/day, feed was prepared in the 50 L drums.

The procedure for preparing feed was to turn off the feed pump before disconnecting the feed tubing from the drums and discarding any remaining substrate. The inside of the drums was sprayed with 70% ethanol before scrubbing with an abrasive sponge. Ethanol was also sprayed into the feed nozzle of the drums to ensure the connection between the drums and tubing was cleaned. The drums and feed nozzles were then rinsed twice using a minimal amount of hot water. The drums were then filled to ~75% of the desired final volume (depending on how much feed was required) before stock solutions were measured out in measuring cylinders (pre-washed with 70% ethanol and rinsed) and poured into the drums. The drums were then filled up to the desired total volume using a jet of water to ensure the mixture was homogeneous. Volumes were marked off on the inside of the drums for determination of the volume to add. Using this method, signs of contamination of the substrate (presence of turbidity) were only observed five to six days after substrate preparation. Therefore, four days' worth of substrate was prepared every four days following moving the feed drums into the refrigerated room (i.e. for most of the first experiment and the entire granulation experiment).

Routine maintenance

In addition to cleaning the feed drums when preparing feed, it was found necessary to clean the tubing connecting the reactor to the feed drums every two days to prevent build-up of contaminants on the inside of the tubing. This was achieved by pumping ~75 mL of biocide solution (Sealed Air Biocide D Extra, 3 g/L) through both sets of feed tubing, followed by forcing ~500 mL of hot water through each

set of tubing using a 60 mL syringe. More hot water – around 100-200 mL per set of reactor feed tubing – was then pumped through the tubes to displace any air in the tubes and to wash out the remaining biocide solution from the feed pump tubing. The feed tubing also required occasional massaging to loosen and remove build-up of biomass, which increased the efficacy of the biocide solution. The overflow flasks were also cleaned on average once a week to minimise the growth of algae and build-up of sludge which could block the effluent port of the flasks.

3.3.2 Analytical techniques

COD

In the first experiment, soluble COD was measured regularly (at least once a week) for the first three months, after which it was recorded intermittently. In the granulation experiment, soluble COD was measured daily. In both experiments, COD was measured according to the closed reflux, colorimetric method (5220 D.) (APHA, 1999). Merck COD reagent set (1.14555 HR) was used in conjunction with a digestion block and the Nova Spectroquant photometer. Samples were centrifuged and the supernatant used for determination of the soluble COD. Potassium hydrogen phthalate (PHP) (1,175 g-COD/g-PHP) in deionised water was used as a standard, at concentrations of 85, 212.5, 425, 637.5 and 850 mg-PHP/L, corresponding to COD values of 100, 250, 500, 750 and 1000 mg-COD/L respectively. The standard curve generated is presented in Figure 6-3 in Appendix D.2.1. Deionised water was used as reagent blank, and all COD measurements were made in duplicate. The volumes of samples and reagents were halved for economical and waste production purposes as it made no bearing on the results obtained. The COD results are presented as the percentage of soluble COD removed from the system, calculated as the difference between the influent and effluent soluble CODs, divided by the influent soluble COD.

pH

As for COD, pH was measured regularly during the first three months of the first experiment, after which it was recorded intermittently. pH was measured daily in the granulation experiment. In both experiments, pH was measured using an Accsen (AEL32T) pH electrode and Accsen (PH8) pH meter. A small sample of ~4 mL was taken using a 15 mL Falcon tube. This was done as carefully as possible to prevent rapid dissolution of CO_2. A lid was immediately fitted to the tube while walking to the pH meter. The Falcon tube was stored in a test tube rack while the pH probe was rinsed with deionised water. The pH probe was stored in the same size and type of Falcon tube, therefore the lid provided a seal while the pH measurement was taken. It was found that sliding the probe out of the Falcon tube and taking the pH reading immediately again using the same sample caused an error of +0.05-0.10 around the pH of 6.55 due to the evolution of CO_2 gas. The pH meter was calibrated daily using pH 4.0 and 7.0 buffer solutions.

VFA

The concentrations of lactic, acetic, propionic and butyric acids were measured using high performance liquid chromatography (HPLC). A Waters Breeze 2 system equipped with a Bio-Rad Organics Acids ROA column and a UV (210 nm wavelength) detector. The system was run isocratically using a mobile phase of 0.01 M H_2SO_4 at a flow rate of 0.6 mL/min. Standards containing the abovementioned VFA at concentrations of 100-600 mg/L in 100 mg/L intervals were used to generate standard curves to allow quantification of the VFA measured.

Biogas volume & composition

The cumulative biogas volume produced was measured using Wet Tip Gas Meters (http://wettipgasmeter.com/). These meters were calibrated to count every 35 mL of biogas produced, and the number of counts was recorded daily, along with the time of reading to allow calculation of the biogas productivity.

Gas samples for gas composition analysis were collected in Tedlar gas sampling bags (Sigma). A Perkin-Elmer Autosystem gas chromatograph equipped with a Supelco wax column (1.2 mm x 37 m) and flame ionisation detector (FID) was used for the determination of the CH_4 fraction of the biogas.

The FID and oven temperatures were set at 280°C and 50°C respectively. Nitrogen was used as a carrier gas at a flow rate of 1.5 mL/min. Measurements were performed by injecting 100 µL of gas. Standards containing 25% and 50% CH_4 were used to generate a standard curve with each analysis. The balance of the gas composition was assumed to comprise of CO_2.

Free & saline ammonia

Free and saline ammonia (FSA) concentration was determined using the preliminary distillation/titration methods (4500-NH_3 B & C) (APHA, 1999).

Total & volatile suspended solids

The total suspended solids (TSS) test procedure followed is analogous to method "2540 B. Total Solids Dried at 103-10.5°C" (APHA, 1999), except that samples were dried at 95°C to prevent boiling. Ceramic crucibles were dried at 95°C overnight and their masses measured the following day. Around 10 mL of sample was then collected directly from the reactors during operation (i.e. with the sludge bed in its usual state of expansion) in each crucible and dried overnight at 95°C. The concentrations obtained are therefore relevant to the TSS and VSS content of the sludge bed in its operational state, in which the sludge bed is expanded due to the upwards flowing liquor as well as biogas production. The masses of the dried samples were measured, before ignition in a furnace at 550°C for 20 min. The ash-containing crucibles were allowed to cool in the 95°C oven before the masses were measured, allowing quantification of the volatile suspended solids (VSS). All sample masses were measured directly from the 95°C oven to prevent errors due to absorption of moisture.

Photography and microscopy

In the Granulation experiment, photographs were taken of the sludge bed samples used to perform the VSS and TSS tests to document the physical appearance of the granules. It was attempted to minimise the effects of variations in the lighting conditions by taking the photographs under artificial lighting. However, some minor variation between the lighting conditions was still experienced. The procedure followed was to decant ~5 mL of each sludge sample onto a plastic petri dish. The petri dish was then elevated on a glass beaker to raise it off of the dark background of the lab benches, and photographs were taken ~10 cm from the beaker using a cell phone camera (iPhone 4S).

Micrographs were also taken of pieces of granules from R1 and R2 at the end of the Granulation experiment. A small sample (~10 mL) was taken from the lowest sampling port of each reactor. Granule samples were prepared by breaking the granule with the tip the pipette, which was then used to transfer 1.0 µL of sample containing a tiny piece of the granule debris to a microscope slide. Micrographs were taken using a light microscope (model BX40, Olympus Optical co. Ltd, Japan) equipped with a digital camera and AnalySIS software at 1000X magnification.

4. Stoichiometric Model Development

4.1.1 Model Purpose & Scope

A steady state, purely stoichiometric (no kinetics) model was built in MS Excel for the purposes of further understanding the effects of the dominant weak acid-base systems on the pH in the digesters. The effluent pH of both experimental UASB systems was at the lower end of the desired operating range of 6.5-7.8 (Hulshoff Pol *et al.*, 1983), despite the inclusion of 1500 mg-$NaHCO_3$/L (~18 mmol-$NaHCO_3$/L) and 170 mg-K_2HPO_4/L (0.97 mmol-K_2HPO_4/L) as buffers. It was desired to further understand why such a low pH was generated, as well as the effect of changes in buffer concentrations on the effluent pH. The results of the experiments conducted using the model described in this chapter are presented in section 5.3.

As already mentioned in Section 2.3.2, the pH of an aqueous system is defined by the interactions between compounds that act as acids/bases and H_2O i.e. react with H^+ of OH^- ions in solution or dissociate to increase the H^+ or OH^- ion concentrations. Therefore, to calculate the effluent pH from an AD reactor it is only necessary to know the concentrations of acids and bases, solution ionic strength (if high enough to impact ionic activity), and the temperature of the effluent stream. The effluent composition is determined through stoichiometry and knowledge of the extent to which the feed substrate and intermediate compounds are converted to final and intermediate products. The conversion of feed substrate and intermediates is governed by the kinetics of substrate and intermediate compound degradation within the reactor. However, if the conversion of these compounds is already known, it is not necessary to model the kinetics of the system if only a sensitivity analysis of the effects of weak acid/base species concentrations on effluent pH is of interest.

The development of this model therefore involved deriving the conceptual model, stoichiometry and mathematical expressions that govern the stoichiometry and the weak acid-base chemistry. The effect of ionic strength was not taken into account due to the low ionic strength (~0.02 mol/L) of the substrate used for the experimental system.

4.1.2 Conceptual Model

A schematic of the conceptual model depicting the flows of carbon (C) is presented in Figure 4-1.

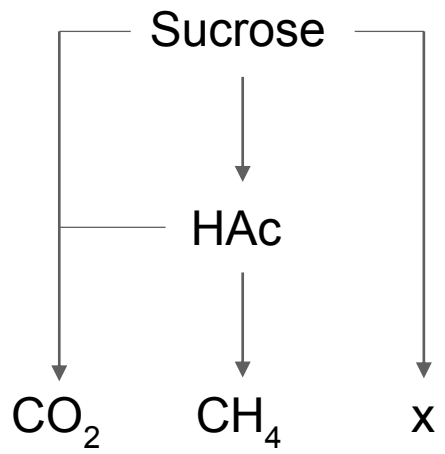

Figure 4-1: Conceptual model used indicating the flows of carbon

In this scheme, sucrose is fermented to acetic acid (HAc) as the most important VFA, which is then converted to CH_4 and CO_2. The assumption of acetic acid being the only VFA formed has little bearing on calculation of the pH due to the VFA all having similar pKa values. For simplicity sake it was assumed that biomass is only produced from the acidogenesis of sucrose and not the methanogenesis step. This assumption is supported by the fact that acidogens exhibit the highest growth yield of 0.089 g-COD/g-$COD_{fermented}$, representing over 77% of the total biomass yield (Sötemann et al. 2005). Furthermore,

because it is desired to predict the pH of the reactors under conditions where the vast majority of the COD is removed, the conversion of VFA specified in the model is in the range of 90%-100% (based on the experimental data shown in Figure 5-2 and Figure 5-3). This means that attributing all biomass growth to the acidogens does not result in significant errors because the yield of methanogenic cells is relatively constant at 90%-100% of the maximum possible growth yield. Hydrolysis is also not included due to sucrose being a readily fermentable substrate.

Further assumptions made are that only the phosphate, ammonium, carbonate and HAc weak acid/base subsystems and the partial pressure of CO_2 ($ppCO_2$) influence the digester pH. Therefore, in addition to the C flows shown, the concentrations of the compounds NH_3/NH_4^+, H_3PO_4, $H_2PO_4^-$, HPO_4^{2-}, PO_4^{3-}, H_2CO_3, HCO_3^-, CO_3^{2-} are included in model and are used to calculate the pH. It is also assumed that the aqueous phase acid/base subsystems are all in equilibrium, and that the aqueous phase in in equilibrium with the reactor headspace.

4.1.3 Derivation of Mathematical Relationships

Stoichiometry

The stoichiometric equation derived from the conceptual model (Figure 4-1) is presented below as Equation 13

$$C_{12}H_{22}O_{11} + Y_N \cdot NH_3 \rightarrow Y_x \cdot C_5H_7O_2N_a + Y_A \cdot (1 - X_{HAc}) \cdot C_2H_4O_2 + Y_M \cdot X_{HAc} \cdot CH_4 + Y_C \cdot CO_2 \quad \text{Equation 13}$$

where

$C_{12}H_{22}O_{11}$ is the molecular formula of sucrose

Y_N is the yield coefficient of NH_3

Y_x is the yield coefficient of biomass

$C_5H_7O_2N_a$ is the molecular formula of biomass (x)

Y_A is the yield coefficient of $C_2H_4O_2$ (HAc), used to represent VFA formed

Y_M is the yield coefficient of CH_4

Y_C is the yield coefficient of CO_2

The biomass that is formed is assigned the molecular formula of $C_5H_7O_2N_a$ as a general formula for anaerobic sludge (Sötemann, Ristow, *et al.*, 2005). The biomass term in the stoichiometry is treated as representing both the cell and EPS masses of the sludge granules. As such, the N-content of the biomass was kept as a variable ("a") to be calculated from the uptake of N measured experimentally to account for the total N uptake and therefore NH_3 removal from the system. The value of Y_N was calculated from experimental data as follows (Equation 14):

$$Y_N = \frac{(FSA_e - FSA_f)}{mgCOD_{converted}} \cdot \frac{COD_S}{M_{NH3}} \quad \text{Equation 14}$$

where

FSA_f is the free and saline NH_3 (FSA) concentration in the feed (mg-N/L), measured as 61.5 mg-N/L

FSA_e is the FSA concentration of the effluent (mg-N/L), measured as 38.5 mg-N/L

M_{NH_3} is the molar mass of NH_3, equal to 17 g/mol

$mgCOD_{converted}$ is the taken as the feed COD concentration measured (1590 mg-COD/L)

M_N is the molar mass of N, equal to 14 g/mol

COD_S is the molar COD of sucrose, equal to 384 g-COD/mol

The uptake of N was measured only during the first experiment, therefore this data was used to calculate the value of Y_N. This uptake of N is assumed to be similar between the two experiments performed due to the similar behaviour of the sludge granules in both experiments. Furthermore, the uptake of NH_3 can be calculated as 0.0145 mg-N/mg-COD_{feed}, which is relatively similar to the value of 0.02 mg-N/mg-COD_{feed} reported as required by Sam-Soon et al. (1990). It was also assumed that the feed COD converted is equivalent to the COD fed due to acidogenesis being a far faster process than methanogenesis.

The value of Y_x was calculated using the data from Sam-Soon et al. (1987), where they reported a sludge yield of 0.09 g-VSS/g-$COD_{removed}$ and a sludge COD/VSS ratio of 1.23 g-COD/g-VSS. In the context of this model, the value of 0.09 g-VSS/g-$COD_{removed}$ was taken to be equal to 0.09 g-VSS/g-$COD_{converted}$, where g-$COD_{converted}$ refers to sucrose that is fermented to HAc, and not necessarily subsequently reduced to CH_4. Again, this is substantiated as causing minimal error for the purposes of this model due to the majority of biomass growth taking place during acidogenesis, and by only investigating the conditions where methanogenesis is 90% efficient (i.e. 90% of the HAc formed through acidogenesis is converted to CH_4). The calculation of Y_x from these assumptions is as follows:

$$Y_x = 0.09\frac{gVSS_x}{gCOD_{converted}} \cdot 1.23\frac{gCOD_x}{gVSS_x} \cdot \left(\frac{1}{COD_x}\right) \cdot COD_S \qquad \text{Equation 15}$$

where

COD_x is the molar COD of the biomass (184 g-COD/mol_x), and excludes the contribution from the N component of the biomass, as this would not be measured during COD analysis (APHA, 1999).

The value of “a” in the formula used for biomass ($C_5H_7O_2N_a$) could then be calculated using Equation 16 (derived from the N-balance):

$$a = \frac{-Y_N}{Y_x} \qquad \text{Equation 16}$$

The yield coefficients of HAc (Y_A) and CH_4 (Y_M) were calculated from a COD balance as follows:

$$COD_{S,in} = COD_{x,formed} + COD_{A,formed} + COD_{M,formed} \qquad \text{Equation 17}$$

where

$COD_{S,in}$ is the COD fed into the reactor

$COD_{x,formed}$ is the COD of the biomass formed

$COD_{A,formed}$ is the COD of the net amount of HAc formed

$COD_{M,formed}$ is the COD of CH_4 formed

The COD contribution of the N (NH_3) is again not accounted for, as this is not measured during the COD test and would add an equal COD contribution to both sides of Equation 17 in any case since the same quantity of N appears on both sides of the equation. Substituting the respective equations for the COD-containing compounds above yields Equation 18:

$$X_s \cdot [S]_f \cdot COD_S = Y_x \cdot [S]_f \cdot X_s \cdot COD_x + Y_A \cdot [S]_f \cdot X_s \cdot (1 - X_{HAc}) \cdot COD_{HAc} + Y_M \cdot [S]_F \cdot X_S \cdot X_{HAc} \cdot COD_M \qquad \text{Equation 18}$$

where

X_s is the conversion of sucrose

$[S]_f$ is the molar concentration of sucrose in the feed (mol/L)

X_{HAc} is the conversion of the HAc formed

COD_{HAc} and COD_M are the molar COD of HAc and CH_4 respectively, both with a value of 64 g-COD/mol

Further dividing Equation 18 through by $(X_s \cdot [S]_f)$ yields Equation 19:

$$COD_S = Y_x \cdot COD_x + Y_A \cdot (1 - X_{HAc}) \cdot COD_{HAc} + Y_M \cdot X_{HAc} \cdot COD_M \quad \text{Equation 19}$$

Therefore, at a 0% conversion of HAc ($X_{HAc} = 0$):

$$Y_A = \frac{COD_S - Y_x \cdot COD_x}{COD_{HAc}} \quad \text{Equation 20}$$

and at a 100% conversion of HAc ($X_{HAc} = 100\%$):

$$Y_M = \frac{COD_S - Y_x \cdot COD_x}{COD_M} \quad \text{Equation 21}$$

Since $COD_{HAc} = COD_M$, $Y_A = Y_M$

The yield coefficient of CO_2 (Y_C) can then be calculated through a C-balance as follows:

$$12 \cdot 1 = 5 \cdot Y_x + 1 \cdot Y_C + 1 \cdot Y_M \cdot X_{HAc} + 2 \cdot Y_A \cdot (1 - X_{HAc}) \quad \text{Equation 22}$$

Rearranging Equation 22, solving for Y_C, and acknowledging that $Y_A = Y_M$ yields Equation 23:

$$Y_C = Y_A \cdot X_{HAc} + (12 - 5 \cdot Y_x - 2 \cdot Y_A) \quad \text{Equation 23}$$

A summary of the values of the stoichiometric parameters (yield coefficients and value of "a") calculated using Equation 13-Equation 23 is presented in Table 4-1.

Table 4-1: Summary of the model stoichiometric parameters

Parameter	Value
Y_N	-0.397
Y_x	0.231
a	1.72
Y_A	5.34
Y_M	5.34
Y_C	$5.34 \cdot X_{HAc} + 0.173$

Influent proton balance equation

Performing a proton balance (Equation 24) on a solution with fully specified total species concentrations of weak acids/bases provides the basis for the mathematical relationship between the H^+ concentration and the weak acid and base concentrations.

$$\sum H^+ \, gained = \sum H^+ \, lost \quad \text{Equation 24}$$

It is helpful to construct a proton balance diagram to aid in the derivation of the proton balance equation. To perform the proton balance on the feed, the proton balance diagram illustrated in Figure 4-2 was drawn. In the middle row are the chemical compounds added to the solution. One row above represents the species formed if the weak acid/base compounds added gain a proton from the solution, and two rows the species which have gained two protons. One row below represents the species that have lost a proton to the bulk solution.

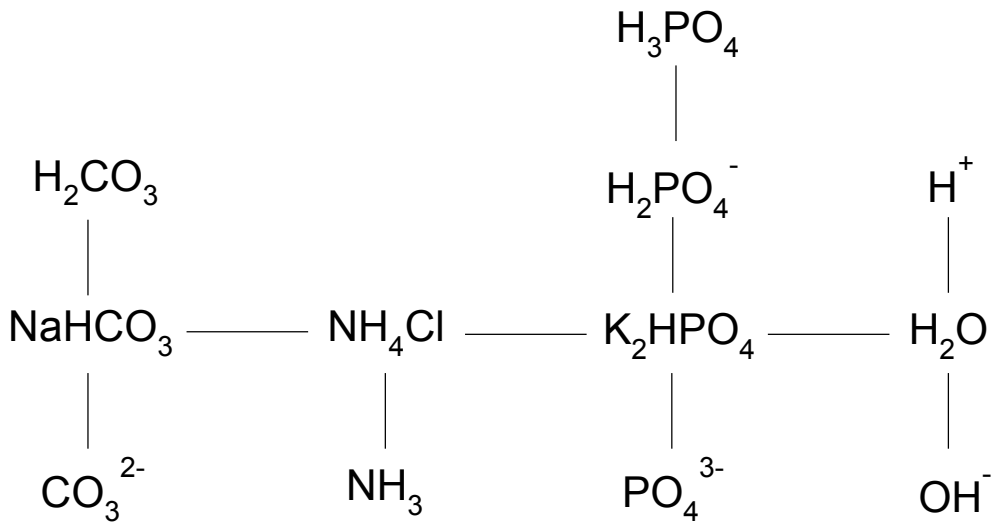

Figure 4-2: Influent proton balance diagram

With the aid of Figure 4-2, the influent proton balance equation (Equation 25) was derived:

$$[H^+] + [H_2CO_3] + [H_2PO_4^-] + 2[H_3PO_4] = [CO_3^{2-}] + [NH_3] + [PO_4^{3-}] + [OH^-] \quad \text{Equation 25}$$

To relate the ion concentrations in Equation 25 to the concentrations of weak acid/base compounds added to solution, the total species concentrations are first defined by Equation 26-Equation 28:

$$C_T = [H_2CO_3] + [HCO_3^-] + [CO_3^{2-}] \quad \text{Equation 26}$$

$$P_T = [H_3PO_4] + [H_2PO_4^-] + [HPO_4^{2-}] + [PO_4^{3-}] \quad \text{Equation 27}$$

$$N_T = [NH_3] + [NH_4^+] \quad \text{Equation 28}$$

Because all carbonate, phosphate and FSA species present in solution are formed from the re-speciation of the $NaHCO_3$, K_2HPO_4 and NH_4Cl added to the feed, C_T, P_T and N_T of the feed solution ($C_{T,f}$, $P_{T,f}$, $N_{T,f}$) are equal to the molar concentrations of $NaHCO_3$, K_2HPO_4 and NH_4Cl added to the feed. Equation 29-Equation 35 were then derived from Equation 26-Equation 28 and the definitions of the equilibrium/dissociation constants (Equation 64-Equation 71 in Appendix A:) to relate the individual ionic species concentrations present in Equation 25 to the total species concentrations C_T, P_T and N_T.

$$[H_2CO_3] = \frac{C_T}{1 + \frac{K_{C1}}{[H^+]} + \frac{K_{C1}K_{C2}}{[H^+]^2}} \quad \text{Equation 29}$$

$$[\mathrm{H_2PO_4^-}] = \frac{\mathrm{P_T}}{1 + \frac{[\mathrm{H^+}]}{\mathrm{K_{P1}}} + \frac{\mathrm{K_{P2}}}{[\mathrm{H^+}]} + \frac{\mathrm{K_{P2}K_{P3}}}{[\mathrm{H^+}]^2}} \quad \text{Equation 30}$$

$$[H_3PO_4] = \frac{P_T}{1 + \frac{K_{P1}}{[H^+]} + \frac{K_{P1}K_{P2}}{[H^+]^2} + \frac{K_{P1}K_{P2}K_{P3}}{[H^+]^3}} \quad \text{Equation 31}$$

$$[CO_3^{2-}] = \frac{C_T}{1 + \frac{[H^+]^2}{K_{C1}K_{C2}} + \frac{[H^+]}{K_{C2}}} \quad \text{Equation 32}$$

$$[NH_3] = \frac{N_T}{1 + \frac{[H^+]}{K_N}} \quad \text{Equation 33}$$

$$[PO_4^{3-}] = \frac{P_T}{1 + \frac{[H^+]^3}{K_{P1}K_{P2}K_{P3}} + \frac{[H^+]^2}{K_{P2}K_{P3}} + \frac{[H^+]}{K_{P3}}}$$ Equation 34

$$[OH^-] = \frac{K_W}{[H^+]}$$ Equation 35

where

K_N is the dissociation constant for the weak acid NH_4Cl

K_{C1} and K_{C2} are the first and second dissociation constants of H_2CO_3 respectively

K_{P1}, K_{P2} and K_{P3} are the first, second and third dissociation constants of H_3PO_4 respectively

K_W is the dissociation constant for water

Substituting Equation 29-Equation 35 into Equation 25 and moving all terms to the RHS yields Equation 36.

$$\begin{aligned} 0 = {} & \frac{N_T}{1 + \frac{[H^+]}{K_N}} + \frac{K_W}{[H^+]} + \frac{P_T}{1 + \frac{[H^+]^3}{K_{P1}K_{P2}K_{P3}} + \frac{[H^+]^2}{K_{P2}K_{P3}} + \frac{[H^+]}{K_{P3}}} + \frac{C_T}{1 + \frac{[H^+]^2}{K_{C1}K_{C2}} + \frac{[H^+]}{K_{C2}}} \\ & - \frac{C_T}{1 + \frac{K_{C1}}{[H^+]} + \frac{K_{C1}K_{C2}}{[H^+]^2}} - \frac{P_T}{1 + \frac{[H^+]}{K_{P1}} + \frac{K_{P2}}{[H^+]} + \frac{K_{P2}K_{P3}}{[H^+]^2}} \\ & - \frac{2P_T}{1 + \frac{K_{P1}}{[H^+]} + \frac{K_{P1}K_{P2}}{[H^+]^2} + \frac{K_{P1}K_{P2}K_{P3}}{[H^+]^3}} - [H^+] \end{aligned}$$ Equation 36

The right-hand side (RHS) of Equation 36 provides a function that can be targeted to be set to zero through manipulation of the H^+ concentration by the Solver add-in in Microsoft Excel, in which the model is implemented. The H^+ concentration that results in the function being equal to zero corresponds with the pH at which the protons gained equal those lost by the weak acid/base compounds added ($C_{T,f}$, $N_{T,f}$, $P_{T,f}$). It must be noted that the values of the equilibrium/dissociation constants used to describe the feed speciation were calculated for 20°C, which is the temperature at which the feed pH was measured.

Inputs and effluent concentrations

In addition to specification of the influent $NaHCO_3$, K_2HPO_4 and NH_4Cl concentrations, the influent sucrose concentration, influent flow rate, and the conversions of sucrose and HAc formed also require specification. The conversions of sucrose and HAc are defined by Equation 37 and Equation 38 respectively.

$$X_S = \frac{[S]_{in} - [S]_{out}}{[S]_{in}}$$ Equation 37

$$X_{HAc} = \frac{[HAc]_{formed} - [HAc]_{out}}{[HAc]_{formed}}$$ Equation 38

where

$$[HAc]_{formed} = [S]_{in} \cdot X_S \cdot Y_A$$ Equation 39

The effluent concentrations and gaseous CO_2 and CH_4 productivities are defined in terms of the influent total species concentrations, stoichiometry, and conversions as follows:

$$A_T = Y_A \cdot [S_f] \cdot X_S \cdot (1 - X_{HAc})$$ Equation 40

$$C_T = C_{T,f} + Y_C \cdot [S_f] \cdot X_S - \frac{\dot{n}_{CO_2}}{v}$$ Equation 41

$$N_T = N_{T,f} + Y_N \cdot [S_f] \cdot X_S$$ Equation 42

$$\dot{V}_M = v \cdot Y_M \cdot [S_f] \cdot X_S \cdot X_{HAc} \cdot \frac{RT}{P}$$ Equation 43

where

$$A_T = [HAc] + [Ac^-]$$ Equation 44

v is the feed flow rate (L/day)

$\dot{V}_M$ is the volumetric productivity of methane (L/day)

R is the universal gas constant (= 0.0821 L.atm/mol.K)

T is the temperature at standard conditions (25°C)

P is the pressure at standard conditions (1 atm)

$\dot{n}_{CO_2}$ is the volume of CO2 gas produced

The volume of CO_2 produced is calculated using the relationship between $[H_2CO_3]$ and the headspace $ppCO_2$ given by Henry's Law below:

$$K_{C0} = \frac{[H_2CO_3]}{ppCO_2}$$ Equation 45

where

$$ppCO_2 = P \cdot \frac{\dot{n}_{CO_2}}{\dot{n}_{CO_2} + \dot{n}_{CH_4}}$$ Equation 46

and

$$\dot{n}_{CH_4} = v \cdot Y_M \cdot [S_f] \cdot X_S \cdot X_{HAc}$$ Equation 47

However, $[H_2CO_3]$ is dependent on the reactor pH and C_T according to Equation 29. Rearranging Equation 45 and substituting the RHS of Equation 29 and Equation 46 for the values of $[H_2CO_3]$ and $ppCO_2$ yields

$$P \cdot \frac{\dot{n}_{CO_2}}{\dot{n}_{CO_2} + \dot{n}_{CH_4}} = \frac{C_T}{K_{C0} \cdot \left(1 + \frac{K_{C1}}{[H^+]} + \frac{K_{C1}K_{C2}}{[H^+]^2}\right)}$$ Equation 48

However, the value of C_T is also dependent on the production of CO_2 in accordance with Equation 41. Substituting Equation 41 for the value of C_T yields Equation 49:

$$P \cdot \frac{\dot{n}_{CO_2}}{\dot{n}_{CO_2} + \dot{n}_{CH_4}} = \frac{C_{T,f} + Y_C \cdot [S_f] \cdot X_S - \frac{\dot{n}_{CO_2}}{v}}{K_{C0} \cdot \left(1 + \frac{K_{C1}}{[H^+]} + \frac{K_{C1}K_{C2}}{[H^+]^2}\right)}$$ Equation 49

α and β are defined as per Equation 50 and Equation 51 respectively for convenience of solving for $\dot{n}_{CO_2}$:

$$\alpha = K_{C0} \cdot \left(1 + \frac{K_{C1}}{[H^+]} + \frac{K_{C1}K_{C2}}{[H^+]^2}\right)$$ Equation 50

$$\beta = C_{T,f} + Y_C \cdot [S_f] \cdot X_S - \frac{\dot{n}_{CO_2}}{v}$$ Equation 51

Substituting Equation 50 and Equation 51 into Equation 49 and rearranging yields Equation 52:

$$\alpha \cdot P \cdot \dot{n}_{CO_2} = \left(\dot{n}_{CO_2} + \dot{n}_{CH_4}\right)\left(\beta - \frac{\dot{n}_{CO_2}}{v}\right)$$ Equation 52

Simplifying and rearranging Equation 52 reveals a quadratic equation for $\dot{n}_{CO_2}$:

$$\dot{n}_{CO_2}{}^2 + \left(\alpha \cdot P \cdot v - \beta \cdot v + \dot{n}_{CH_4}\right) \cdot \dot{n}_{CO_2} - \dot{n}_{CH_4} \cdot \beta \cdot v = 0$$ Equation 53

Defining $\left(\alpha \cdot P \cdot v - \beta \cdot v + \dot{n}_{CH_4}\right)$ as “b” and $\left(\dot{n}_{CH_4} \cdot \beta \cdot v\right)$ as “c”, the value of $\dot{n}_{CO_2}$ can be solved for using the quadratic formula (Equation 54).

$$\dot{n}_{CO_2} = \frac{-b \pm \sqrt{b^2 - 4 \cdot c}}{2}$$ Equation 54

Since “b” holds a positive value, the second (square root) term must be added to render the production of CO_2 positive. Therefore, the value of $\dot{n}_{CO_2}$ is calculated using Equation 55:

$$\dot{n}_{CO_2} = \frac{-b + \sqrt{b^2 - 4 \cdot c}}{2}$$ Equation 55

Effluent pH calculation

The proton balance diagram for the effluent is illustrated in Figure 4-3.

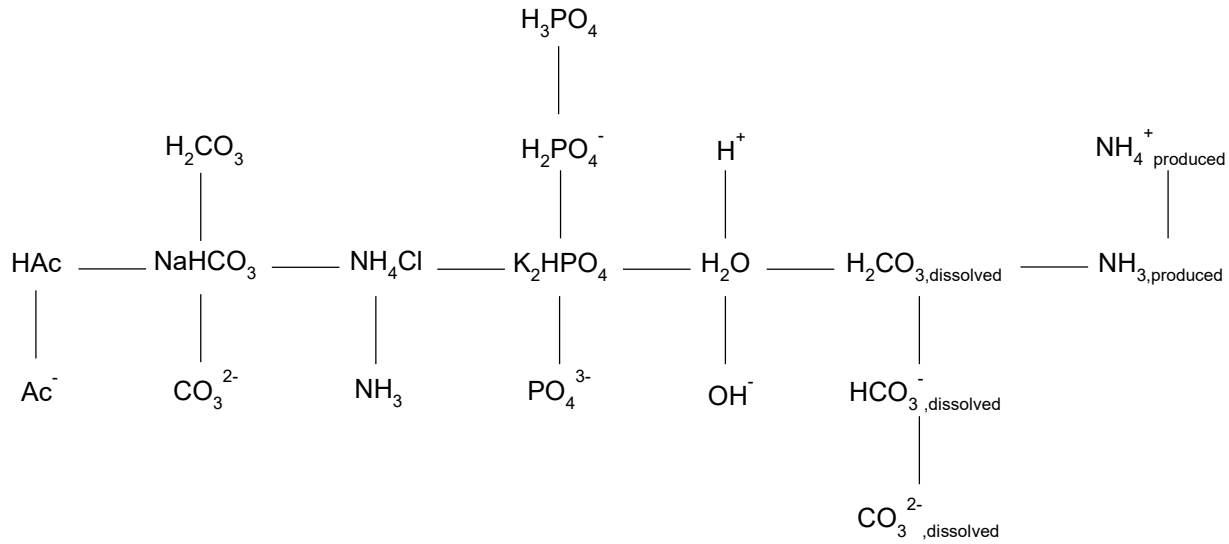

Figure 4-3: Effluent proton balance diagram

This diagram builds on the influent proton balance diagram (Figure 4-2), with the addition of the HAc, $H_2CO_{3,dissolved}$ and $NH_{3,produced}$ columns. These compounds are included in the same row as the compounds added to the feed ($NaHCO_3$, NH_4Cl, K_2HPO_4, H_2O) because these are the forms in which they are produced in the AD process. In the case of $NH_{3,produced}$, this term is actually negative due to the net removal of NH_3 from the system. However, it is termed as being produced because the yield coefficient of NH_3 in the stoichiometry is negative. The proton balance equation derived with the aid of Figure 4-3 is shown below (Equation 56):

$$[H^+] + [H_2CO_3] + [H_2PO_4^-] + 2[H_3PO_4] + [NH_4^+]_{produced} = [NH_3] + [A^-] + [CO_3^{2-}] + [OH^-] + [PO_4^{3-}] + \left[HCO_{3,dissolved}^-\right] + 2\left[CO_{3,dissolved}^{2-}\right] \quad \text{Equation 56}$$

where

$$[NH_4^+]_{produced} = Y_N \cdot [S_f] \cdot X_S \cdot \frac{[NH_4^+]}{N_T} \quad \text{Equation 57}$$

$$[A^-] = \frac{A_T}{1 + \frac{[H^+]}{K_a}} \quad \text{Equation 58}$$

$$\left[HCO_{3,dissolved}^-\right] = (C_T - C_{T,f}) \cdot \frac{[HCO_3^-]}{C_T} \quad \text{Equation 59}$$

$$\left[CO_{3,dissolved}^{2-}\right] = (C_T - C_{T,f}) \cdot \frac{[CO_3^{2-}]}{C_T} \quad \text{Equation 60}$$

and

$$\frac{[NH_4^+]}{N_T} = \frac{1}{1 + \frac{K_N}{[H^+]}} \quad \text{Equation 61}$$

No H_2CO_3, HCO_3^- or CO_3^{2-} is explicitly produced from the process stoichiometry. However, some of the CO_2 produced dissolves in the effluent biogas depending on the pH. This CO_2 that does dissolve is equivalent to $(C_T - C_{T,f})$, and becomes H_2CO_3, which then mostly dissociates (at the pH of operation) to form HCO_3^- and a minute quantity of CO_3^{2-}, as shown in Figure 4-4.

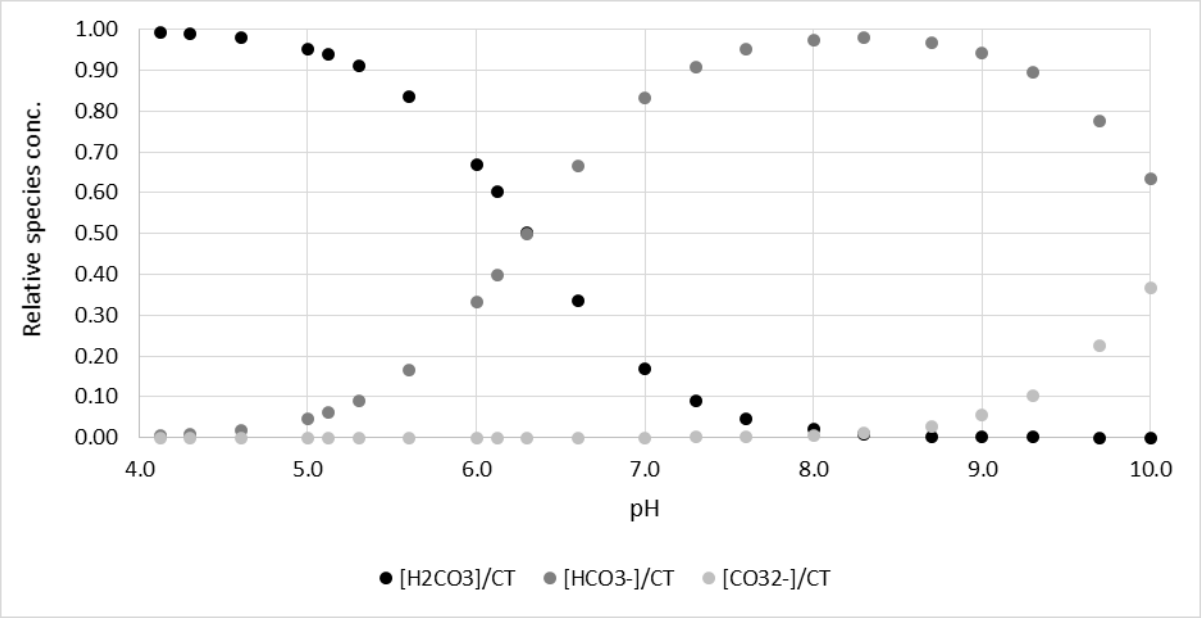

Figure 4-4: Concentrations of H_2CO_3, HCO_3^- and CO_3^{2-} relative to C_T as a function of the pH

Substituting Equation 29-Equation 35 and Equation 57-Equation 60 for the terms in the effluent proton balance equation (Equation 56), and moving all terms to the RHS yields Equation 62:

$$0 = \frac{N_T}{1+\frac{[H^+]}{K_N}} + \frac{A_T}{1+\frac{[H^+]}{K_a}} + \frac{C_T}{1+\frac{[H^+]^2}{K_{C1}K_{C2}}+\frac{[H^+]}{K_{C2}}} + \frac{K_W}{[H^+]} + \frac{P_T}{1+\frac{[H^+]^3}{K_{P1}K_{P2}K_{P3}}+\frac{[H^+]^2}{K_{P2}K_{P3}}+\frac{[H^+]}{K_{P3}}} + \left(C_T - C_{T,f}\right)\cdot\frac{[HCO_3^-]}{C_T} + 2\cdot\left(C_T - C_{T,f}\right)\cdot\frac{[CO_3^{2-}]}{C_T} - [H^+] - \frac{C_T}{1+\frac{K_{C1}}{[H^+]}+\frac{K_{C1}K_{C2}}{[H^+]^2}} - \frac{P_T}{1+\frac{[H^+]}{K_{P1}}+\frac{K_{P2}}{[H^+]}+\frac{K_{P2}K_{P3}}{[H^+]^2}} - \frac{2\cdot P_T}{1+\frac{K_{P1}}{[H^+]}+\frac{K_{P1}K_{P2}}{[H^+]^2}+\frac{K_{P1}K_{P2}K_{P3}}{[H^+]^3}} - \frac{Y_N\cdot[S_f]\cdot X_S}{1+\frac{K_N}{[H^+]}} \quad \text{Equation 62}$$

This CO_2 dissolution is governed by the simultaneous equilibrium between the pH of the reactor and the $ppCO_2$ in the headspace. The RHS of Equation 62 will be equal to zero only when the protons gained and lost by the weak acid/base present in the liquid phase balance, and the gas and liquid phase equilibrium condition between $[H_2CO_3]$ and $ppCO_2$ is satisfied. As for the influent proton balance, Solver is used to set the RHS of Equation 62 to zero by manipulating the effluent H^+ concentration, which solves for the equilibrium pH of the reactor effluent.

4.1.4 Model Validation

A spreadsheet implementation of the Sludge Digestion Model described by Sotemann et al. (2005) was used to validate the results obtained by the stoichiometric model described above in this chapter. Results of the Sludge Digestion Model (Sötemann *et al.*, 2005) were compared with Scenario 2 of the stoichiometric model. The reason for this is that the Sludge Digestion Model assumes hydrolysis to be the rate-limiting step, and so does not include acetic acid generation. Scenario 2 of the stoichiometric

model assumes 100% conversion of acetic acid, and therefore presents a comparable scenario with the Sludge Digestion Model. The results of the main AD performance variables as predicted by both models are included in Table 6-2 in Appendix E. Furthermore, a Carbon balance and COD balance for the stoichiometric model are presented in Table 6-3 and Table 6-4 respectively, proving consistency of the mathematical expressions used.

5. Experimental Results and Discussion

5.1 First UASB experiment

The aim of this experiment was to operate the two UASB reactors described in Section 3.1.1 and referred to as R1 and R2, at increasing organic loading rates (OLRs). The purpose of this experiment was to collect steady state data at each OLR above 6 g-COD/L.day. The sole carbon-source for R1 was sucrose, whereas R2 was initially fed a mixture of sucrose and carboxymethyl cellulose (CMC).

5.1.1 System Performance and development

A broad summary of the first UASB experiment indicating the dates corresponding to the applied OLR is given in Table 5-1.

Table 5-1: Summary of the performance of the UASB reactor systems in the first experiment

Day	OLR (g/L.day)		HRT (h)	Effluent pH	Soluble COD* removal (%)	Biogas composition (% CH_4)	
	R1	R2				R1	R2
1	1	1	36	6.8-7	>90%	-	-
66†	2	1	18	6.6-6.8	>90%	-	-
80	3.6	1.8	10	~6.5	>90%	-	-
163α	5.4	5.4	6.7	~6.5	80-90%	50%	56%
290	9	9	4	~6.5	70-80%	54%	55%

*Note that in the case of R2 this value only applies to the removal of the sucrose component of the feed for the first OLR of 1 g/L.day
†At this point CMC was removed from the feed for R2 resulting in R2 receiving a lower OLR than R1
αAt this point R2 received the same feed sucrose concentration and therefore the same OLR as R1

Biogas production was observed soon after inoculation, and by Day 15 >90% and >50% of the COD was being removed from Reactor 1 (R1) and Reactor 2 (R2) respectively, with effluent pH >6.8. However, in spite of R1 removing >90% of the influent COD, the percentage of COD removed from R2 never rose significantly above 50%. This indicated that the CMC was not being degraded. Furthermore, R2 in particular experienced a number of episodes in which the sludge bed would begin to float due to the entrapment of biogas formed within the bed. This was assigned to the high viscosity in R2 resulting from the CMC, in combination with a less turbulent sludge bed environment from the lower biogas production, allowing the granules in the sludge bed to stick together. This lack of satisfactory performance at the initial OLR of 1 g-COD/L.day deterred the progression of the study. Eventually the recycle flow rate was increased to ~60 L/day (corresponding to a recycle ratio of ~20 and a superficial upflow velocity of ~0.7 m/h) and the hydraulic retention time (HRT) was halved (with a corresponding doubling in OLR) on Day 66 in an attempt to increase the turbulence in the sludge bed. At the same time, the CMC component of the feed for R2 was removed, and R2 received a lower concentration of COD and experienced a lower OLR as a result. The sucrose component of R2's feed was increased over the following months until it equalled that being fed to R1.

After 5 days at the new OLR, both reactors were again removing >90% of the COD fed, and on Day 80 the OLR was further increased to 3.6 g-COD/L.day. At this point, the hydraulic retention time (HRT) couldn't be further lowered due to the need for a larger vessel to prepare and store feed in. In addition to this, substrate was becoming contaminated frequently due to a lack of means of sterilisation. This meant that both reactors were often fed a slightly fermented substrate, which also appeared to detriment reactor performance.

On Day 120 new feed drums were installed in the walk-in refrigerated room. It took nearly a month of operation to establish the correct frequency with which feed tubing and the feed drums required cleaning. During this time, reactor performance was dissatisfactory in that floating sludge incidents were still being observed. In addition to this, the presence of a scum layer on the surface of the reactor liquor caused blockage of the recycle and/or effluent ports, causing the recycle flow to stop, or in a few cases

the washout of some sludge. However, >90% of the soluble COD fed to the reactor was still being removed from the aqueous phase (i.e. being converted to either sludge or CH_4).

Eventually it was decided on Day 163 that poor settleability of the sludge and its tendency to float may be due to too little turbulence within the sludge bed, hence the OLR was increased again to ~5 g-COD/L.day by increasing the feed flow rate. However, the problem with floating sludge persisted. By this stage it was clearly observable that the structure of the granules had deteriorated. Many granules looked broken and damaged, and a fluffy white layer coated them. A picture of a sludge sample representative of the state of the sludge in both reactors is shown in Figure 5-1.

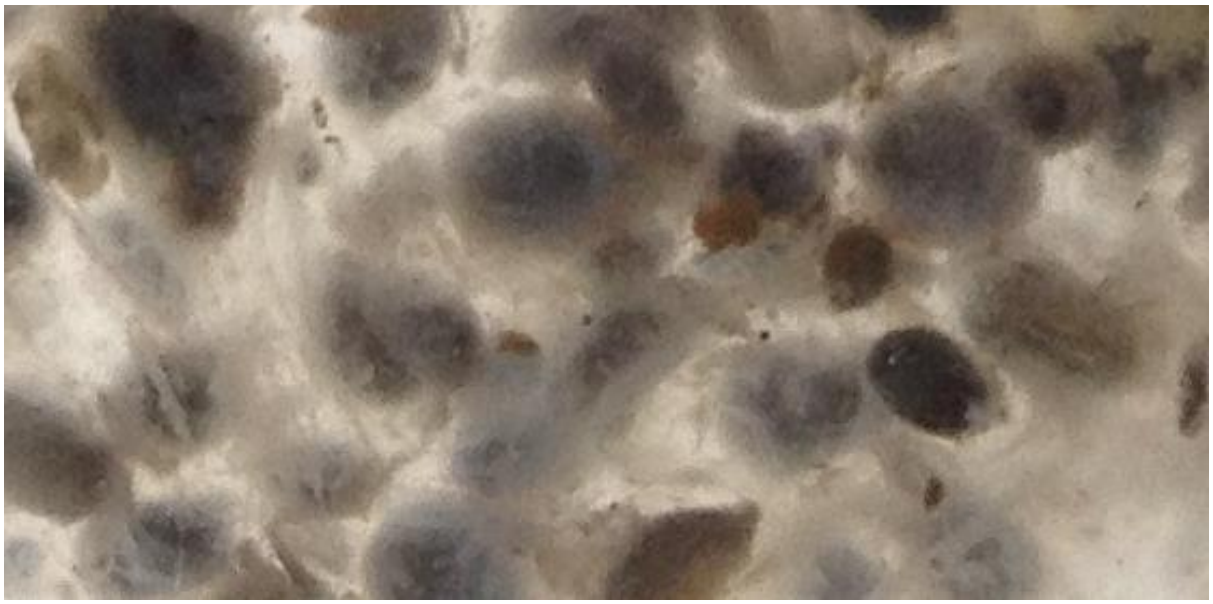

Figure 5-1: Sludge granules after being underfed for four months

This fluffy layer trapped biogas bubbles and caused the sludge to float. In incidents where the sludge bed was floating, N_2 gas was sparged multiple times using a 140 mL syringe to break up the sludge mass and liberate the trapped gas bubbles. It was attempted a number of times to flush out the fluffy white substance using 10 L of tap water. This material was thought to be a contaminant, and appeared to be replacing the sludge granules. However, this approach was completely ineffective, and within a day the sludge bed would appear as it had the day before flushing.

Over the course of this experiment the effluent pH of both reactors steadily dropped until around Day 200 R1 and R2 had an effluent pH of 6.31 and 6.43 respectively. As low pH conditions are not ideal for granule growth, the pH and buffer capacity of the feed was increased by increasing the $NaHCO_3$ concentration from 1000 mg/L to 1500 mg/L. This increased the effluent pH to 6.5-6.6, but there was little observable improvement in the condition of the sludge over the course of the next month.

After reading literature reports of similar issues it was discovered that the fluffy white substance was likely to comprise mostly of exogenous polymeric substance (EPS). EPS is produced to mediate the bondage of microorganisms within a biofilm, or in this case granule (Fukuzaki *et al.*, 1995). In UASB systems, EPS comprises mostly protein and polysaccharides which are thought to provide the linkage between microbial cells via polyvalent cations (Fukuzaki *et al.*, 1995). As the amount of N being supplied (13.7 mg-N/g-COD) was the amount calculated for cell growth only, this would be too little to allow for both cell and EPS production. The N concentration in the feed was increased to 68 mg-N/g-COD, which is in excess of the 20 mg-N/g-COD recommended by Sam-Soon et al. (1990). Furthermore, it was discovered that the substrate composition was deficient in S. The concentration of $MgSO_4.7H_2O$ was also increased from 6.39 to 16.7 mg/g-COD. Of the polyvalent cations found in anaerobic sludge granules, Ca is usually found in significant quantities within sludge granules (Fukuzaki *et al.*, 1995; Yu *et al.*, 2001), but was not initially added to the substrate for this study due both to the presence of 12 mg-Ca^{2+}/L in the tapwater (a greater concentration than that calculated as being required for cell growth) and the addition of Ca in the form of $CaCl.2H_2O$ causing precipitation of other compounds in the

substrate. To account for this, 191 mg-$CaCl_2.2H_2O$/L was incorporated into the feed in an attempt to increase the settleability of the sludge and to prevent the formation of the fluffy outer layer. The concentration of Fe was also increased from 1.83 to 6.67 mg-$FeCl_3$/g-COD since Fe is also often found to accumulate in anaerobic sludge granules (Schmidt and Ahring, 1996).

VSS and TSS tests performed on sludge bed and effluent samples on Day 282 revealed a VSS/TSS ratio of 88% and 90% for R1 and R2, indicating a very low inorganic solids content of the sludge. This reflects the low influent concentration of the major inorganic sludge components Ca and Fe. The same test showed that the effluent TSS concentration was around 360 mg-L, indicating the poor effluent quality resulting from the fluffy growth.

However, amendment of the substrate nutrient and buffer concentrations failed to yield more distinct granules. The OLR was increased to 9 g-COD/L.day on Day 290 in an attempt to increase the turbulence of the sludge bed. However, by this stage the settleability of the original sludge granules had deteriorated too much, especially with the attachment or entrapment of gas bubbles, causing washout of most of the sludge. The experiment was terminated on Day 318.

5.1.2 Discussion

In summary, the progress of this experiment was prevented by deterioration of the sludge granules used to inoculate both reactors. The conditions thought to have caused the deterioration of the granular inoculum include underfeeding the sludge, feeding partially fermented substrate containing acidogenic biomass, and not providing enough nutrients. Contamination of the feed substrate in the 5 L and 10 L Schott bottles initially used as feed containers posed the issue of scale-up of feed preparation. As a result, the reactors were initially underfed, and the feed was often contaminated by opportunistic fermentative bacteria present in the air. Although partially fermented, or “sour”, substrate has been treated effectively in UASB reactors (Lettinga *et al.*, 1980), feeding reactors with substrate containing the acidogenic biomass which results from this souring has been documented as being detrimental to granule formation (Vanderhaegen *et al.*, 1992). Moreover, underfeeding the sludge results in a less turbulent sludge bed environment due to a lower specific biogas production (volume of biogas produced per volume of sludge). In this low-shear environment, the filamentous growth of the hydrophobic methanogenic *Methanosaeta spp.* is not limited to shorter filaments, and the growth of loosely-bound (LB) exogenous polymeric substances (EPS) with a higher proteinaceous EPS (PN-EPS) content is favoured (Wang *et al.*, 2017). R2 was more adversely affected by this phenomenon due to being fed half the readily-biodegradable COD initially, resulting in roughly half the biogas production compared with R1. This explains the higher frequency of sludge bed flotation incidents in R2 compared with R1.

In the fourth month of the experiment this situation was resolved through the installation of feed drums in a walk-in fridge. However, by this stage the sludge granules had developed a fluffy white outer layer (pictured in Figure 5-1) which was viscous and prone to the attachment and entrapment of gas bubbles, giving the sludge bed a tendency to float.

It is noteworthy that even at a low pH of 6.5 and under conditions not conducive to granule formation, the majority (70-90%) of the soluble COD was converted into either sludge (biomass and EPS) or CH_4. This indicates the robustness of the microbial consortia present even under these sub-optimal conditions. However, the type of sludge produced under these substrate-limited conditions performs poorly in a UASB reactor, where settleability and stability within the reactor are required. As the experiment progressed, most of these solids were present as sludge agglomerates (similar to the white substance shown in Figure 5-1). This sludge meets the visual criteria of LB-EPS as described by Fukuzaki et al. (1995) as a “thick polymeric coat… resulting in fluffy granule formation”, and by Wang et al. (2017) as “loose and dispersible slime layer found in the outer layer of sludge flocs without an obvious edge”.

Also worth noting is that within two weeks of inoculating R2, the entire sludge bed began to float. This showed that the characteristics of the sludge agglomerates respond relatively quickly to environmental changes. This phenomenon was also observed in the study by Wang et al. (2017), where sludge granules with positive characteristics (summarised by a low sludge flotation potential (SFP)) were developed from a flotation-prone sludge in 30 days.

5.2 Granulation experiment

The granulation experiment was conducted to establish the cause of the granulation issues that occurred in the first experiment. The importance of the role of mixing within the sludge bed was emphasised in the relevant literature, hence the effect of additional hydraulic mixing on sludge granulation was investigated. The two UASB reactors are referred to as R1 and R2 and are described in Section 3.1.1 were used. R1 was operated with effluent recycling to provide additional hydraulic mixing, while R2 was operated without effluent recycling.

5.2.1 Results

System performance

The performance of the two UASB reactors was monitored through measurement of the soluble COD removal, biogas productivity and composition, and pH. The soluble COD removal efficiency (percentage of COD removed), CH_4 productivity and OLR are plotted for R1 and R2 in Figure 5-2 and Figure 5-3 respectively. As discussed in Section 2.4.1, the COD converted in a UASB reactor forms either biomass or CH_4. The CH_4 productivity is presented as the equivalent COD of CH_4 produced per litre reactor working volume per day to allow for direct comparison of the portion of the COD fed to the reactor (OLR) that yielded CH_4.

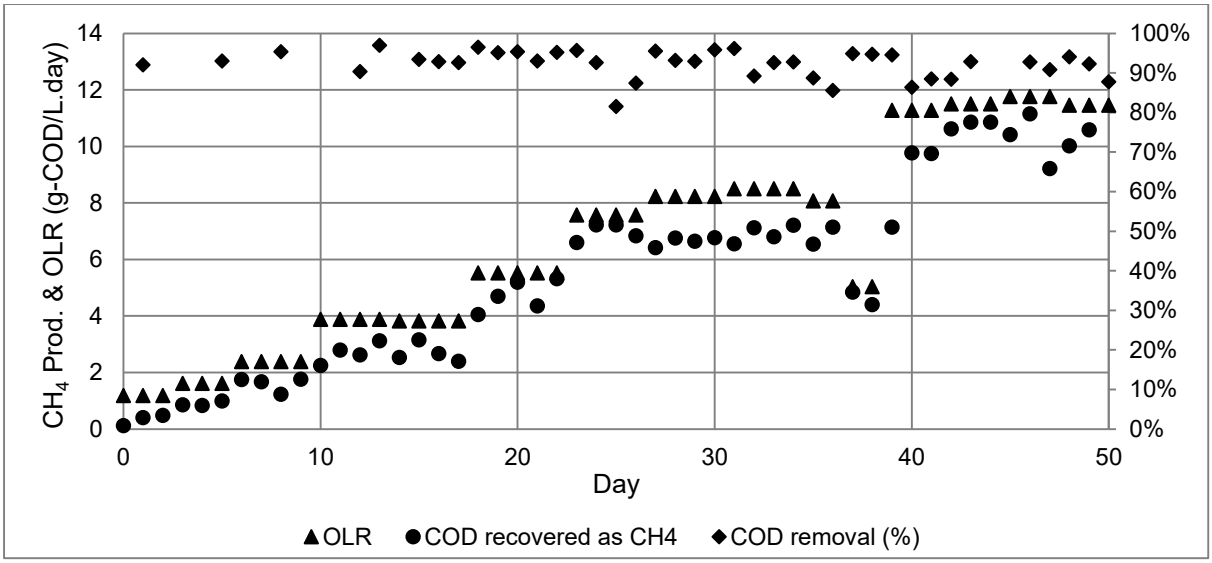

Figure 5-2: Performance of R1 in terms of COD removal and CH_4 productivity

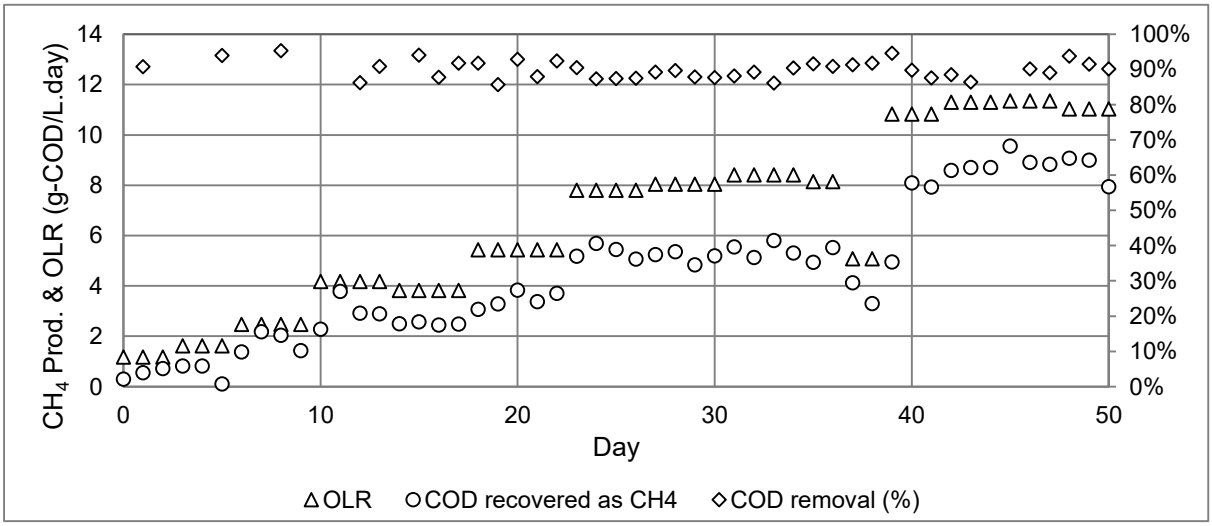

Figure 5-3: Performance of R2 in terms of COD removal and CH_4 productivity

As shown in Figure 5-2 and Figure 5-3, the majority of the COD fed to the reactors was removed from the aqueous phase and recovered as CH_4. The average soluble COD removal was 92 ± 3% for R1 and 90 ± 3% for R2. It is clear that a lower CH_4 yield was measured for R2 than for R1. The percentage of COD removed that was recovered as CH_4 over the entire experimental period was calculated as 91% for R1 and 76% for R2.

It should be noted that in the beginning of the experiment the effluent port of R2 was occasionally blocked by solid debris. This resulted in a rise in the liquid level in the reactor, forcing more biogas through the gas meters and causing an error in the biogas productivity measurement. An error in the measurement would also often occur after the blockage cleared due to part of the biogas produced being required to displace the accumulated reactor liquor until the pressure in the reactor headspace was once again equilibrated with that in the gas meter and overflow flasks. Such events were noted to occur on days 4, 7, 8 and 11 for R2, which is reflected in the disparity between the results recorded for these days and those preceding or following them (Figure 5-3).

The biogas composition was measured at five points spread across the experiment, the results of which are presented in Table 5-2. The values calculated for the equivalent COD of CH_4 produced (presented in Figures Figure 5-2 and Figure 5-3) were calculated using the biogas compositions in Table 5-2 according to Appendix D.2. There is a relatively large variation in measured biogas compositions.

Table 5-2: Biogas composition over the course of the granulation experiment

Day	Biogas composition (%CH_4)	
	R1	R2
5	64%	58%
19	57%	55%
28	53%	49%
40	54%	58%
50	56%	54%

The results of the effluent pH for R1 and R2 are presented in Figure 5-4 and Figure 5-5 respectively. The pH of the feed is not shown on the graphs and was between 8.00 and 8.10. The effluent pH is much lower, and drops over the course of the first 3-4 weeks from 6.8-6.9 to ~6.5 for both reactors.

Measurements of the concentrations of the most abundant VFA usually found in AD, namely acetic acid (HAc), propionic acid (HPr) and butyric acid (HBu) were performed over one five-day period to investigate the VFA profile generated after increasing the OLR. The results shown in Figure 5-6 and Figure 5-7 show one data point before and four data points following the increase in OLR from ~5.5 to ~8.0 g-COD/L.day. Both reactors produced some VFA on Day 24, most notably HAc, after the increase in OLR on Day 23. However, the composition of the VFA produced is different between R1 and R2, with HBu produced in R1 and HPr produced in R2.

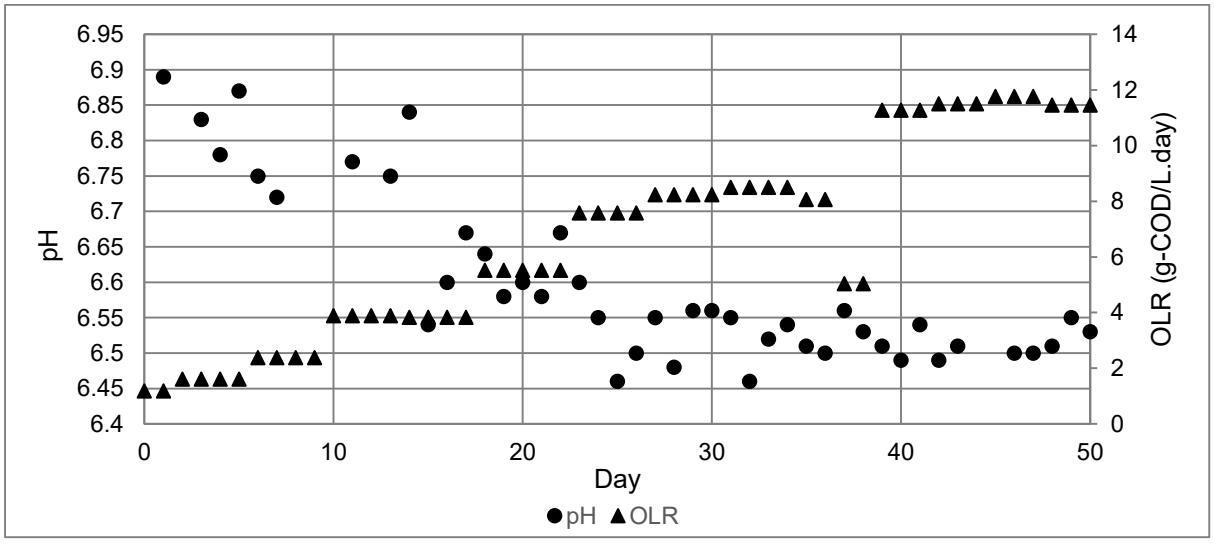

Figure 5-4: R1 effluent pH

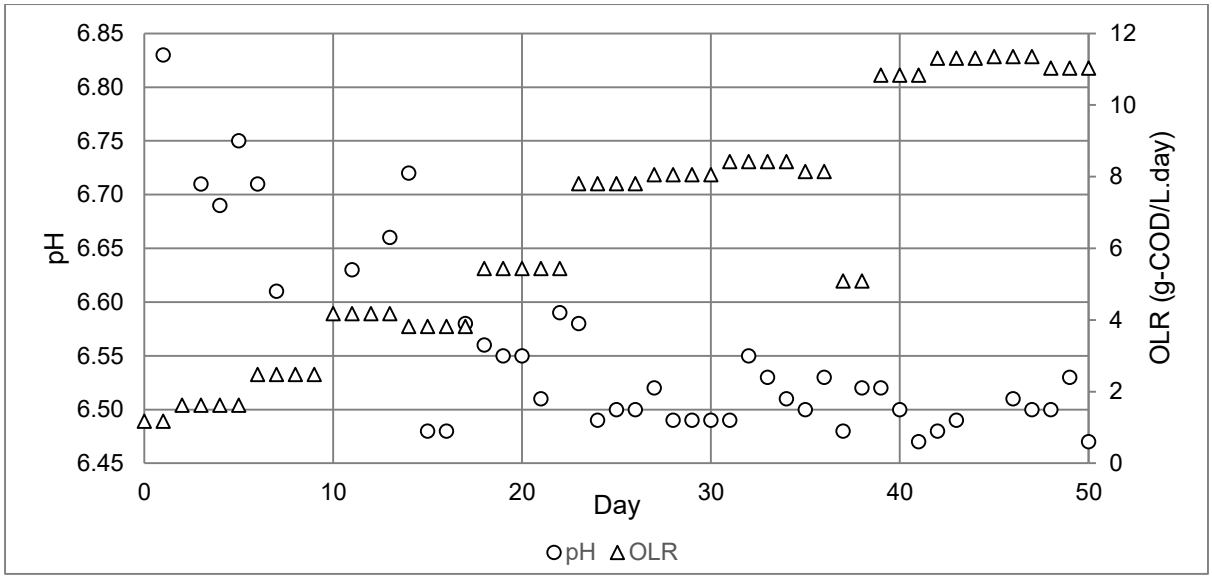

Figure 5-5: R2 effluent pH

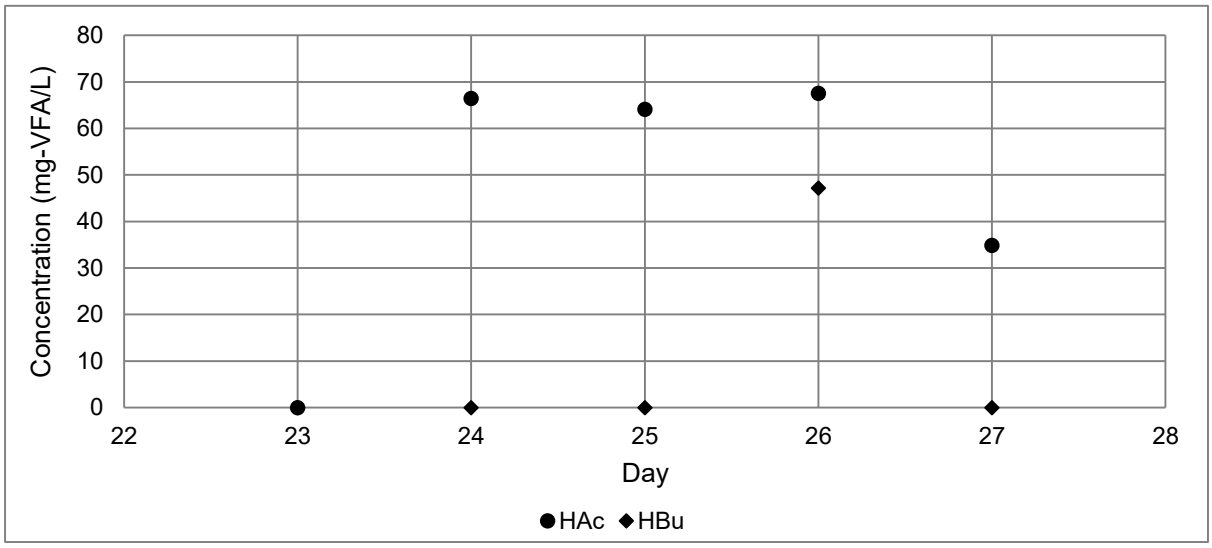

Figure 5-6: VFA profile for R1 after increasing the OLR on Day 23

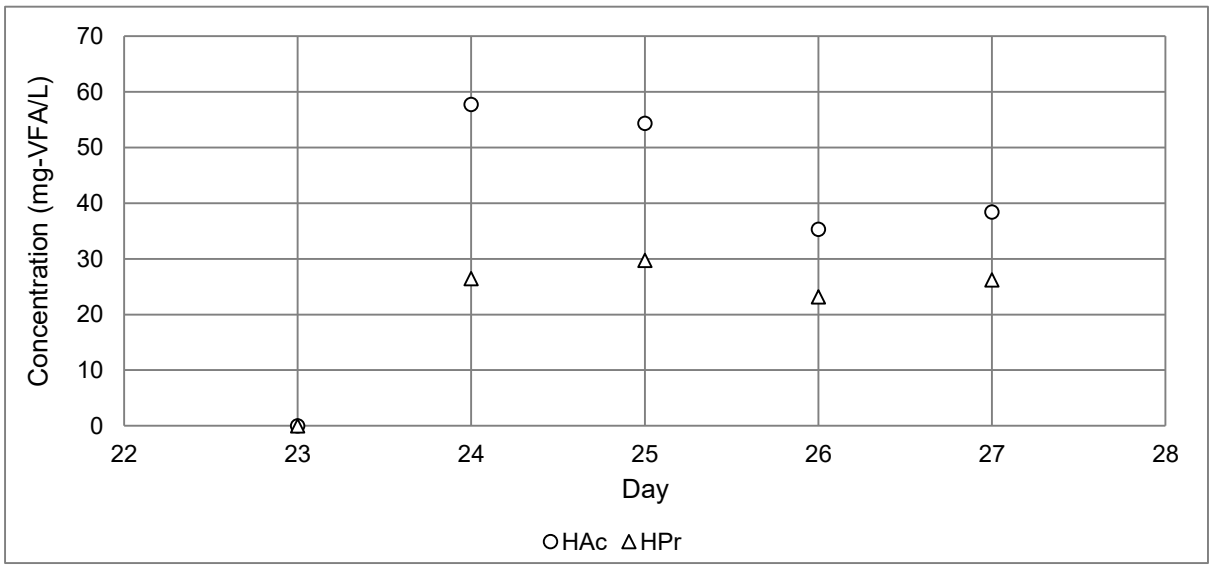

Figure 5-7: VFA profile for R2 after increasing the OLR on Day 23

Sludge bed characterisation

Total suspended solids (TSS) and volatile suspended solids (VSS) were measured along the height of each reactor to quantify the sludge loading rate (SLR), as well as to characterise the density and inorganic content of the sludge beds. The TSS and VSS measurements were processed to determine the average TSS and VSS concentrations within each reactor and the SLR, the results of which are presented along with the superficial upflow velocity in Table 5-3. The results from the TSS and VSS measurements are presented in Figure 5-8.

Table 5-3: Average TSS, VSS, VSS/TSS ratios of the reactor contents, SLR, and upflow velocity over the course of the experiment

Day	TSS (g/L)		VSS (g/L)		VSS/TSS ratio (%)		SLR (g-COD/g-VSS.day)		Upflow velocity (m/h)	
	R1	R2	R1	R2	R1	R2	R1	R2	R1	R2
0	21.1	21.1	14.6	14.6	69.2	69.2	0.041	0.040	0.17	0.0017
13	24.0	15.7	18.4	12.3	76.7	78.3	0.106	0.169	0.38	0.058
33	22.3	22.1	17.2	17.7	77.1	80.1	0.247	0.238	0.60	0.13
50	30.5	28.7	25.5	24.3	83.6	84.7	0.224	0.227	0.29	0.17

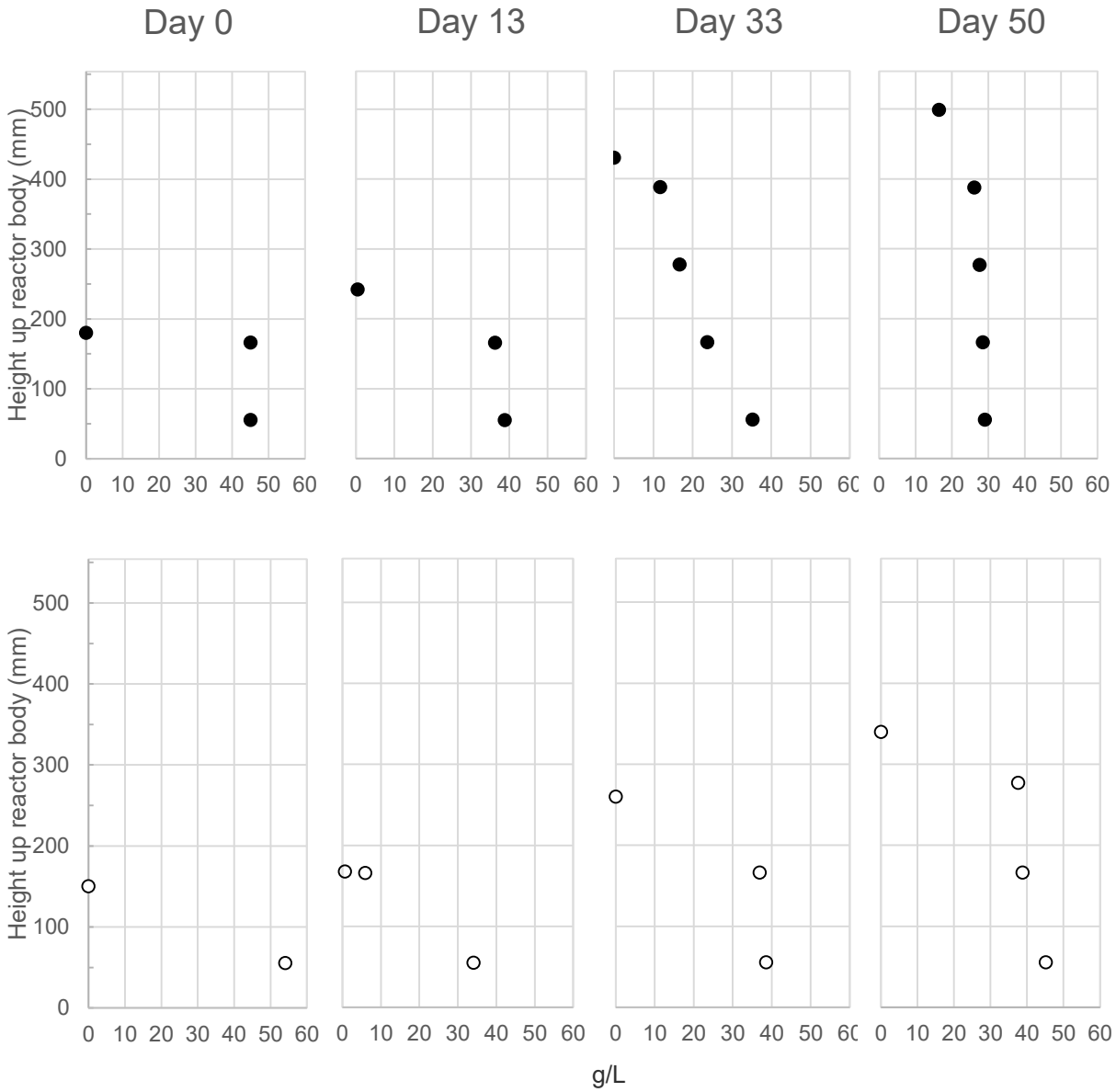

Figure 5-8: VSS concentration profiles along the heights of RI (●) and R2 (○)

Qualitative results

As with the first experiment, biogas production was observed within hours of inoculation. In R2, biogas bubbles were initially trapped beneath the sludge bed, causing flotation of the entire sludge bed four hours after inoculation. However, while rising toward the top of the reactor body the sludge mass broke up spontaneously and settled back down at the bottom of the reactor. A photograph of the trapped gas bubbles is shown in Figure 5-9. This was the only sludge flotation incident occurring in the experiment.

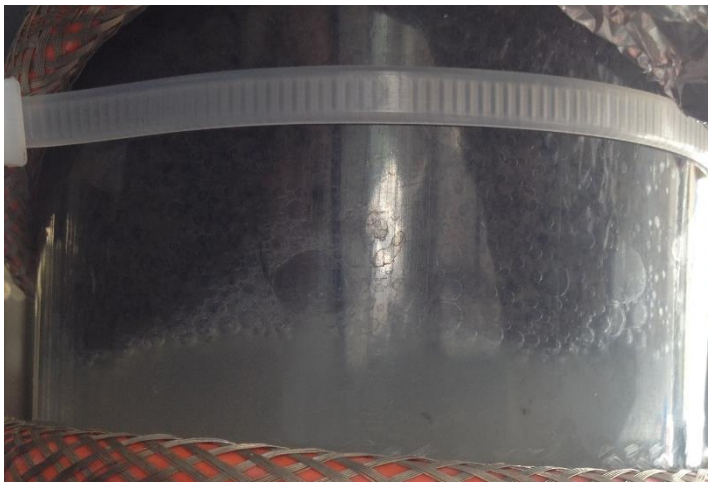

Figure 5-9: Trapped gas bubbles beneath the sludge bed in R2 four hours after inoculation

For most of the experiment the sludge bed in R1 was observed to be slightly fluidised and more expanded than in R2 as a result of the recycle increasing the superficial upflow velocity. Furthermore, the biogas bubbles produced in R1 were smaller, and greater by number. In contrast, the sludge bed in R2 was observed to be more compact and movement of the visible granules (those against the reactor wall) was rarely observed, indicating the potential for dead zones within the sludge bed. Gas bubbles in R2 were more easily trapped in the bed, growing in size until much larger than those formed in R1, eventually causing an eruption of sludge granules when they escaped from the top of the bed. The expanded sludge bed in R1 is depicted by the VSS profiles presented in Figure 5-8, where the presence of VSS at a greater height indicates a larger or more expanded sludge bed in R1 than in R2. To prevent the expanding sludge bed in R1 from entering the gas-liquid-solid separator (GLSS), the recycle flow rate was lowered on Day 40 from 40 L/day to 14 L/day. However, the expansion of the sludge bed in R1 eventually resulted in the need for removal of excess sludge on days 43 and 47, where around 450 mL were withdrawn from the sludge bed on both occasions.

Photographs and micrographs of sludge samples were also taken to provide a qualitative record of the visual appearance of the sludge granules. Photographs were taken with every TSS/VSS measurement (i.e. four times over the course of the experiment) and micrographs were taken of a sludge sample from the lowest sampling port at the end of the experiment. The photographs are presented in Figure 5-10 to Figure 5-15, and micrographs in Figure 5-16 and Figure 5-17. Observing Figure 5-10 to Figure 5-13 reveals that, out of the dates on which the photographs were taken, the most distinctly homogeneous granules were obtained on Day 33 (Figure 5-12). Figure 5-10 shows that the granules in the inoculum are all relatively clear, and most are growing around a solid support material which appears as a darker centre. In Figure 5-11, these granules appear slightly denser (the solid support is less visible), and they are also slightly more homogeneous. In Figure 5-12, the photograph reveals the darkest, most homogeneous, and perceptively densest granules. However, Figure 5-13 shows a layer of newer growth on the outside of the granules that appears to be less dense (clearer/lighter in colour) and with a less distinctive edge. Figure 5-14 is a photograph of this sludge from Day 50 taken again using the camera's flash. The flash clearly reveals the presence of a white outer layer surrounding an inner darker layer. The sludge from R2 generally looks less homogeneous, but also less consistently fluffy and white as the sludge from R1. Furthermore, agglomerates of fluffy white sludge are clearly observable in the sludge from R1, but are barely noticeable (although still present in the sludge from R2). A photograph showing the fluffy white sludge from R1 more clearly is presented as Figure 5-15.

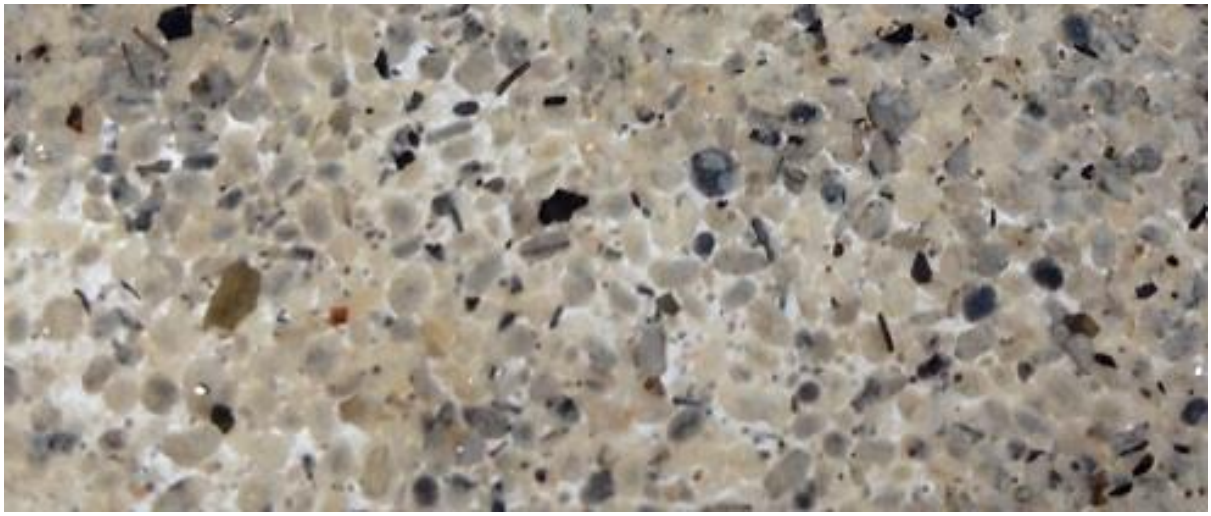

Figure 5-10: Photograph of the inoculum taken one day before inoculation

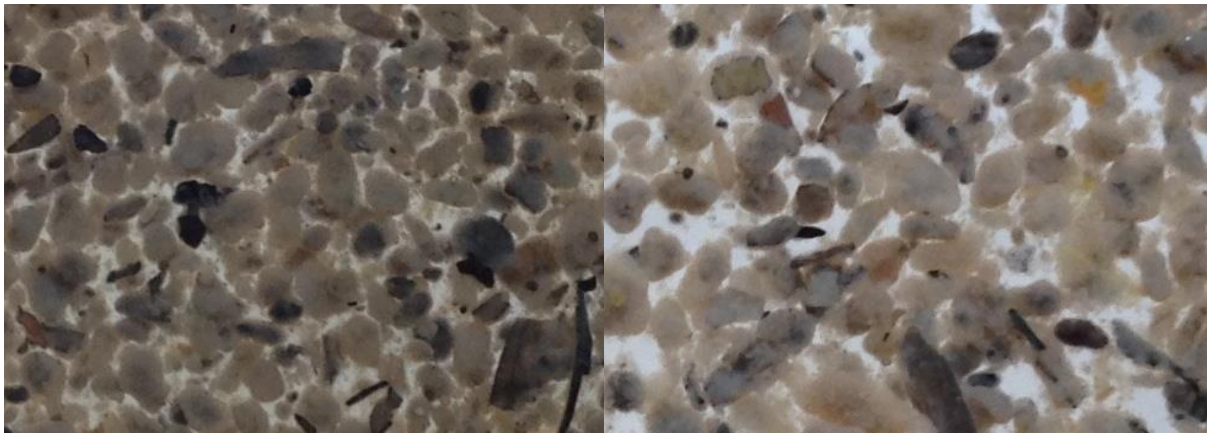

Figure 5-11: Photographs of sludge from R1 (left) and R2 (right) taken on Day 13

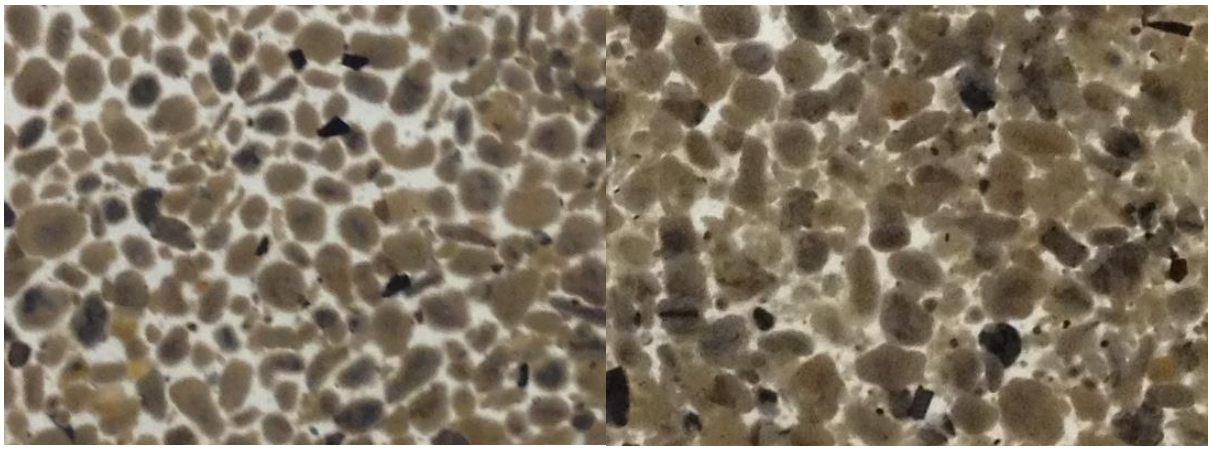

Figure 5-12: Photographs of sludge from R1 (left) and R2 (right) taken on Day 33

Figure 5-16 and Figure 5-17 shows the edges of pieces of sludge granules at 1000x magnification taken from the sludge beds of R1 and R2 respectively. The edge of the granule piece from R2 is clearly marked by a brown colour, and is better defined and denser than that from R1. The granule from R1 seems to comprise mostly of long (>1000 µm) filaments, which protrude from the edge of the granule piece. This renders the edge of the piece of the granule from R1 less distinct, and marked only by an area less densely populated by filaments.

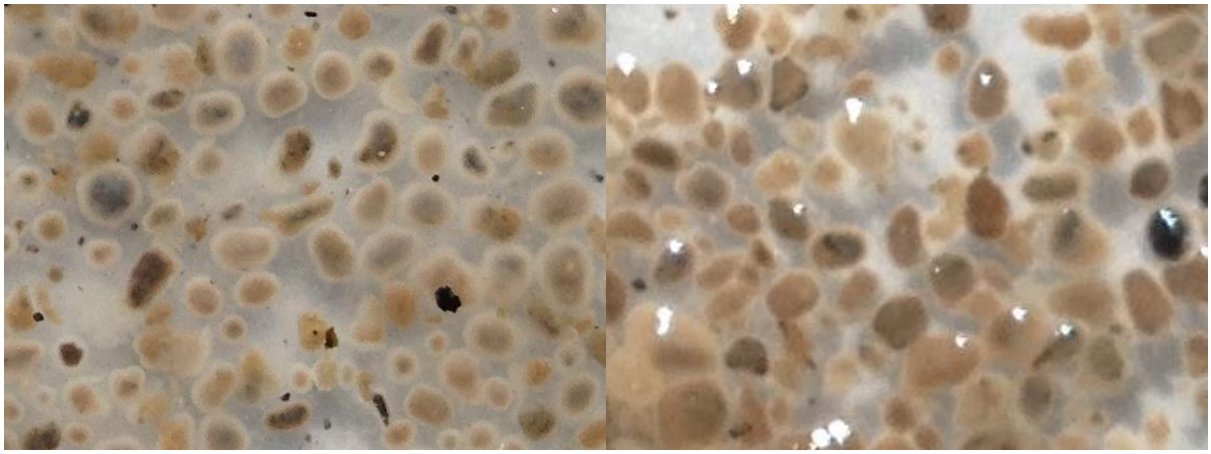

Figure 5-13: Photographs of sludge from R1 (left) and R2 (right) taken on Day 50

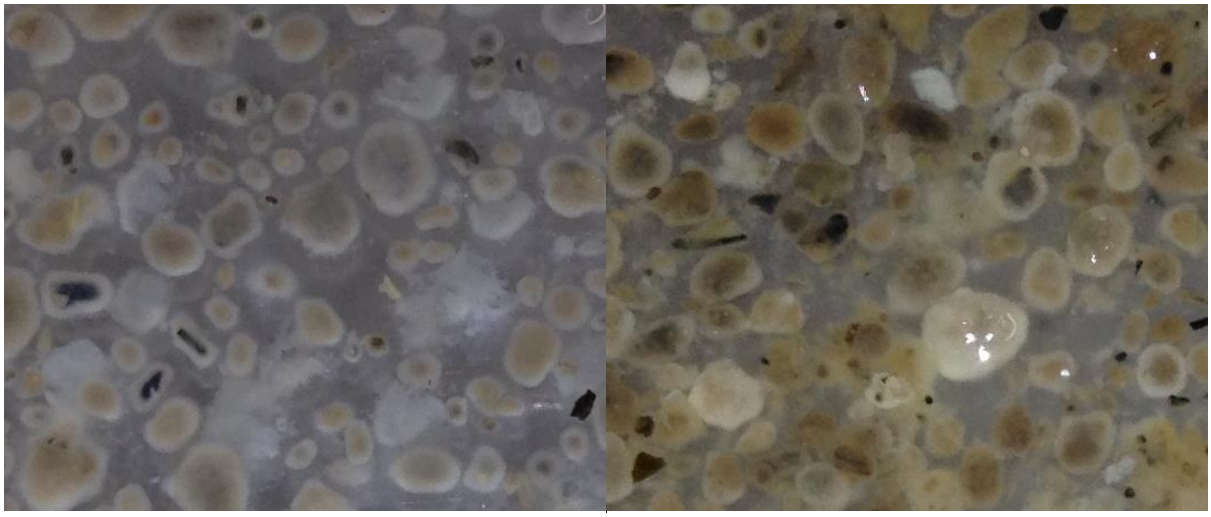

Figure 5-14: Photograph of sludge from R1 (left) and R2 (right) taken on Day 50 with flash

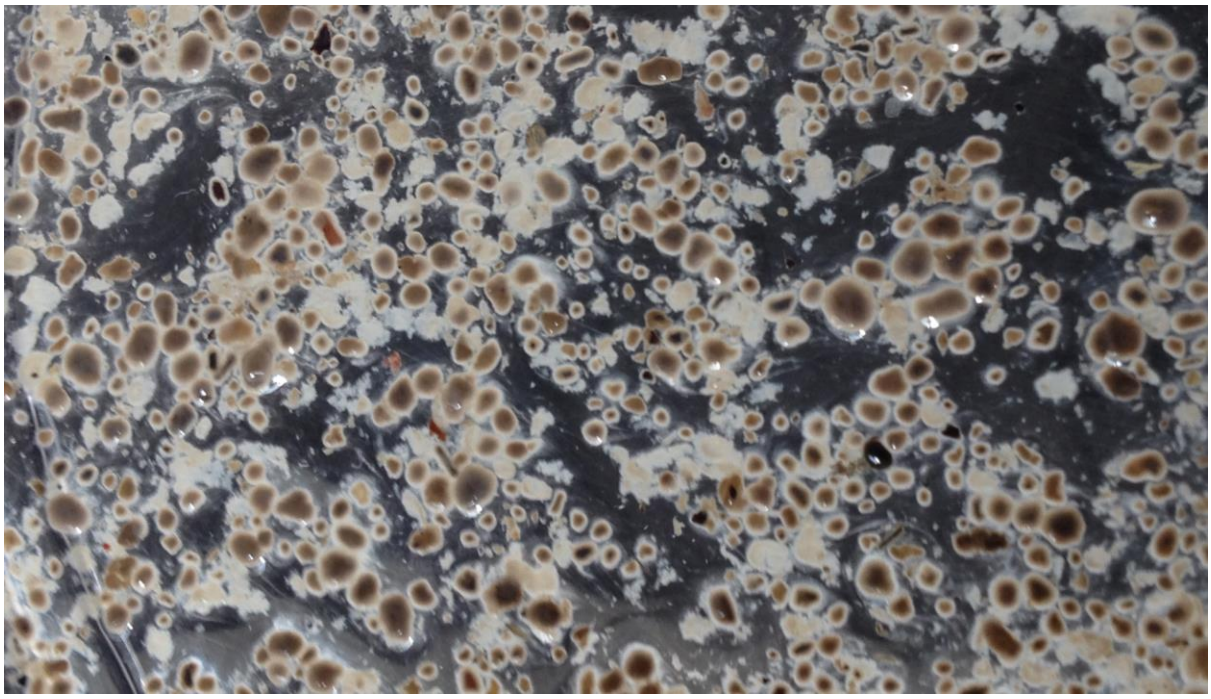

Figure 5-15: Photograph of sludge from R1 sludge bed on Day 50 showing the presence of fluffy white agglomerates

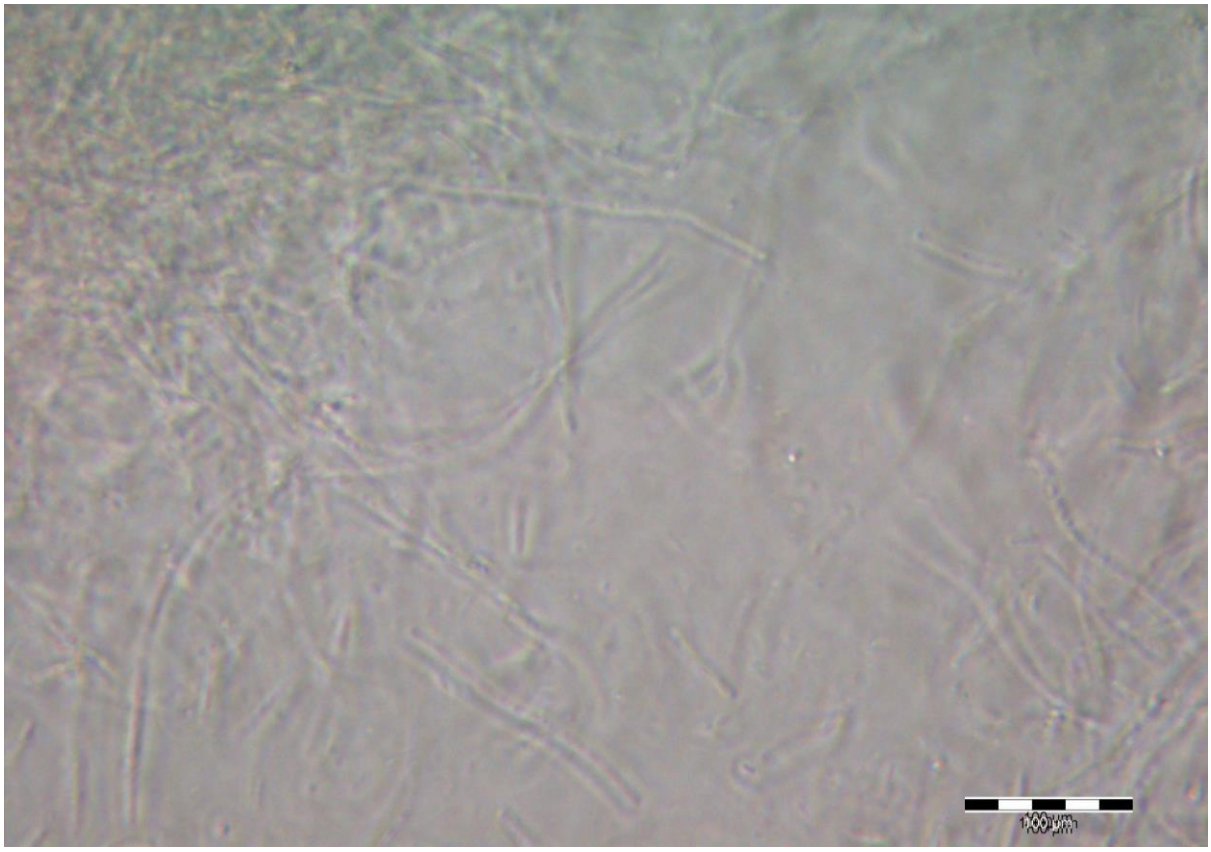

Figure 5-16: Micrograph of the edge of a piece of a granule from R1

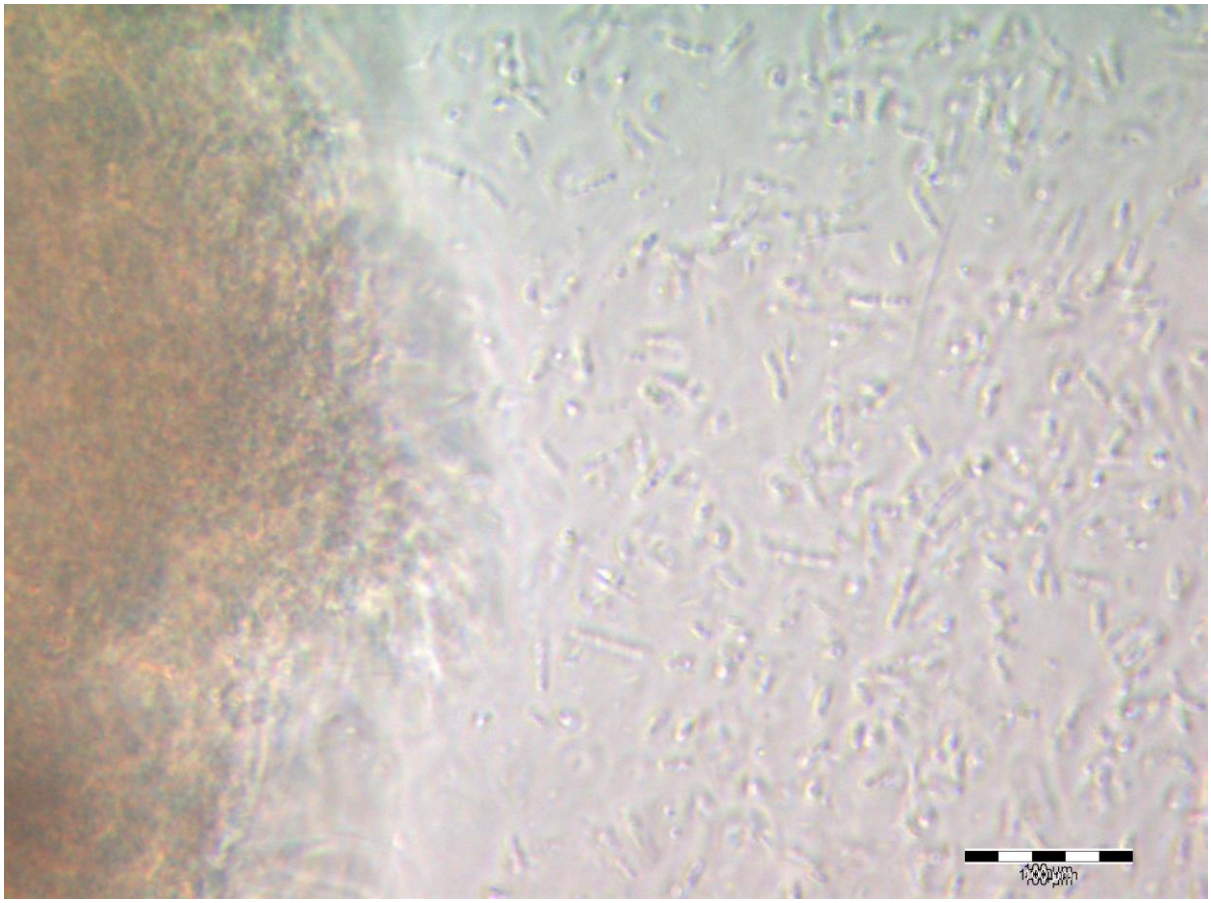

Figure 5-17: Micrograph of the edge of a piece of a granule from R2

5.2.2 Discussion

System performance

Both reactors performed well in terms of soluble COD removal, with ~90% of the soluble COD fed to the reactors removed consistently. The COD removal efficiency measured is relatively independent of the OLR, indicating that the reactors were operating well below their maximum capacity. Of the COD removed from the aqueous phase a greater portion was recovered as CH_4 for R1 (91%) than for R2 (76%). As discussed in Section 2.4.1, COD is only removed from the aqueous phase through its conversion to biomass or CH_4 and CH_4 yields of ~80-90% are expected. The CH_4 yields for R1 and R2 are both close to this range, and it is likely that the higher yield of CH_4 measured for R1 can be at least partly explained by a greater degree of oversaturation of dissolved CH_4 in R2. Oversaturation of CH_4 is an issue reported on previously in publications of studies on UASB reactors (Singh and Viraraghavan, 1998; Kim *et al.*, 2011; Ferrer *et al.*, 2012), and occurs due to a lack of contact between the gaseous and liquid phases within the reactor. The contact between these phases is enhanced in R1 due to circulation of the reactor liquor, resulting in a greater number of gas bubbles of smaller volume being produced with an associated higher interfacial surface area. Furthermore, the reactor is more homogenously mixed, increasing the rate at which liquor at the interface between the reactor headspace and liquid phase is renewed, as well as preventing dead zones. The saturation concentration of CH_4 at 37°C and a CH_4 partial pressure of 0.55 atm (roughly the CH_4 partial pressure experienced in both reactors) can be calculated according to Henry's Law (Ferrer *et al.*, 2012) as ~10 mg-CH_4/L, which is equivalent to ~40 mg-COD_{CH4}/L. This corresponds to ~3% of the COD converted, so if the CH_4 is oversaturated by a factor of two (as was reported by Kim et al. (2011) and Pauss et al. (1990)) this would render a total CH_4 recovery (dissolved + undissolved CH_4) of 84% for R2. However, the degree of oversaturation of dissolved CH_4 has been observed to be as high as 12 times the equilibrium value predicted by Henry's Law (Pauss *et al.*, 1990). It is therefore possible that dissolved CH_4 could account entirely for the difference in the measured CH_4 recovery. However, it is also likely that some error exists in the CH_4 recoveries as calculated due to the use of only five biogas composition measurements to represent the entire 50 day experimental period.

A slightly lower average conversion of COD was measured in R2 (90%) than in R1 (92%). This is thought to result from the lower contact time between sludge and substrate in R2, which resulted from the more compact and less mixed sludge bed in R2. The same hydraulic retention time (HRT) was experienced in both reactors, but because the reactor liquor was not in contact with the sludge bed for as much time in R2 (a greater portion of R2 contained no sludge bed than in R1) there was less contact time between the highly active sludge and its substrate.

The effluent pH behaved similarly for both reactors, dropping from the initial value of ~6.9 down to ~6.5 over the course of 3.5 weeks. A pH of 6.5 is on the border of the range in which methanogenesis is strongly affected. Furthermore, a drop in pH is usually a sign of VFA accumulation as a result of overloading the methanogen population (Moosbrugger *et al.*, 1993). It was because of this pH drop that the OLR was not increased according to the original experimental plan i.e. immediately after COD removal reached above 80%. However, the effluent pH appears to have been relatively independent of the OLR, and the fact that it changed slowly and followed a consistent trend over the course of weeks indicates that it may have been related to a change in the sludge characteristics. Corresponding with the drop in pH is an increase in the VSS/TSS ratio of the sludge for both reactors. This means that the inorganic solids content of the sludge decreased. Since $CaCO_3$ has been found to be a primary inorganic component of sludge granules, it is possible that $CaCO_3$ was leached out of the inoculum over the course of the experiment due to the low pH in the reactors. This would cause an increase in the effluent alkalinity and pH. Although the sludge VSS/TSS ratio increases throughout the entire experiment, the effect of $CaCO_3$ being leached out of the sludge on effluent pH would have become less significant as the influent flow rate increased and diluted the $CaCO_3$ that dissolved. It is noted that this decrease in the inorganic solids content would lower the bulk density of the granules, which could be perceived as a factor that exacerbated, or even caused, the tendency for sludge flotation. However, this is thought to be unlikely for two reasons. Firstly, well-granulated sludge has been documented to contain anything between 10-90% inorganic material (Schmidt and Ahring, 1996), indicating that not all sludge granules contain a high inorganic material content. Secondly, the literature on granulation did

not reveal a case where dissolution of the inorganic components was responsible for granulation failure, provided that the concentrations of inorganic components in the feed were in excess of that required for cellular synthesis. Instead, the reasons for deterioration of the sludge granules are presented in the following sub-section Granulation performance.

The VFA profiles presented in Figure 5-6 and Figure 5-7 also show that no VFA were present on Day 23, confirming that VFA accumulation could not be responsible for the low reactor pH. However, increasing the OLR on Day 23 did result in the accumulation of small amount of VFA (peaking at ~115 and ~85 mg-VFA_{total}/L for R1 and R2 respectively), with a corresponding drop in the effluent pH from ~6.6 to ~6.5. This VFA concentration falls within the VFA concentration range of 0.5-2.0 mmol-VFA/L typical of digesters under normal operation (Lahav and Morgan, 2004). In terms of the composition of the VFA, acetate was detected in the effluent from both reactors. However, of the higher VFA, only butyrate was present in the effluent from R1, while the effluent from R2 contained only propionate. This difference in metabolic behaviour of the two reactors indicates that in addition to the differences in the morphology of the cells in the granules, there was also likely a difference in the ecology between the granules from R1 and R2.

Granulation performance

The term ‘quality’ is used in this context to refer to the presence of positive sludge granule characteristics, namely high microbial (particularly methanogenic) activity, high settleability and a low sludge flotation potential (SFP). The SFP is a measure of how prone a particular sludge sample is to adhering to gas bubbles and floating, and can be measured directly through SFP tests. Fundamentally, the SFP is affected by granule properties such as the structural composition of the granule exogenous polymeric substances (EPS), as well as the hydrophobicity, viscosity and surface charge of the sludge (Wang *et al.*, 2017). The structural composition of EPS has been classified by Nielsen and Jahn (1999) as tightly-bound EPS (TB-EPS) and loosely-bound EPS (LB-EPS). TB-EPS is “tightly and stably bound to the cell surface”, while LB-EPS is a “loose and dispersible slime layer” that is found at the outer layer of sludge aggregates and appears at the outer layer of sludge granules with no clearly discrete edge (Wingender *et al.*, 1999). The hydrophobicity and surface charge affect the strength of the bonds between gas bubbles and the sludge granules, where a more hydrophobic sludge sample with a less negative surface charge is more likely to adhere to gas bubbles and float (Wang *et al.*, 2017). Wang et al. (2017) found that the characteristics leading to a low SFP are strongly correlated with a lower LB-EPS/TB-EPS ratio i.e. the presence of more LB-EPS increases the tendency for sludge to float. The reasoning behind this is that these physical properties are a function of the chemical composition of the sludge, most notably the ratio of proteinaceous EPS (PN-EPS) to polysaccharide EPS (PS-EPS) (Wang *et al.*, 2017). This is because proteins are more hydrophobic than polysaccharides (Jorand *et al.*, 1998), and their amino groups carry a positive charge which decreases the negativity of the surface charge of the sludge, in contrast to the negative charge carried by the carboxyl groups from the PS-EPS (Liao *et al.*, 2001). Therefore sludge with a high PN-EPS/PS-EPS ratio is more likely to adhere to gas bubbles and float. In the study by Wang et al. (2017), the PN-EPS/PS-EPS ratio was found to decrease with a decrease in the LB-EPS/TB-EPS ratio, therefore sludge with a lower LB-EPS/TB-EPS ratio should have a lower PN-EPS/PS-EPS ratio and be less likely to float. It is thought that that relationship between the LB-EPS/TB-EPS and PN-EPS/PS-EPS ratios is not causal, but rather that mixing conditions within the reactor affect them similarly. Wang et al. (2017) suggest that poor mixing leads to dead zones within the sludge bed, resulting in localised areas where substrate limitations cause the microorganisms to utilise PS-EPS as an energy source. Simultaneously, the starving microorganisms are more prone to cell lysis, which would release proteins. Poor mixing is also responsible for allowing the accumulation of LB-EPS, which is not sheared off as it would be under high-shear conditions. The relationship between the LB-EPS/TB-EPS ratio and sludge viscosity is causal since LB-EPS is more water retentive than TB-EPS (Yang and Li, 2009), resulting in sludge with a high LB-EPS/TB-EPS ratio to be more viscous and poorly settleable (Wang *et al.*, 2017).

In the present study, the quality of the granules is inferred from the measured system performance variables (COD removal efficiency etc.), sludge bed density, occurrence of sludge flotation incidents, and visual appearance. System performance provides an indication of the biological activity of the sludge i.e. the presence of active microorganisms in the quantities necessary to perform the AD process

to completion. Sludge bed density, occurrence of sludge flotation incidents and visual appearance provide an indication of the physical state of the sludge, from which conclusions regarding its susceptibility to flotation can be drawn. A denser sludge bed indicates more settleable sludge granules and/or denser sludge granules. As described in the paragraph above, visual appearance – most notably observation of the presence/abundance of LB-EPS – can be used to qualitatively assess the granule quality.

Although the inoculum used for this experiment (Newlands Sludge) was granular, it was of a lower quality than the granules used for inoculation in the first experiment (Prospecton Sludge). This is indicated by the lower total solids content (density) of the Newlands Sludge, and qualitatively by the observed (higher) viscosity of the Newlands sludge. The Newlands sludge granules also appear to have a less distinct edge, indicating a higher quantity of LB-EPS than the Prospecton Sludge. Most importantly, a sludge flotation incident occurred four hours after inoculation with the Newlands Sludge, but such an incident was only observed to occur after two weeks of underfeeding with the Prospecton Sludge. This comparison indicates that the starting sludge in the granulation experiment displayed a relatively high SFP for granular sludge.

Throughout this experiment the performance of R1 and R2 was similar, with satisfactory soluble COD removal (>90%) and biogas production occurring in both reactors. Reactor performance is therefore not used to compare the sludges from R1 and R2. However, it does indicate that the Newlands Sludge used as the inoculum was highly methanogenically active, and that this characteristic was maintained in both reactors throughout the experiment. In addition to this, no flotation incidents were recorded in either reactor after the first day, indicating that the reactor conditions provided were sufficient to somewhat maintain the settleable nature of the sludge.

However, over the course of the experiment the quality of the granules did not progress as desired. The characteristics of the sludge did appear to improve in both reactors during the first half of the experiment. The granules shown in Figure 5-11 and Figure 5-12 are more homogeneous, indicating a lower presence of non-granular agglomerates that can be seen in Figure 5-10 and again at the end of the experiment in Figure 5-15. The granules shown in Figure 5-13 (from Day 50) display a clear outer layer of growth resembling LB-EPS, over an inner denser layer. Figure 5-14 (from Day 50) taken with the flashlight of the camera reveals agglomerates of LB-EPS, which can be seen even more clearly in Figure 5-15. These are signs of the bulking-type sludge described by Hulshof Pol et al. (1983). The fact that the state of the sludges in R1 and R2 initially improved, before beginning to deteriorate at the end of the experiment indicates that conditions within the reactors were borderline favourable to granulation.

In hindsight, the factor that has been identified as being responsible is once again underfeeding. In the present study, the main parameter used to design the experiment was the OLR, which was based on other studies investigating the start-up of UASB reactors using digested sewage sludge as the inoculum (Hulshoff Pol *et al.*, 1983; Fang and Chui, 1993; Behling *et al.*, 1997; Singh and Viraraghavan, 1998; Ghangrekar *et al.*, 2005). As discussed in Section 2.4.3, the start-up of a UASB reactor using digested sewage sludge as an inoculum tends to follow a distinct trend in which the majority of the solids from the sludge bed are washed out of the reactor. Hulshoff Pol et al. (1983) found that in the start-up of a UASB using digested sewage sludge that the average sludge concentration (measured as volatile suspended solids (VSS)) in the reactor decreased from the starting value of 12-15 g-VSS/L to 2 g-VSS/L, indicating that as little as 15% of the starting sludge VSS may be left after the initial washout phase. However, in the case of using an already granular (and therefore settleable) inoculum this washout phenomenon does not occur, and the majority of the inoculum is retained within the reactor. This means that – in addition to any increase in activity over flocculent sludge due to the nature/internal organisation of sludge granules – the effective sludge loading rate (SLR) can be ~6-7 times lower when a settleable/granular sludge is used as the inoculum at the same VSS concentration as digested sewage sludge. For instance, in the case of this experiment by Hulshoff Pol et al. (1983) where digested sewage sludge was used as the inoculum, granule formation was observed at an OLR of 4.28 g-COD/L.day, when the average VSS concentration in the reactor was 2 g-VSS/L. This corresponds to a SLR of above 2 g-COD/g-VSS.day. However, if all the starting VSS was retained in the reactor the SLR would have been ~0.3 g-COD/g-VSS.day at the same OLR of 4.28 g-COD/L.day.

This indicates that the SLR provides a far more useful indicator of the feed flow rate that is tolerable to the sludge in the reactor than the OLR, because it is based on a measure of the quantity of biomass present. It has already been mentioned that the OLR was not increased sooner in the present study in spite of the high COD removal because of the low pH measured being a potential indicator of the presence of VFA, indicating that the sludge could be overfed. This impression was given by the steady decrease in pH over the first 3.5 weeks of the experiment, over which period the OLR was increased five times. However, if the SLR had been used as the main criterion for increasing the OLR it would have been clear that the sludge was being underfed. The SLRs experienced in R1 and R2 were relatively similar throughout the experiment, and ranged from 0.040-0.247 g-COD/g-VSS.day (Table 5-3). However, Hulshof Pol et al. (1983) recommend operating UASB reactors at a SLR above 0.6 g-COD/g-VSS.day to prevent the growth of flocculent bulking-type sludge when using VFA as the carbon source. Carbohydrate-based substrates are considered to yield more EPS (Schmidt and Ahring, 1996) and better quality granules than VFA (Vanderhaegen *et al.*, 1992), indicating that operating conditions may not need be as stringent for satisfactory granulation to occur. Ghangrekar et al. (2005) found that using an initial SLR between 0.1-0.25 g-COD/g-VSS.day was optimal when using sucrose as the carbon source and digested sewage sludge as the inoculum. However, Ghangrekar et al. (2005) failed to note that the effective SLR increases as a result of sludge washout. For the sake of comparison, if the initial SLR is assumed to increase by a factor of six due to washout of VSS in the initial start-up phases, then the results of Ghangrekar et al. (2005) translate to using an initial SLR of 0.6-1.5 g-COD/g-VSS.day. The maximum OLR at which a mesophilic UASB reactor has been operated while maintaining removal of the majority (~75%) of the influent COD (to the author's knowledge) was performed by Fang and Chui (1993). They found that a maximum specific CH_4 productivity of 1.7 g-COD_{CH4}/g-VSS.day was reached when the SLR reached 3 g-COD/g-VSS.day. However, only 75% of their influent COD was soluble and readily biodegradable, which was also shown by the removal of only 75% of the influent COD at the higher OLR/lower HRT tested. This corresponds to a maximum SLR of 2.25 g-COD/g-VSS.day where a completely readily biodegradable and soluble carbon source is used, indicating the upper limit for operation. The above reasoning is further supported by the fact that the full-scale UASB reactors in which the inoculum granules were grown were operated at an SLR of 0.61 g-COD/g-VSS.day. Unfortunately the importance of the SLR was not fully understood at the time of devising this experiment, thus this parameter was overlooked.

In spite of the issue with regards to underfeeding, the results from this experiment are still deemed suitable to inform Hypothesis 1. It is possible that the results obtained under these borderline-starvation conditions are even more relevant for testing the efficacy of using hydraulic mixing via effluent recycle to aid the granulation process. This is because conditions for granulation were sub-optimal, giving an indication of the potential for effluent recycle to help in situations where granulation is not proceeding favourably. Also, although the recycle ratio for R1 was lowered before the end of the experiment, this was done in reaction to the expansion of the sludge, indicating that the conditions used prior to lowering the recycle ratio were favourable to the formation of bulking-type sludge. The photographs of the sludges from R1 and R2 shown in Figure 5-11 to Figure 5-15 do not reveal a large difference between the sludges from these reactors, except that the granules in R2 were less homogeneous, and contained less LB-EPS at the end of the experiment. The latter point in particular is reasoned from the presence of a significantly greater quantity of the fluffy white agglomerates fitting the description of LB-EPS observed in the sludge bed samples from R1. Furthermore, the density of the two sludge beds differs greatly, indicating that the sludge granules obtained in R2 are far more settleable than those obtained in R1. Figure 5-8 shows that at the end of the experiment the sludge bed in R1 is more expanded, taking up the entire reactor working body volume, and has a maximum VSS density of 26-29 g-VSS/L. In contrast, the sludge bed from R2 occupied 63% of the reactor working body volume at the end of the experiment, with a density between 38-45 g-VSS/L. This comparison is not entirely fair considering that R1 was still experiencing a higher superficial upflow velocity than R2. However, at this stage of the experiment this difference in superficial upflow velocity was not as great due to lowering the recycle ratio in R1 and biogas production resulting in much of the mixing of the sludge beds. Finally, the micrographs of the sludge from the end of the experiment reveal the presence of predominantly long (>1000 µm) filaments growing in the granule sampled from R1 (Figure 5-16), while the granule from R2 (Figure 5-17) did not contain any filaments longer than ~200 µm. This observation further validates that the growth of bulking-type sludge was only exhibited in R1 and not in R2, since this type of sludge is

associated with the growth of long filaments of presumably *Methanosaeta Spp.* It is on these bases that Hypothesis 1 is refuted, since the evidence obtained suggests that more settleable sludge granules are obtained in the absence of an effluent recycle under the conditions investigated.

This conclusion was unexpected, but not entirely inexplicable. Although the increased fluid flow in R1 from the effluent recycle increased the mixing within in the reactor on average, observed as semi-fluidization of the sludge bed, the biogas bubbles produced were also smaller and more numerous than in R2. These smaller gas bubbles visually displayed less explosive forces than the larger bubbles observed to erupt from the sludge bed in R2, which appears to have made them less effective at shearing off and preventing the growth of LB-EPS and long filaments of *Methanosaeta Spp*. Wang et al. (2017) found that pneumatic mixing was the most effective form of mixing for cultivating positive granule characteristics, with hydraulic mixing being the least effective. This indicates that the mixing caused by the evolution of biogas is more important than that from the liquid upflow, and the increased liquid upflow in R1 appears to have sabotaged this 'pneumatic' mixing from the biogas. This concept – that pneumatic mixing is the most important factor for cultivation of quality granules – is also supported by the fact that underfeeding results in the formation of bulking-type sludge, since underfeeding the sludge results in a lower specific as production and therefore less pneumatic mixing per volume of sludge. However, Wang et al. (2017) still found that hydraulic mixing lowered the SFP of their sulphidogenic sludge granules. This indicates that for low-gas producing systems the inclusion of hydraulic mixing may still be beneficial, which is to be expected since otherwise there will be very little mixing and the likelihood of channelling and dead zones are higher. It must also be noted that the different microbial community present in sulphidogenic granules may also affect the result.

5.3 Modelling experiment

5.3.1 Results

Introduction

A modelling approach was taken to evaluate Hypothesis 2, as well as to estimate the influent $NaHCO_3$ concentration required for the effluent pH to be neutral. Results were generated for these purposes by varying model inputs for the following scenarios:

1. The base case, in which the effluent pH is determined according to the model as described in Section 4
2. The same as the base case, except all VFA produced is consumed i.e. the effluent VFA concentration is zero
3. The same as the base case, except that alkalinity consumption due to the removal of NH_3 in its non-ionised form for biomass (protoplasm and EPS) production is ignored
4. The same as the base case, but the influent $NaHCO_3$ concentration is varied to obtain a neutral effluent pH

Inputs

In all the above scenarios it is assumed that the influent sucrose concentration is 1.34 g/L (=1.5 g-COD/L) and reacts completely i.e. $X_s = 100\%$. This is because acidogenesis proceeds at a much faster rate than methanogenesis (Lettinga *et al.*, 1980; Speece, 1983), and at the OLR at which the reactors were operated in the experimental investigations VFA conversion (methanogenesis) was typically 90%. It was therefore also assumed in Scenarios 1, 3 and 4 that conversion of VFA was 90% effective i.e. $X_{HAc} = 90\%$. In Scenario 2, it was assumed that $X_{HAc} = 100\%$. Furthermore, the influent weak acid and base total species concentrations inputted were the same as those used for the updated experimental medium (Table 3-3), and are presented in Table 5-4. The only exception to this is Scenario 4, in which the influent C_T concentration corresponds to the concentration required to obtain a neutral effluent pH. Lastly, an influent flow rate of 15 L/day was inputted, corresponding to the highest flow rate at which the experimental reactors were operated. The model therefore mimics the reactor operation during the last period in which the OLR was 11.25 L/day.

Table 5-4: Influent weak acid/base total species concentrations

Influent weak acid/base total species	Added as	Concentration (mol/L)
A_T	N/A	0
C_T	$NaHCO_3$	0.0179
N_T	NH_4Cl	0.00729
P_T	K_2HPO_4	0.000970

To generate the results for Scenario 3 the last term from Equation 62, which is responsible for accounting for the release of protons from NH_4^+ molecules dissociating due to the uptake of NH_3, was removed. Therefore the effluent NH_3 concentration was still the same as the effluent in the base case, but the release of protons as a result of the NH_3 uptake is ignored. It must be noted that the model predicted the influent pH as 8.03, which matches the measured influent pH during the granulation experiment.

Results

The effluent weak acid/base total species concentrations, CH_4 productivity and biogas composition are presented in Table 5-5 for the above Scenarios.

Table 5-5: Results for modelling of Scenarios 1-4

Scenario	1	2	3	4
pH	6.60	6.70	6.67	7.00
A_T (mol/L)	0.00208	0	0.00208	0.00208
C_T (mol/L)	0.0271	0.0293	0.0281	0.0580
N_T (mol/L)	0.00574	0.00574	0.00574	0.00574
P_T (mol/L)	0.000970	0.000970	0.000970	0.000970
CH_4 recovery (g-COD_{CH4}/L.day)	8.99	8.99	8.99	8.99
Gas comp. (%CH_4)	64.7	67.4	67.0	62.1

In Scenario 4 it was found that an influent $NaHCO_3$ concentration of 0.05 mol-$NaHCO_3$/L (4.2 g-$NaHCO_3$/L) was required to obtain a neutral effluent pH.

5.3.2 Discussion

The results presented in Table 5-5 are somewhat surprising, but the pH prediction, CH_4 recovery and gas composition obtained for the base case (Scenario 1) fit well with that measured for the experimental systems during the last period of operation (in which the feed flow rate was 15 L/day i.e. as modelled). This comparison between the experimental results and the results predicted by the base case model is presented in Table 5-6.

Table 5-6: Comparison of the pHs, CH_4 recoveries and gas compositions predicted by the model and measured experimentally

	R1	R2	Scenario 1
Average pH	6.51	6.50	6.60
CH_4 recovery (g-COD_{CH4}/L.day)	10.33	8.74	8.99
Average gas composition (%CH_4)	54%	58%	65%

The effluent pH of 6.60 predicted by the model is close to that measured, especially when considering the change in pH from the influent (which was both measured and predicted to be 8.0). The CH_4 recovery predicted falls between the CH_4 recoveries obtained experimentally. Lastly, the gas composition predicted by the model is less accurate, but still reasonably close to that obtained in R2. It is also possible that the gas compositions measured were not extremely accurate since only one measurement was made in the last operational period of the Granulation experiment.

The results in Table 5-5 are surprising because the two mechanisms proposed to predominantly account for the drop in pH, namely the presence of HAc in the effluent and the removal of un-ionised NH_3, are not predicted to be the main cause of the pH drop. Conversion of all the HAc produced is predicted to only raise the pH to 6.70 (Scenario 2), while the effect of NH_3 uptake only accounts for dropping the pH from 6.67-6.60 (Scenario 3). To further understand this, Equation 36 (influent proton balance equation) was subtracted from Equation 62 (effluent proton balance equation) to scrutinise the mathematical terms responsible for the difference in influent and effluent pHs, yielding Equation 63.

$$\frac{A_T}{1+\frac{[H^+]}{K_a}} - \frac{Y_N \cdot [S_f] \cdot X_S}{1+\frac{K_N}{[H^+]}} + (C_T - C_{T,f}) \cdot \frac{[HCO_3^-]}{C_T} + 2 \cdot (C_T - C_{T,f}) \cdot \frac{[CO_3^{2-}]}{C_T} \quad \text{Equation 63}$$

The first term in Equation 63 is responsible for the release of 0.00205 mol-H^+/L due to the dissociation of the HAc produced. The second term is responsible for the release of 0.00154 mol-H^+/L due to the uptake of un-ionised NH_3. Finally, the last two terms in Equation 63 are responsible for the release of 0.00613 mol-H^+/L due to the dissolution of CO_2 as H_2CO_3, which then re-speciates forming (mostly) HCO_3^- and some CO_3^{2-}. Therefore, the carbonic acid produced due to the dissolution of CO_2 to establish the equilibrium between the headspace CO_2 partial pressure and the aqueous H_2CO_3 concentration (and in turn the C_T concentration) contributed the most to the drop in pH. This result is not unreasonable, since the carbonate subsystem is known to be the dominant weak acid/base in most terrestrial waters (Loewenthal *et al.*, 1989), and the substrate prepared here did not include high concentrations of other weak acids/bases. It is on this basis that Hypothesis 2 is refuted. However, it is worthwhile noting that the acidity resulting from the production of HAc and uptake of NH_3 were indeed of a similar magnitude in this instance. Furthermore, it is recommended that effluent H_2CO_3* alkalinity measurements be made experimentally to verify the effluent C_T predicted by the model.

Also worth noting is that the C_T concentrations predicted for the various scenarios were different due to a higher quantity of CO_2 dissolving at a higher pH. In Scenario 4, it was found that the influent $NaHCO_3$ concentration would have had to have been almost tripled (from 1.5 g/L to 4.2 g/L) to maintain a neutral effluent pH. This is an unreasonably high $NaHCO_3$ requirement for both laboratory and full-scale installations. A recommended method of raising the effluent pH would be to co-digest the sugar with a proteinaceous substrate to take advantage of the alkalinity production from conversion of the protein into NH_3, which then absorbs a proton forming NH_4^+.

Finally, the results obtained for Scenario 2 are similar to the results obtained for the main AD performance variables as predicted by the Steady State Sludge Digestion Model (Sötemann *et al.*, 2005). The differences in the gas composition and pH predicted by the two models is likely mostly a result of the difference in elemental composition assumed for the biomass coupled with uptake of phosphorus in the Sludge Digestion Model (which was not a feature of the Stoichiometric Model).

6. Conclusions

Two experimental investigations were performed involving the start-up and operation of two upflow anaerobic sludge bed (UASB) reactors. The first experiment performed was aimed at operating the UASB reactors at various organic loading rates (OLR) to gather data for model development. However, deterioration of the sludge granules used for inoculation led to termination of this experiment and the development of a new experimental investigation aimed at solving the granulation issues. Both these experiments performed well in terms of COD removal and methane generation, but suffered from the same deterioration of the sludge granules, resulting in flotation of the sludge beds and/or washout of sludge. The parameter identified as being most responsible for this phenomenon is the sludge loading rate (SLR). It was found that the SLRs employed in the experimental investigations were too low (<0.6 g-COD/g-VSS.day), resulting in the formation of bulking-type sludge that is prone to flotation. It is therefore recommended that the SLR is used to design the start-up regime for UASB reactors. Furthermore, it is recommended that the effect of sludge washout on the SLR to ensure the optimal SLR is maintained throughout start-up.

The effect of the inclusion of effluent recycle on granule settleability was investigated in the second (granulation) experiment. Hypothesis 1 predicted that the recycling of the effluent increases the turbulence within the reactor, thus resulting in the formation of more settleable sludge granules with a lower loosely-bound exogenous polymeric substance (LB-EPS) content. It was found that the reactor recycle aids the transport of CH_4 from the liquid to the gaseous phase, therefore minimising oversaturation of CH_4 and thereby enhancing its recovery. However, the inclusion of the effluent recycle stream expedited the deterioration of the sludge settleability under the starvation conditions investigated. It is on this basis that Hypothesis 1 was refuted.

In both experimental investigations the effluent pHs of both reactors was around 6.5, which is significantly lower than the feed pH of 8.0. A pH of 6.5 is at the lower end of the desired range of operation of UASB reactors. Hypothesis 2 was therefore developed to investigate this issue, stating that the drop in pH was due to the uptake of NH_3 and production of VFAs and that these processes affected the pH to a similar extent. A modelling approach was adopted to test Hypothesis 2 through quantifying the effects of the processes affecting the weak acid and base systems, and in turn their effect on the effluent pH. The model predicts an influent pH of 8.03 and effluent pH of 6.60 for the experimental systems investigated. This is close to the values measured experimentally, providing support for validation of the model's accuracy. However, it is recommended that effluent H_2CO_3* alkalinity measurements be made to validate the predicted effluent total carbonate species concentration. It was found that the greatest contribution to the decrease in pH across the experimental reactor systems was the dissolution of CO_2 formed to establish the equilibrium between the headspace partial pressure and aqueous-phase H_2CO_3 concentration. This process of CO_2 dissolution was found to release 0.00613 mol-H^+/L. This is more significant than the effects of VFA production and NH_3 uptake, which resulted in the release of 0.00205 mol-H^+/L and 0.00154 mol-H^+/L respectively. It is on this basis that Hypothesis 2 is refuted. However, it should be noted that in this particular case VFA production and NH_3 uptake were indeed found to release a similar quantity of protons, and thus affect the digester pH similarly. It was also predicted that the concentration of $NaHCO_3$ in the feed be increased from 1.5 g/L to 4.2 g/L to obtain an effluent pH of 7.0 should this compound be used for pH control.

References

Adney, W. S., Rivard, C. J., Shiang, M. and Himmel, M. E. (1991) 'Anaerobic digestion of lignocellulosic biomass and wastes', *Applied Biochemistry and Biotechnology*, 30(2), pp. 165–183. doi: 10.1007/BF02921684.

Ahring, B. K., Schmidt, J. E., Winther-Nielsen, M., Macario, A. J. L. and Conway de Macario, E. (1993) 'Effect of Medium Composition and Sludge Removal on the Production, Composition, and Architecture of Thermophilic (55C) Acetate-Utilizing Granules from and Upflow Anaerobic Sludge Blanket Reactor', *Applied and Environmental Microbiology*, 59(8), pp. 2538–2545. doi: 10.1148/radiol.11110951.

Angelidaki, I., Ellegaard, L. and Ahring, B. K. (2003) 'Applications of the anaerobic digestion process.', *Advances in biochemical engineering/biotechnology*, 82, pp. 1–33.

APHA (1999) *Standard methods for the examination of water and wastewater*. 20th edn, *Government Gazette*. 20th edn.

Barrera, E. L., Spanjers, H., Romero, O., Rosa, E. and Dewulf, J. (2014) 'Characterization of the sulfate reduction process in the anaerobic digestion of a very high strength and sulfate rich vinasse', *Chemical Engineering Journal*. Elsevier B.V., 248, pp. 383–393. doi: 10.1016/j.cej.2014.03.057.

Batstone, D. J., Keller, J., Angelidaki, I., Kalyuzhnyi, S. V., Pavlostathis, S. G., Rozzi, a., Sanders, W. T., Siegrist, H. and Vavilin, V. a. (2002) 'The IWA Anaerobic Digestion Model No 1 (ADM1).', *Water Science and Technology*, 45(10), pp. 65–73.

De Beer, D., O'Flaharty, V., Thaveesri, J., Lens, P. and Verstraete, W. (1996) 'Distribution of extracellular polysaccharides and flotation of anaerobic sludge', *Applied Microbiology and Biotechnology*, 46(2), pp. 197–201. doi: 10.1007/s002530050805.

Behling, E., Diaz, a., Colina, G., Herrera, M., Gutierrez, E., Chacin, E., Fernandez, N. and Forster, C. F. (1997) 'Domestic wastewater treatment using a UASB reactor', *Bioresource Technology*, 61(3), pp. 239–245. doi: 10.1016/S0960-8524(97)00148-X.

Bolong, N., Ismail, A. F., Salim, M. R. and Matsuura, T. (2009) 'A review of the effects of emerging contaminants in wastewater and options for their removal', *Desalination*. Elsevier B.V., 238(1-3), pp. 229–246. doi: 10.1016/j.desal.2008.03.020.

Brouckaert, C. J., Ikumi, D. and Ekama, G. a (2010) 'Modelling of Anaerobic Digestion for Incorporation Into a Plant-Wide Wastewater Treatment Model', in. Durban: WISA Biennial Conference.

Ten Brummeler, E., Hulshoff Pol, L. W. and Dolfing, J. (1985) 'Methanogenesis in an upflow anaerobic sludge blanket reactor at pH 6 on an acetate-propionate mixture', *Applied and Environmental Microbiology*, 49(6), pp. 1472–1477.

Buswell, a. M. and Mueller, H. F. (1952) 'Mechanism of Methane Formation', *Industrial and engineering chemistry*, 44(3), pp. 550–552. doi: 10.1021/ie50507a033.

Chen, J. and Lun, S. Y. (1993) 'Study on mechanism of anaerobic sludge granulation in UASB reactors', *Water Science and Technology*, 28(7), pp. 171–178.

Chen, Y., Cheng, J. J. and Creamer, K. S. (2008) 'Inhibition of anaerobic digestion process: A review', *Bioresource Technology*, 99(10), pp. 4044–4064. doi: 10.1016/j.biortech.2007.01.057.

Chernicharo, C. A. L., van Lier, J. B., Noyola, A. and Ribeiro, T. B. (2015) 'Anaerobic sewage treatment : state of the art , constraints and challenges', *Reviews in Environmental Science and Bio/Technology*. Springer Netherlands, 14(4), pp. 649–679. doi: 10.1007/s11157-015-9377-3.

Chui, H. (1994) *Effect of Substrate on the Performance and Sludge Characteristics of UASB reactors*. University of Hong Kong. doi: 10.1017/CBO9781107415324.004.

Chui, H., Fang, H., ASCE, M. and Li, Y. (1994) 'Removal of formate from wastewater by anaerobic process', *Journal of Environmental Engineering*, 120(5), pp. 1308–1320.

Chui, H. K., Engineering, S., Road, P. and Kong, H. (1993) 'Microstructural analysis of anaerobic granules', 7(7), pp. 407–410.

Chynoweth, D. P., Owens, J. M. and Legrand, R. (2000) 'Renewable methane from anaerobic digestion of biomass', *Renewable Energy*, 22(1-3), pp. 1–8. doi: 10.1016/S0960-1481(00)00019-7.

Cordell, D. and White, S. (2011) 'Peak phosphorus: Clarifying the key issues of a vigorous debate about long-term phosphorus security', *Sustainability*, 3(10), pp. 2027–2049. doi: 10.3390/su3102027.

Dogan, T., Ince, O., Oz, N. A. and Ince, B. K. (2005) 'Inhibition of Volatile Fatty Acid Production in Granular Sludge from a UASB Reactor', *Journal of Environmental Science and Health, Part A*, 40(3), pp. 633–644. doi: 10.1081/ESE-200046616.

Donoso-Bravo, A., Mailier, J., Martin, C., Rodríguez, J., Aceves-Lara, C. A. and Wouwer, A. Vande (2011) 'Model selection, identification and validation in anaerobic digestion: A review', *Water Research*, 45(17), pp. 5347–5364. doi: 10.1016/j.watres.2011.08.059.

Eastman, J. a and Ferguson, J. F. (1981) 'Solubilization of particulate organic carbon during the acid phase of anaerobic digestion', *Journal of the Water Pollution Control Federation*, 53(3), pp. 352–366. doi: 10.2307/25041085.

Ekama, G. A., Brouckaert, C. J., Brouckaert, B. M. and Ikumi, D. S. (2015) 'Integration of complete elemental mass balanced stoichiometry and aqueous phase chemistry for bioprocess modelling of liquid and solid waste treatment systems: Part 2-Bioprocess stoichiometry', *Water SA*.

Fang, H. and Chui, H. (1993) 'Maximum COD Loading Capacity in UASB Reactors at 37°C', *Journal of Environmental Engineering*, 119(1), pp. 103–119.

Fang, H., Chui, H. and Li, Y. (1994) 'Microbial structure and activity of UASB granules treating different wastewaters', *Water Science and Technology*, 30(12), pp. 87–96.

Ferrer, J., Seco, A., Martí, N. and Gimenez, J. (2012) 'Methane recovery efficiency in a wastewater : Evaluation of methane losses with the effluent', *Bioresource Technology*, 118, pp. 67–72. doi: 10.1016/j.biortech.2012.05.019.The.

Fukuzaki, S., Nish, N. and Naga, S. (1995) 'High Rate Performance and Characterization of Granular Methanogenic Sludges in Upflow Anaerobic Sludge Blanket Reactors Fed with Variou Defined Substrates.pdf', 79(4), pp. 354–359.

Garcia, J.-L., Patel, B. K. . and Ollivier, B. (2000) 'Taxonomic, Phylogenetic, and Ecological Diversity of Methanogenic Archaea', *Anaerobe*, 6(4), pp. 205–226. doi: 10.1006/anae.2000.0345.

Ghangrekar, M. M., Asolekar, S. R. and Joshi, S. G. (2005) 'Characteristics of sludge developed under different loading conditions during UASB reactor start-up and granulation', *Water Research*, 39(6), pp. 1123–1133. doi: 10.1016/j.watres.2004.12.018.

Grady Jr, C. P. L., Daigger, G. T., Love, N. G. and Filipe, C. D. M. (2011) *Biological wastewater treatment*. CRC press.

Gujer, W. and Zehnder, A. J. B. (1983) 'Conversion Processes in Anaerobic Digestion', *Water Science and Technology*, 15(8-9), pp. 127–167. Available at: http://wst.iwaponline.com/content/15/8-9/127.abstract.

Haberl, H. *et al.* (2012) 'Correcting a fundamental error in greenhouse gas accounting related to bioenergy', *Energy Policy*. Elsevier, 45, pp. 18–23. doi: 10.1016/j.enpol.2012.02.051.

Haile, F., Ghoor, T., Ikumi, D., Wadhawan, T., Brouckaert, C. J., Murthy, S., Al-Omari, A. and Ekama, G. (2015) 'A Stoichiometric and Elementally Balanced Model for Simulating Anaerobic Digester Failure', in.

Halalsheh, M., Koppes, J., Den Elzen, J., Zeeman, G., Fayyad, M. and Lettinga, G. (2005) 'Effect of SRT and temperature on biological conversions and the related scum-forming potential', *Water Research*, 39(12), pp. 2475–2482. doi: 10.1016/j.watres.2004.12.012.

Hassam, S., Ficara, E., Leva, a. and Harmand, J. (2015) 'A generic and systematic procedure to derive a simplified model from the anaerobic digestion model No. 1 (ADM1)', *Biochemical Engineering Journal*. Elsevier B.V., 99(1), pp. 193–203. doi: 10.1016/j.bej.2015.03.007.

Heisler, J. *et al.* (2008) 'Eutrophication and harmful algal blooms: A scientific consensus', *Harmful Algae*, 8(1), pp. 3–13. doi: 10.1016/j.hal.2008.08.006.

Helgeson, H. C. (1967) 'Thermodynamics of complex dissociation in aqueous solution at elevated temperatures', *Journal of Physical Chemistry*, 71(10), pp. 3121–3136. doi: 10.1021/j100869a002.

Hulshoff Pol., L. W., Dolfing, J., Zeeuw, W. J. De and Lettinga, G. (1982) 'Cultivation of well adapted pelletized methanogenic sludge', *Biotechnology Letters*, 4(5), pp. 329–332.

Hulshoff Pol, L. (1989) 'The phenomenon of granulation of anaerobic sludge', pp. 1–120.

Hulshoff Pol, L. W., De Castro Lopes, S. I., Lettinga, G. and Lens, P. N. L. (2004) 'Anaerobic sludge granulation', *Water Research*, 38(6), pp. 1376–1389. doi: 10.1016/j.watres.2003.12.002.

Hulshoff Pol, L. W., De Zeeuw, W. J., Velzeboer, C. T. M. and Lettinga, G. (1983) 'Granulation in UASB-reactors', *Water Science and Technology*, 15(8-9), pp. 291–304.

Ikumi, D., Harding, T., Brouckaert, C. and Ekama, G. (2012) *Plant Wide Integrated Biological,Chemical and Physical Bioprocesses Modelling of Wastewater Treatment Plants in Three Phases (Aqueous-Gas-Solid)*. Cape Town.

Jorand, F., Boué-Bigne, F., Block, J. C. and Urbain, V. (1998) 'Hydrophobic/hydrophilic properties of activated sludge exopolymeric substances', *Water Science and Technology*, pp. 307–315. doi: 10.1016/S0273-1223(98)00123-1.

Kennedy, C. (1990) 'Ionic strength and the dissociation of acids', *Biochemical Education*, 18(1), pp. 35–40. doi: 10.1016/0307-4412(90)90017-I.

Kim, J., Kim, K., Ye, H., Lee, E., Shin, C., McCarty, P. L. and Bae, J. (2011) 'Anaerobic fluidized bed membrane bioreactor for wastewater treatment', *Environmental science & technology*, 45(2), pp. 576–81. doi: 10.1021/es1027103.

Kleerebezem, R., Joosse, B., Rozendal, R. and Van Loosdrecht, M. C. M. (2015) 'Anaerobic digestion without biogas?', *Reviews in Environmental Science and Bio/Technology*. Springer Netherlands, (October). doi: 10.1007/s11157-015-9374-6.

Lahav, O. and Morgan, B. E. (2004) 'Titration methodologies for monitoring of anaerobic digestion in developing countries - A review', *Journal of Chemical Technology and Biotechnology*, 79(12), pp. 1331–1341. doi: 10.1002/jctb.1143.

Law, Y., Ye, L., Pan, Y. and Yuan, Z. (2012) 'Nitrous oxide emissions from wastewater treatment processes', *Philosophical Transactions of the Royal Society B: Biological Sciences*, 367(1593), pp. 1265–1277. doi: 10.1098/rstb.2011.0317.

Lee, W. S., Chua, A. S. M., Yeoh, H. K. and Ngoh, G. C. (2014) 'A review of the production and applications of waste-derived volatile fatty acids', *Chemical Engineering Journal*. Elsevier B.V., 235, pp. 83–99. doi: 10.1016/j.cej.2013.09.002.

Lettinga, G. and Hulshoff Pol, L. (1991) 'UASB-Process design for various types of wastewates', *Water Science and Technology*, 24(8), pp. 87–107.

Lettinga, G., van Velsen, a F. M., Hobma, S. W., de Zeeuw, W. and Klapwijk, a (1980) 'Use of the upflow sludge blanket (USB) reactor concept for biological wastewater treatment, especially for anaerobic treatment', *Biotechnology and Bioengineering*, 22(4), pp. 699–734. doi: 10.1002/bit.260220402.

Liao, B. Q., Allen, D. G., Droppo, I. G., Leppard, G. G. and Liss, S. N. (2001) 'Surface properties of sludge and their role in bioflocculation and settleability', *Water Research*, 35(2), pp. 339–350. doi: 10.1016/S0043-1354(00)00277-3.

van Lier, J. B., van der Zee, F. P., Frijters, C. T. M. J. and Ersahin, M. E. (2015) 'Celebrating 40 years anaerobic sludge bed reactors for industrial wastewater treatment', *Reviews in Environmental Science and Bio/Technology*. Springer Netherlands, 14(4), pp. 681–702. doi: 10.1007/s11157-015-9375-5.

Loewenthal, R. E., Ekama, G. a. and Marais, G. V. R. (1989) 'Mixed weak acid/base systems. Part 1 - mixture characterisation', *Water SA*, pp. 3–24.

van Loosdrecht, M. C. M. and Zehnder, A. J. B. (1990) 'Energetics of bacterial adhesion', *Experientia*, 46(8), pp. 817–822. doi: 10.1007/BF01935531.

Lyberatos, G. and Skiadas, I. V (1999) 'Modelling of anaerobic digestion - a review', *Global NEST Journal*, 1(2), pp. 63–76. doi: 10.2478/v10026-008-0011-9.

Mahoney, E. M., Varangu, L. K. and Cairns, W. L. (1987) 'The effect of calcium on microbial aggregation during uasb reactor start-up', *Water Science and Technology*, 19(1-2), pp. 249–260.

Mao, C., Feng, Y., Wang, X. and Ren, G. (2015) 'Review on research achievements of biogas from anaerobic digestion', *Renewable and Sustainable Energy Reviews*. Elsevier, 45, pp. 540–555. doi: 10.1016/j.rser.2015.02.032.

McCarty, P. L., Bae, J. and Kim, J. (2011) 'Domestic wastewater treatment as a net energy producer - can this be achieved?', *Environmental science & technology*, 45(17), pp. 7100–6. doi: 10.1021/es2014264.

McCarty, P. L. and Mosey, F. (1991) 'Modelling of anaerobic digestion process - a discussion of concepts', *Water Science Technology*, 24(8), pp. 17–33.

Moosbrugger, R. E., Wentzel, M. C., Ekama, G. A. and Marais, G. (1993) 'Weak acid/bases and pH control in anaerobic systems - a review', *Water SA*, p. 10.

Moosbrugger, R., Loewenthal, R. and Marais, G. (1990) 'Pelletisation in a UASB system with protein (casein) as substrate', *Water SA*, 16(3).

Morvai, L., Mihaltz, P. and Czako, L. (1992) 'The kinetic basis of a new start-up method to ensure the rapid granulation of anaerobic sludge', *Water Science and Technology*, 25(7), pp. 113–122.

Morvai, L., Miháltz, P., Czakó, L., Péterfy, M. and Holló, J. (1990) 'The influence of organic load on granular sludge development in an acetate-fed system', *Applied Microbiology and Biotechnology*, 33(4), pp. 463–468. doi: 10.1007/BF00176667.

Mosey, F. E. (1983) 'Mathematical Modelling of the Anaerobic Digestion Process: Regulatory Mechanisms for the Formation of Short-Chain Volatile Acids from Glucose', *Water Science and Technology*, 15(8-9), pp. 209–232.

Mu, Y. and Yu, H.-Q. (2006) 'Biological Hydrogen Production in a UASB Reactor with Granules. 1: Physicochemical Characteristics of Hydrogen-Producing Granules', *Biotechnology Advances*, 94(5), pp. 980–987. doi: 10.1002/bit.

Musvoto, E. V, Wentzel, M. C., Loewenthal, R. E. and Ekama, G. a (1997) 'Kinetic-based model for mixed weak acid / base systems', *Water SA*, pp. 7700–7700. Available at: http://cat.inist.fr/?aModele=afficheN&cpsidt=2094498.

Nges, I. A. and Liu, J. (2010) 'Effects of solid retention time on anaerobic digestion of dewatered-sewage sludge in mesophilic and thermophilic conditions', *Renewable Energy*. Elsevier Ltd, 35(10), pp. 2200–2206. doi: 10.1016/j.renene.2010.02.022.

Nielsen, H. B. and Angelidaki, I. (2008) 'Strategies for optimizing recovery of the biogas process following ammonia inhibition', *Bioresource Technology*, 99(17), pp. 7995–8001. doi: 10.1016/j.biortech.2008.03.049.

Noyola, A., Padilla-Rivera, A., Morgan-Sagastume, J. M., Güereca, L. P. and Hernández-Padilla, F. (2012) 'Typology of Municipal Wastewater Treatment Technologies in Latin America', *Clean - Soil, Air, Water*, 40(9), pp. 926–932. doi: 10.1002/clen.201100707.

O'Flaherty, V., Mahony, T., O'Kennedy, R. and Colleran, E. (1998) 'Effect of pH on growth kinetics and sulphide toxicity thresholds of a range of methanogenic, syntrophic and sulphate-reducing bacteria', *Process Biochemistry*, 33(5), pp. 555–569. doi: 10.1016/S0032-9592(98)00018-1.

Pauss, A., Andre, G., Perrier, M. and Guiot, S. R. (1990) 'Liquid-to-Gas mass transfer in anaerobic processes: Inevitable transfer limitations of methane and hydrogen in the biomethanation process', *Applied and Environmental Microbiology*, 56(6), pp. 1636–1644.

Peña, M. R., Mara, D. D. and Avella, G. P. (2006) 'Dispersion and treatment performance analysis of an UASB reactor under different hydraulic loading rates', *Water Research*, 40(3), pp. 445–452. doi: 10.1016/j.watres.2005.11.021.

Pind, P. F., Angelidaki, I. and Ahring, B. K. (2003) 'Dynamics of the anaerobic process: Effects of volatile fatty acids', *Biotechnology and Bioengineering*, 82(7), pp. 791–801. doi: 10.1002/bit.10628.

Pullammanappallil, P. C., Chynoweth, D. P., Lyberatos, G. and Svoronos, S. a. (2001) 'Stable performance of anaerobic digestion in the presence of a high concentration of propionic acid', *Bioresource Technology*, 78(2), pp. 165–169. doi: 10.1016/S0960-8524(00)00187-5.

Rajeshwari, K. ., Balakrishnan, M., Kansal, A., Lata, K. and Kishore, V. V. . (2000) 'State-of-the-art of anaerobic digestion technology for industrial wastewater treatment', *Renewable and Sustainable Energy Reviews*, 4(2), pp. 135–156. doi: 10.1016/S1364-0321(99)00014-3.

Rijsberman, F. R. (2006) 'Water scarcity: Fact or fiction?', *Agricultural Water Management*, 80(1-3 SPEC. ISS.), pp. 5–22. doi: 10.1016/j.agwat.2005.07.001.

Sam-Soon, P. a. L. N. S., Loewenthal, R. E., Dold, P. L. and Marais, G. V. R. (1987) 'Hypothesis for

pelletisation in the upflow anaerobic sludge bed reactor', *Water SA.*, pp. 69–80.

Sam-Soon, P., Loewenthal, R. E., Wentzel, M., Moosbrugger, R. and Marais, G. (1991) 'Effects of a recycle in upflow anaerobic sludge bed(UASB) systems', *Water SA*, pp. 37–46.

Sam-Soon, P., Loewenthal, R., Wentzel, M. and Marais, G. (1990) 'Effect of nitrogen limitation on pelletisation in upflow anaerobic sludge bed(UASB) systems', *Water SA*, 16(3), pp. 165–170.

Saravanan, V. and Sreekrishnan, T. R. (2006) 'Modelling anaerobic biofilm reactors—A review', *Journal of Environmental Management*, 81(1), pp. 1–18. doi: 10.1016/j.jenvman.2005.10.002.

Schmidt, J. E. and Ahring, B. K. (1996) 'Granular sludge formation in upflow anaerobic sludge blanket (UASB) reactors', *Biotechnology and Bioengineering*, 49(3), pp. 229–246. doi: 10.1002/(SICI)1097-0290(19960205)49:3<229::AID-BIT1>3.0.CO;2-M.

Seghezzo, L., Zeeman, G., Van Liel, J. B., Hamelers, H. V. M. and Lettinga, G. (1998) 'a Review: the Anaerobic Treatment of Sewage in Uasb and Egsb Reactors', *Bioresource Technology*, 65, pp. 175–190. doi: 10.1016/S0960-8524(98)00046-7.

Şentürk, E., Ince, M. and Onkal Engin, G. (2010) 'Treatment efficiency and VFA composition of a thermophilic anaerobic contact reactor treating food industry wastewater', *Journal of Hazardous Materials*, 176(1-3), pp. 843–848. doi: 10.1016/j.jhazmat.2009.11.113.

Singh, K. S. and Viraraghavan, T. (1998) 'Start-up and operation of UASB reactors at 20 C for municipal wastewater treatment', *Journal of Fermentation and Bioengineering*, 85(6), pp. 609–614. doi: 10.1016/S0922-338X(98)80014-7.

Solon, K., Flores-Alsina, X., Mbamba, C. K., Volcke, E. I. P., Tait, S., Batstone, D., Gernaey, K. V. and Jeppsson, U. (2015) 'Effects of ionic strength and ion pairing on (plant-wide) modelling of anaerobic digestion', *Water Research*. Elsevier Ltd, 70, pp. 235–245. doi: 10.1016/j.watres.2014.11.035.

Sötemann, S. W., Van Rensburg, P., Ristow, N. W., Wentzel, M. C., Loewenthal, R. E. and Ekama, G. a (2005) 'Integrated chemical/physical and biological processes modeling Part 2 - Anaerobic digestion of sewage sludges', *Water SA*, 31(4), pp. 545–550. doi: 10.4314/wsa.v31i4.5145.

Sötemann, S. W., Ristow, N. W., Wentzel, M. C. and Ekama, G. a (2005) 'A steady state model for anaerobic digestion of sewage sludges', *Water SA*, 31(4), pp. 511–516. doi: 10.4314/wsa.v31i4.5143.

Speece, R. E. (1983) 'Anaerobic biotechnology for industrial wastewater: Review', *Environmental Science & Technology*, 17(9), pp. 520–521. doi: 10.1139/l96-121.

Sperling, M. Von and Chernicharo, C. A. D. L. (2005) 'Biological Wastewater Treatment in Warm Climate Regions - Volume One', p. 634. doi: 10.5860/CHOICE.45-2633.

Thaveesri, J., Daffonchio, D., Liessens, B., Vandermeren, P. and Verstraete, W. (1995) 'Granulation and sludge bed stability in upflow anaerobic sludge bed reactors in relation to surface thermodynamics', *Applied and Environmental Microbiology*, 61(10), pp. 3681–3686.

Vanderhaegen, B., Ysebaert, E., Favere, K., Van Wambeke, M., Peeters, T., Panic, V., Vandenlangenbergh, V. and Verstraete, W. (1992) 'Acidogenesis in relation to in-reactor granule yield', *Water Science and Technology*, 25(7), pp. 21–30.

Wang, B., Wu, D., Ekama, G. a., Huang, H., Lu, H. and Chen, G. H. (2017) 'Optimizing mixing mode and intensity to prevent sludge flotation in sulfidogenic anaerobic sludge bed reactors', *Water Research*, 122, pp. 481–491. doi: 10.1016/j.watres.2017.06.018.

Wang, K., Yin, J., Shen, D. and Li, N. (2014) 'Anaerobic digestion of food waste for volatile fatty acids (VFAs) production with different types of inoculum: Effect of pH', *Bioresource Technology*, 161, pp. 395–401. doi: 10.1016/j.biortech.2014.03.088.

Wang, X., McCarty, P. L., Liu, J., Ren, N.-Q., Lee, D.-J., Yu, H.-Q., Qian, Y. and Qu, J. (2015) 'Probabilistic evaluation of integrating resource recovery into wastewater treatment to improve environmental sustainability', *Proceedings of the National Academy of Sciences*, 112(5), pp. 1630–1635. doi: 10.1073/pnas.1410715112.

Weiland, P. (2003) 'Production and energetic use of biogas from energy crops and wastes in Germany.', *Applied biochemistry and biotechnology*, 109(1-3), pp. 263–274. doi: 10.1385/ABAB:109:1-3:263.

Wiegant, W. M. and de Man, a. W. a. (1986) 'Granulation of biomass in thermophilic upflow anaerobic sludge blanket reactors treating acidified wastewaters', *Biotechnology and Bioengineering*, 28(5), pp. 718–727. doi: 10.1002/bit.260280511.

Wingender, J., Neu, T. R. and Flemming, H. C. (1999) *Microbial Extracellular Polymeric Substances: Characterization, Structure and Function*. doi: 10.1007/978-3-642-60147-7.

Yang, S. fang and Li, X. yan (2009) 'Influences of extracellular polymeric substances (EPS) on the characteristics of activated sludge under non-steady-state conditions', *Process Biochemistry*, 44(1), pp. 91–96. doi: 10.1016/j.procbio.2008.09.010.

Yu, H. Q., Tay, J. H. and Fang, H. H. P. (2001) 'The roles of calcium in sludge granulation during UASB reactor start-up', *Water Research*, 35(4), pp. 1052–1060. doi: 10.1016/S0043-1354(00)00345-6.

Zacharof, M. P. and Lovitt, R. W. (2013) 'Complex effluent streams as a potential source of volatile fatty acids', *Waste and Biomass Valorization*, 4(3), pp. 557–581. doi: 10.1007/s12649-013-9202-6.

Appendix A: Equilibrium equations

The equilibrium dissociation constants for acetic acid (HAc), H_2CO_3, NH_4Cl and H_3PO_4 are defined by Equation 64, Equation 65 and Equation 66, Equation 67, and Equation 68-Equation 70 respectively.

$$K_A = \frac{[Ac^-][H^+]}{[HAc]} \quad \text{Equation 64}$$

$$K_{C1} = \frac{[HCO_3^-][H^+]}{[H_2CO_3]} \quad \text{Equation 65}$$

$$K_{C2} = \frac{[CO_3^{2-}][H^+]}{[HCO_3^-]} \quad \text{Equation 66}$$

$$K_N = \frac{[NH_3][H^+]}{[NH_4Cl]} \quad \text{Equation 67}$$

$$K_{P1} = \frac{[H_2PO_4^-][H^+]}{[H_3PO_4]} \quad \text{Equation 68}$$

$$K_{P2} = \frac{[HPO_4^{2-}][H^+]}{[H_2PO_4^-]} \quad \text{Equation 69}$$

$$K_{P3} = \frac{[PO_4^{2-}][H^+]}{[HPO_4^-]} \quad \text{Equation 70}$$

$$K_W = [H^+][OH^-] \quad \text{Equation 71}$$

where

$$K_A = 10^{-\left(\frac{1170.5}{T} - 3.165 + 0.0134 \cdot T\right)} \quad \text{Equation 72}$$

$$K_{C1} = 10^{-\left(\frac{3404.7}{T} - 14.8435 + 0.03279 \cdot T\right)} \quad \text{Equation 73}$$

$$K_{C2} = 10^{-\left(\frac{2902.4}{T} - 6.498 + 0.02379 \cdot T\right)} \quad \text{Equation 74}$$

$$K_N = 10^{-\left(\frac{1170.5}{T} - 3.165 + 0.0134 \cdot T\right)} \quad \text{Equation 75}$$

$$K_{P1} = 10^{-\left(\frac{799.3}{T} - 4.5535 + 0.01349 \cdot T\right)} \quad \text{Equation 76}$$

$$K_{P2} = 10^{-\left(\frac{1979.5}{T} - 5.3541 + 0.01984 \cdot T\right)} \quad \text{Equation 77}$$

$$K_{P3} = 9.48 \cdot 10^{-13} \quad \text{Equation 78}$$

$K_W = 10^{-14}$ at 25°C Equation 79

$K_W = 2.63 \cdot 10^{-14}$ at 37°C Equation 80

The above correlations for the weak acid dissociation constants (Equation 72-Equation 80) were taken from Helgeson (1967).

Appendix B: Reactor dimensions

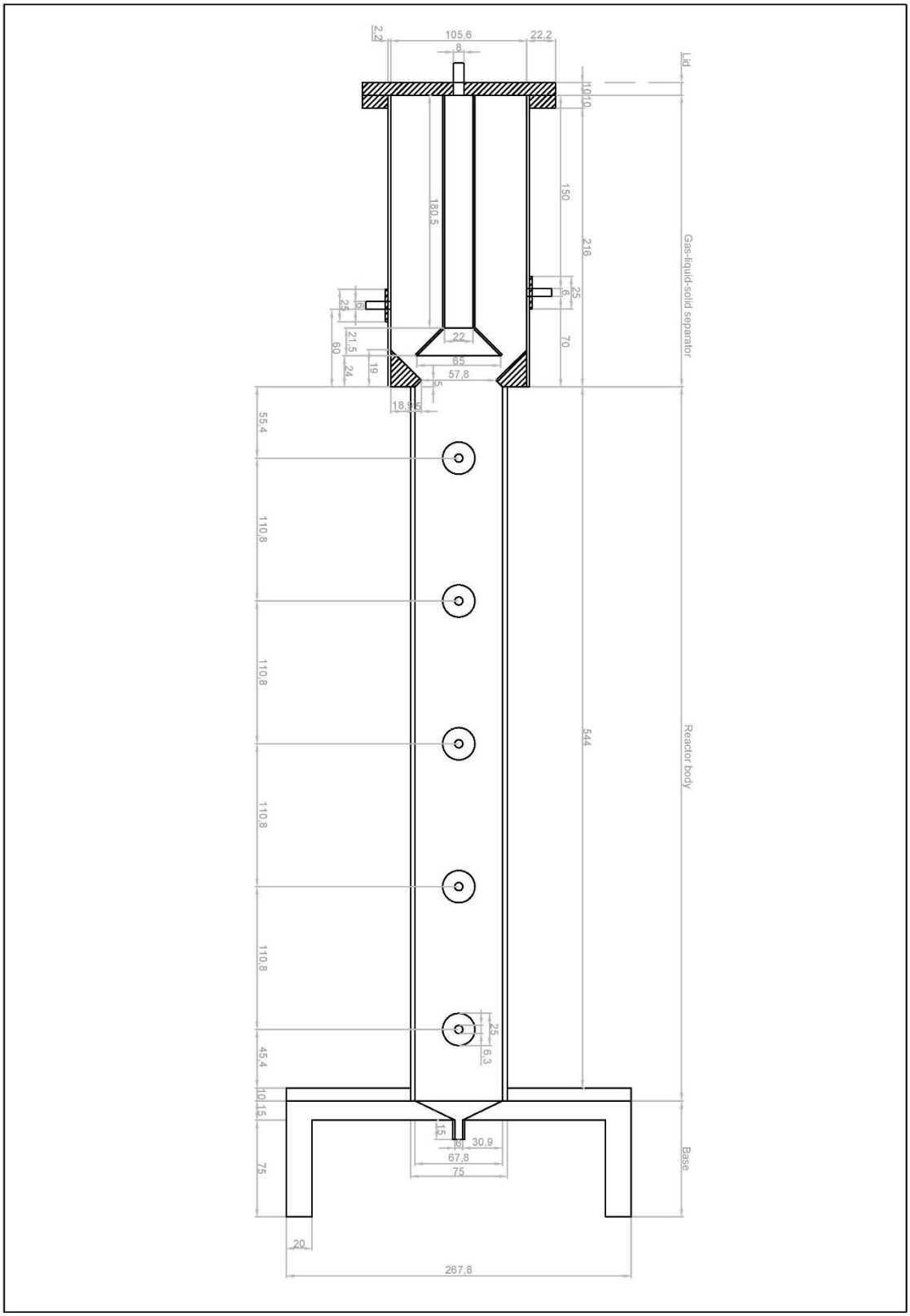

Figure 6-1: Side view of the UASB reactors including dimensions

Appendix C: First experimental plan

Table 6-1: Experimental plan for the original experiment

Phase	Start-up/acclimatisation				1	2	3	4	5	6	7	8	9	10	11
OLR (g-COD/L.day)	1	1.5	2.5	4	6	9	14	22	30	45	65	95	130	160	200
HRT (h)	36	24	14.4	9.0	6.0	4.0	2.57	1.64	1.64	1.64	1.64	1.64	1.64	1.64	1.64
Upflow velocity (m/h)*	0.21	0.28	0.35	0.68	0.68	0.68	0.68	0.68	0.68	0.68	0.68	0.68	0.68	0.68	0.68
COD (g/L)	1.5	1.5	1.5	1.5	1.5	1.5	1.5	1.5	2.05	3.07	4.43	6.48	8.86	10.9	13.6
Feed flow rate (L/day)	1.3	2.0	3.3	5.3	8.0	12.0	18.7	29.3	29.3	29.3	29.3	29.3	29.3	29.3	29.3
Recycle flow rate (L/day)	16.9	22.3	27.0	53.3	50.7	46.7	40.0	29.3	29.3	29.3	29.3	29.3	29.3	29.3	29.3
Recycle ratio	14	12	9	11	7	5	3.1	2.0	2.0	2.0	2.0	2.0	2.0	2.0	2.0

*Note the upflow velocity represents the superficial upflow velocity resulting from the feed and recycle flows

Appendix D: Experimental data and sample calculations

D.1 TSS & VSS

The concenrations of total suspended solids (TSS) and volatile suspended solids (VSS) in the reactors' sludge beds were estimated from the TSS and VSS data generated by sampling from up to five sampling points along the height of each reactor. Since only the TSS and VSS concentrations in the sludge beds were of interest, only sludge bed samples were taken. The number of samples used to generate the profiles of TSS of VSS in the sludge beds therefore depended on the height of the sludge beds (i.e. the number of samples taken corresponds to the number of sampling ports below the top of the sludge beds).

To calculate the average TSS and VSS concentrations in the reactors (presented in Table 5-3), the reactors were divided into the five zones served by the five sampling ports. The TSS and VSS in each zone was assumed to represent the average TSS and VSS in that respectively except in the case of the zone containing the top of the sludge bed. The TSS and VSS present in this top zone were calculated as the TSS and VSS measured in this zone (or in the case that the sludge bed does not reach the height of the sample port serving this zone, the zone below) multiplied by the fraction of the zone that was occupied by the sludge bed. The sludge bed height was also measured along with the TSS and VSS, thus allowing estimation of the fraction of the top zone that was occupied by sludge. However, in the case that the sludge bed occupies less than half the top zone, the sampling port serving this zone will not provide a sludge bed sample, thus the TSS and VSS measured in one zone below is used. A example calculation is presented below for the VSS R2 on Day 33 of the granulation experiment.

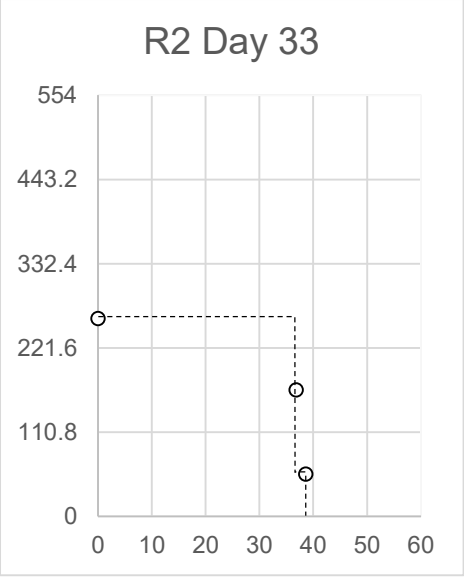

Figure 6-2:The measured VSS along the height of R2 on Day 33 of the granulation experiment with the sludge bed VSS concentration assumed shown by the dashed black line

As can be seen in Figure 6-2 the sludge bed occupies the lowest three zones, and only partially occupies the top (third) zone in which it is present. Furthermore, less than half of the top zone is occupied by sludge, therefore the VSS measured in the second zone is used to estimate the VSS content of the top zone. The average VSS is therefore calculated as follows:

$$VSS_{avg} = 0.2VSS_{zone\ 1} + 0.2VSS_{zone\ 2} + 0.2 \cdot f_{occupied}VSS_{zone\ 2}$$

where

$$f_{occupied} = \frac{260 - 221.6}{332.4 - 221.6} = 0.347$$

where

260 is the measured height of the sludge bed (mm)

221.6 is the height at which the second zone ends/third zone begins (mm)

332.4 is the height at which the third zone ends/fourth zone begins (mm)

$$\therefore VSS_{avg} = 0.2 \cdot 38.6 + 0.2 \cdot 36.9 + 0.2 \cdot 0.347 \cdot 36.9 = 17.7\ g/L$$

D.2 COD

D.2.1 COD standard curve

The standard curve used to convert the measured absorbance values into COD is presented in Figure 6-3:

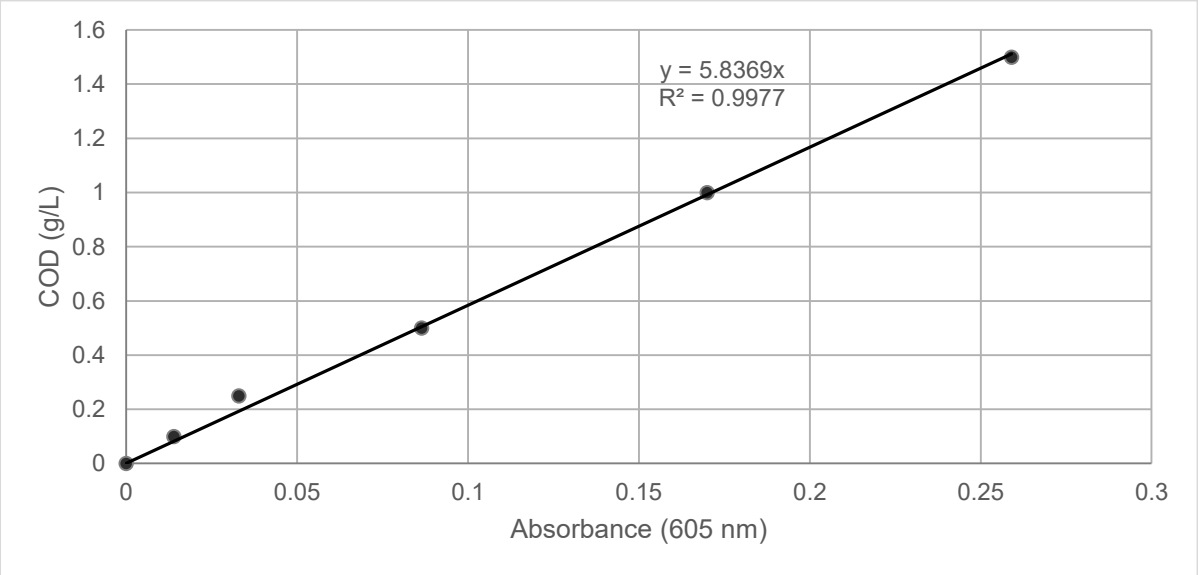

Figure 6-3: Standard curve used to convert the measured absorbance to COD

D.2.2 COD recovered as CH_4

The calculation of CH_4 productivity, presented as g-COD/L.day, was calculated as the product of the measured biogas production (L/day) and the measured biogas composition (%CH_4). Biogas production was measured daily by the number of "tips" recorded on the wet tip gas meter (where each "tip" recorded corresponds to 35 mL of biogas produced). The biogas productivity was then calculated according to Equation 81:

$$Biogas\ productivity = \frac{(Tips_{n+1} - Tips_n) \cdot 0.035\left(\frac{L}{tip}\right) \cdot 24\left(\frac{h}{day}\right)}{Hours\ between\ measurements} \qquad \text{Equation 81}$$

Although biogas production was measured daily during the granulation experiment, biogas composition was only measured five times. Therefore, the CH_4 production for each period between biogas composition measurements was calculated using the biogas composition measured at the beginning of

the period. This CH_4 productivity (L/day) is then converted to volumetric CH_4 productivity as COD (g-COD/L.day) by dividing by the volumetric COD of CH_4 (0.35 L/g-COD) and the reactor working volume (2 L).

For example, calculation of the CH_4 production (g-COD/L.day) from R1 for day 42 is presented below:

$$CH_4\ Productivity_{day\ 42} = \frac{Biogas\ Productivity_{day\ 42}\left(\frac{L}{day}\right) \cdot \%CH_{4,day\ 40}}{0.35\left(\frac{L}{g-COD}\right) \cdot 2\ (L)}$$

$$\therefore CH_4\ Productivity_{day\ 42} = \frac{13.66 \cdot 54\%}{0.35 \cdot 2} = 10.62\ \frac{gCOD}{L.day}$$

To calculate the total amount of COD removed from the aqueous phase that was recovered as CH_4, the total mass of CH_4-COD produced was divided by the total mass of COD removed. The total mass of CH_4-COD was calculated by summing up the daily mass of CH_4-COD produced (as calculated above) by the daily mass of COD removed. The daily mass of COD removed was calculated from the raw data as the difference between the soluble COD in the feed and effluent.

D.3 Superficial upflow velocity

The superficial upflow velocity presented in Table 5-3 is calculated according to Equation 82:

$$u_{Upflow} = \frac{v_{Feed} + v_{Recycle}}{10 \cdot A} \qquad \text{Equation 82}$$

where

u_{Upflow} is the superficial upflow velocity (m/h)

v_{Feed} is the feed flow rate (L/h)

$v_{Recycle}$ is the recycle flow rate (L/h)

A is the reactor cross-setional area (dm^2)

Appendix E: Model results, comparisons and COD and elemental balances

Table 6-2 below presents a comparison of the main AD performance variables as predicted by the model described by Sotemann *et al.* (2005) and the stoichiometric model developed in Chapter 4.

Table 6-2: Comparison of the results obtained from the model described by Sotemann *et al*. (2005) with those obtained in Scenario 2 using the stoichiometric model described in Chapter 4

	Stoichiometric Model Scenario 2	(Sötemann, *et al.*, 2005)
Effluent VFA (mol/L)	0.00	0.00
Effluent pH	6.70	6.60
CH_4 productivity (g-COD_{CH4}/L.day)	10.00	10.00
Gas composition (%$_{CH4}$)	67.4	61.0

Table 6-3 and Table 6-4 have been included to show consistency of the carbon and COD flows respectively within the stoichiometric model.

Table 6-3: Carbon balance of the stoichiometric model

C_{in} (mol/day)	C_{out} (mol/day)				
Sucrose	X (biomass)	CO_2	CH_4	HAc	Total
0.7031	0.068	0.29	0.28	0.063	0.7031

Table 6-4: COD balance of the stoichiometric model

COD_{in} (g/day)	COD_{out} (g-COD/day)			
Sucrose	X (biomass)	CH_4	HAc	Total
22.50	2.49	18.009	2.001	22.50